

JULIUS-MAXIMILIANS UNIVERSITÄT WÜRZBURG



FACULTY FOR PHYSICS AND ASTRONOMY  
CHAIR IN THEORETICAL PHYSICS II

MASTER THESIS

---

LEPTOGENESIS IN THE  $\nu$ MSM  
SELF-CONSISTENT TREATMENT OF THERMAL  
SELF-ENERGIES

---

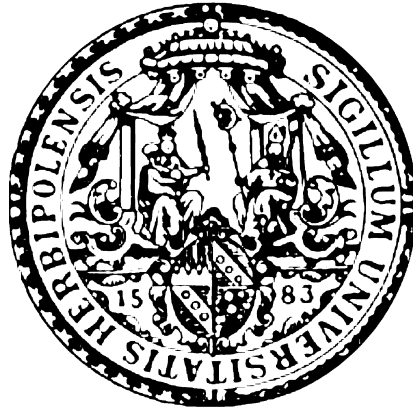
AUTHOR  
Christoph Jürgen Groß

SUPERVISOR  
Prof. Dr. Werner Porod

DATE OF SUBMISSION  
30.06.2015



JULIUS-MAXIMILIANS UNIVERSITÄT WÜRZBURG



FAKULTÄT FÜR PHYSIK UND ASTRONOMIE  
LEHRSTUHL FÜR THEORETISCHE PHYSIK II

MASTERARBEIT

---

LEPTOGENESE IM  $\nu$ MSM  
KONSISTENTE BERECHNUNG VON THERMISCHEN  
SELBSTENERGIEN

---

AUTOR  
Christoph Jürgen Groß

BETREUER  
Prof. Dr. Werner Porod

ABGABEDATUM  
30.06.2015



JULIUS-MAXIMILIANS-UNIVERSITÄT WÜRZBURG

FACULTY FOR PHYSICS AND ASTRONOMY

CHAIR IN THEORETICAL PHYSICS II

# LEPTOGENESIS IN THE $\nu$ MSM

## SELF-CONSISTENT TREATMENT OF THERMAL SELF-ENERGIES

by Christoph Jürgen Groß

### *Abstract*

A self-contained introduction to the Closed Time Path formalism is given, explaining how to extract Feynman rules from the Lagrangian and highlighting the differences to a Quantum Field Theory at zero temperature. The discussion explicitly covers scalars and Dirac fermions, as well as gauge bosons. In the latter case, a naive treatment seems to indicate that BRST invariance is broken at finite temperature. However, it is shown how to address this problem through the utilization of ghost number operators in the partition sum. The  $\nu$ MSM is a promising extension of the Standard Model with right-handed neutrinos. It has the potential to explain numerous questions that point to physics beyond the Standard Model simultaneously. Based on the methods in the Closed Time Path formalism, a self-consistent calculation of self-energies for the right-handed neutrinos is presented. For soft external momenta, the Hard Thermal Loop approximation is used in order to obtain results that are complete to leading order in the couplings.

\* \* \*

In dieser Arbeit wird eine in sich abgeschlossene Einführung zum Closed Time Path Formalismus präsentiert, in der dargelegt wird, wie Feynman Regeln von einer Lagrange Funktion abgeleitet werden können und was die Unterschiede zu einer Quantenfeldtheorie bei verschwindender Temperatur sind. Dies wird explizit für Skalare, Dirac Fermionen und Eichbosonen exerziert. Bei letzteren scheint eine naive Herangehensweise zu zeigen, dass BRST Invarianz bei endlichen Temperaturen verletzt ist. Man kann allerdings zeigen, dass dieses Problem durch die Einführung von Geister Anzahl Operatoren in der Zustandssumme behoben werden kann. Das  $\nu$ MSM ist eine vielversprechende Erweiterung des Standardmodells mit richtshändigen Neutrinos. Es hat das Potential, mehrere Fragestellungen die auf Physik jenseits des Standardmodells hinweisen simultan zu erklären. Basierend auf den Methoden des Closed Time Path Formalismus wird eine konsistente Berechnung der Neutrino Selbstenergie präsentiert. Für weiche externe Impulse wird die Hard Thermal Loop Näherung verwendet um Ergebnisse zu erhalten, die in führender Ordnung Störungsrechnung vollständig sind.



# Einverständniserklärung

Hiermit erkläre ich, dass ich die vorliegende Arbeit selbstständig verfasst, keine anderen als die angegebenen Quellen und Hilfsmittel benutzt und die Arbeit bisher oder gleichzeitig keiner anderen Prüfungsbehörde zur Erlangung eines akademischen Grades vorgelegt habe.

Würzburg, 30. Juni 2015

.....  
*Christoph Jürgen Groß*



# Contents

Abstract • v
Declaration • vii
1 Introduction • 1
2 Thermal Quantum Field Theory • 5
2.1 Quantum Statistics • 5
2.2 Closed Time Path Formalism • 6
2.3 Path Integral • 9
2.4 Klein-Gordon Propagator • 12
2.5 Fermion Propagator • 17
2.6 Interactions • 18
2.7 Gauge Theories • 19
3 The $\nu$ MSM • 27
3.1 Standard Model of electroweak Interactions • 27
3.2 Extension with right-handed Neutrinos • 29
3.2.1 Lagrangian and Parametrization • 29
3.2.2 Majorana Properties • 33
4 Self-Energies • 35
4.1 Dressed Propagators • 35
4.2 Higgs Self Energy • 38
4.2.1 Contributions from Vector Bosons • 38
4.2.2 Contributions from Scalars • 45
4.2.3 Contributions from Fermions • 46
4.2.4 Full thermal Self Energy and dressed Propagator • 47
4.3 Lepton Self Energy • 47
4.3.1 Contributions from Vector Bosons • 47
4.3.2 Contributions from Scalars • 50
4.3.3 Full thermal Self Energy and dressed Propagator • 51
4.4 Neutrino Self Energy • 58
5 Summary and Outlook • 65
A Arbitrary Interval Integrals and the Residue Theorem • 67



# 1

## Introduction

The **Standard Model (SM)** has proven to be a remarkably precise theory for the physics at low energy scales [46, 47]. But despite all its success, tensions with experimental observables - especially in cosmology - remain. This has led to the notion that the SM is not complete but only a low energy effective theory. Of course, there exist a wide variety of extensions and in order to narrow down the list of viable candidates, one must study their phenomenology and compare them to experimental findings.

The **Cosmic Microwave Background (CMB)** is one of the principal sources of information on the early universe. It is comprised of photons that decoupled from matter at the era of recombination and represents the most perfect realization of an ideal black body spectrum in nature. Its origin makes it thus the perfect probe to investigate the universe shortly after the Big Bang, when it was  $\sim 3\,000\text{ K}$  hot, or  $\sim 360\,000\text{ yrs}$  old [60]. It was discovered, more or less accidentally, by Arno Penzias and Robert Wilson in 1965 [48] when they investigated an excess noise temperature in a 20 foot antenna at the Crawford Hill Laboratory and shortly after interpreted as the thermal emission from the last scattering by Robert Dicke and James Peebles et al. [22]. In the following years, theoretical predictions on small anisotropies in the CMB caused by primordial density fluctuations were published [53, 55]. The intriguing implication was the possibility to extract the fractions of baryonic and dark matter in the universe directly from measurements of the angular spectrum of these fluctuations in the CMB. This feat required very precise temperature measurements, a problem that was ultimately tackled by the use of space bound microwave probes. In 1992, scientists finally reported the discovery of said CMB anisotropies in the first-year accumulated data from the **Cosmic Microwave Background Explorer (COBE)** [58]. The subsequent **Wilkinson Microwave Anisotropy Probe (WMAP)** started in 2001 [31] and later the Planck satellite was launched in 2009 [2]. The analysis of the data collected by these missions represents one possibility of how to calculate the baryon asymmetry in the universe, that is the difference between baryon and antibaryon number density. This is usually normalized with the photon density in order to obtain a dimensionless number

## 1 Introduction

$$\eta_b = \frac{n_b - n_{\bar{b}}}{n_\gamma} \simeq 2.739 \cdot 10^{-8} \Omega_b h^2 = \begin{cases} 6.16_{-0.16}^{+0.15} \cdot 10^{-10} & \text{WMAP [39]} \\ (6.072 \pm 0.090) \cdot 10^{-10} & \text{Planck [3]} \end{cases} \quad (1.1)$$

Herein,  $\Omega_b h^2$  is the ratio of baryon density to the critical energy density in the universe with the Hubble rate given by  $H_0 = 100 h \text{ km/s/Mpc}$  [60]. This result leads to the conclusion that there exists a greater abundance of matter than antimatter in the universe. This finding immediately leads to the question of how this asymmetry came to be. A widely accepted model for the very early development of the universe is the idea of cosmic inflation, a period of quasi-exponential growth of co-moving scales, driven by the vacuum energy of a scalar field - the inflaton. This solves by construction two important problems in cosmology: the flatness and the horizon problem. The first addresses the observational fact that the universe today is nearly perfectly flat with curvature  $\Omega_k \simeq 0$ . This can be inferred from the redshift of type Ia supernovae [49, 54] in combination with the CMB measurements mentioned above. While this is not per se inconsistent with standard cosmology, it would require for a very fine tuned curvature in the early universe in Friedmann cosmology without inflation. The second problem revolves around the aforementioned nearly perfect isotropy of the CMB. A calculation of the size of the horizon at the time of recombination yields an angular diameter of only  $1.6^\circ$  in the sky [60]. As a consequence, a nearly homogeneous universe seems unnatural without a period of inflation that would have stretched out all inhomogeneities. These arguments strongly support the idea of inflation. However, after this period of rapid growth, the energy budget of the universe would be completely locked up in kinetic and potential energy of the inflaton, which is afterward transformed into radiation by the process of reheating. With no matter, the universe looks completely baryon-symmetric at that time and processes that can dynamically produce the observed asymmetries are needed - this is known as baryogenesis.

One should note that this method is not the only way to estimate the baryon over photon ratio. Before detailed measurements of the CMB were available, various groups inferred the primordial helium abundance from spectroscopic measurements of HII regions with low metallicity (meaning a lack of elements other than hydrogen and helium) [30, 45]. The amount of helium produced in the early universe depends weakly on the baryon density and the found values agree roughly with the results from CMB measurements.

For successful baryogenesis in the early universe, the three Sakharov conditions [57] need to be fulfilled:

1. violation of baryon number
2.  $C$  and  $CP$  violation
3. deviation from thermal equilibrium

The first condition is intuitively clear: In order to evolve from a baryon symmetric state directly after inflation to a baryon asymmetric state, obviously baryon number must not be a conserved quantity. In the SM, this is provided by so-called sphaleron processes [41, 59]. Second,  $C$  and  $CP$  are two discrete symmetries. The former denotes charge conjugation which exchanges

particles with antiparticles by conjugating all internal quantum numbers, such as  $Q \rightarrow -Q$  for any charge in a gauge theory.  $P$  on the other hand is known as parity conjugation and acts on 3-dimensional space  $\vec{x} \rightarrow -\vec{x}$  changing the handedness of particles. In a world where  $C$  or  $CP$  were exact symmetries, there would be no difference in cross-sections or decay rates for particles and anti-particles. In the SM,  $P$  is broken in the electroweak sector. Also,  $CP$  is weakly broken by imaginary phases in the Yukawa couplings of the scalar Higgs to the quarks. In a minimal parametrization found by Kobayashi and Maskawa [37], there is exactly one parameter that breaks  $CP$  in the  $3 \times 3$  mixing matrix for up- and down-type quarks in the coupling to the  $W$ -boson. The violation was experimentally observed in rare  $K^0$  decays in 1964 for the first time [18] and more recently also in the decays of  $B^0$  [1, 9]. In combination, the breaking of  $P$  and  $CP$  imply that  $CP$  must be broken as well in the SM. The third and last Sakharov condition requires a deviation from thermal equilibrium which is characterized by translational invariance in time. An evolution from a baryon symmetric state to a baryon asymmetric state breaks this time invariance and therefore can only happen out of equilibrium. In the case of the SM, all these factors would come together at the electroweak phase transition, where thermal corrections to the Higgs potential become small enough for the universe to decay to a symmetry breaking vacuum state. However, the determination of the Higgs mass at the LHC seems to imply that the electroweak phase transition is only second order and the baryon asymmetry of the universe predicted by the SM is only  $\eta \sim 10^{-18}$  [25, 56] - eight orders of magnitude below the found value.

The goal of this work is the description of a minimal extension of the SM with right-handed neutrinos, providing an additional source of  $CP$  violation that may cure the problem of baryon asymmetry in the universe. The evolution of the asymmetries obviously depends on reaction rates of the new particle species which can be obtained from two-point correlation functions. These are to be calculated within the framework of thermal Quantum Field Theory (QFT), which will be introduced in Chapter 2. The extension of the SM with right-handed neutrinos is discussed in Chapter 3 and a self-consistent way of calculating self-energies in this model at finite temperature is laid out in Chapter 4. A summary of the methods and findings of this work is then provided in Chapter 5.



# 2

## Thermal Quantum Field Theory

This chapter is aimed at providing a basis and framework for the discussions to follow. While an effort is made to present a consistent and self-contained introduction to the theory of QFT at finite temperature, this topic cannot possibly be explored exhaustively within the limited reach of a master thesis. Therefore, the reader is advised to consult one of the many excellent text books on the matter for a deeper understanding of the field [21, 32, 42].

### 2.1 Quantum Statistics

The vast majority of processes at the microscopic scale of elementary particles in the universe today can be described as taking place in a vacuum at zero temperature. For instance, the cosmic microwave background constitutes a thermal bath of photons at a temperature of 2.7 K, corresponding to mere  $2.3 \times 10^{-4}$  eV. However, there are still situations accessible to physicists where thermal effects are prominent in high energy physics, although these systems are typically far from thermal equilibrium and therefore delicate in their theoretical description. An example can be found in the quark gluon plasma, created at a heavy ion collision in particle accelerators. There exists however a very important application for the theory of systems in or near thermal equilibrium: particle cosmology. Considering the early universe, particle collisions happened within a thermal plasma with the temperature fixing the overall energy scale. A theory that attempts to describe the phenomena that arise in such an environment is typically based upon statistical physics and the notion of ensembles. These are defined in Fock space

$$\mathcal{H} = \bigoplus_{N=0}^{\infty} \mathcal{H}^N, \quad (2.1)$$

where  $\mathcal{H}^N$  is the  $N$ -particle Hilbert space. Members of the ensemble are not limited to pure states  $|\psi_n^N\rangle \in \mathcal{H}$ , but are generally given by the density matrix

$$\rho = \sum_{N=0}^{\infty} \sum_{n=1}^{\dim \mathcal{H}^N} p_n^N |\psi_n^N\rangle \langle \psi_n^N|. \quad (2.2)$$

## 2 Thermal Quantum Field Theory

A system in thermal equilibrium is completely characterized by a small set of numbers: the temperature  $T$  and a set of chemical potentials  $\mu_i$ . The density matrix for such a system can be written as

$$\rho_{\text{eq}} = \frac{\exp\left[-\beta\left(H - \sum_i \mu_i Q_i\right)\right]}{\text{tr}\left\{\exp\left[-\beta\left(H - \sum_i \mu_i Q_i\right)\right]\right\}}. \quad (2.3)$$

Here,  $\beta = 1/T$  is the inverse temperature,  $H$  is the Hamiltonian of the theory and the  $Q_i$  are the charges associated with the chemical potentials. The role of vacuum expectation values in a cold QFT is replaced by averages over the whole ensemble in quantum statistics. For any operator  $\mathcal{A}$ , the average is defined as

$$\langle \mathcal{A} \rangle \equiv \text{tr}[\mathcal{A}\rho], \quad (2.4)$$

with the trace spanning all states in Fock space. These fundamentals of quantum statistics are used to construct a QFT at finite temperature by considering the thermal averages of field operators. At zero temperature, only the vacuum expectation value is considered when evaluating  $n$ -point functions that make up the building blocks of the theory. Going to the ensemble in the thermal plasma, the vacuum element represents only one of many contributions, each weighted by a statistical factor. Thus, effects that arise from interactions with the thermal plasma are included into the Green functions of the theory.

## 2.2 Closed Time Path Formalism

Several formulations of QFT at finite temperature exist, the two most prominent being the **Imaginary Time Formalism (ITF)** and the **Real Time Formalism (RTF)**. In the ITF, calculations are performed in Euclidian space-time with Green functions being defined for imaginary times. While calculations in this former framework are generally less complicated than in the latter, this also comes with the disadvantage of having to continue results analytically to real times if one is interested in timelike correlations. If on the other hand, one is interested in systems that may develop away from equilibrium - which may e.g. be the case when particle species freeze out during the adiabatic cooling of the universe - correlations over time are very important and it may be advisable to work in the RTF. Herein, a system is prepared in thermal equilibrium at time  $t = 0$  but may evolve away at later times:

$$\rho(t) = \rho_{\text{eq}} \quad \text{for } t \leq 0. \quad (2.5)$$

For  $t > 0$ ,  $\rho$  is defined by (2.2), where it is assumed that the weights  $p_n^N$  are constant in time. This implies that within this formalism the entropy is conserved, as it can be expressed as a function that only depends on the  $p_n^N$ . For an adiabatically expanding universe, this assumption

is fulfilled to good approximation at very high temperatures  $T \gg T_{EW} \sim 150 \text{ GeV}$ , where the number of effective degrees of freedom remains constant.

In the Schrödinger picture, the time dependence of the system is completely contained in the states

$$i \frac{\partial}{\partial t} |\psi_n^N(t)\rangle = H |\psi_n^N(t)\rangle \quad (2.6)$$

and one immediately finds the Liouville equation for the density matrix

$$i \frac{\partial \rho(t)}{\partial t} = [H, \rho(t)]. \quad (2.7)$$

This differs from the time evolution of operators in the Heisenberg picture by a minus sign. If the Hamiltonian commutes with the density matrix, the state is stationary and describes a system in thermal equilibrium. However, if the system is not in equilibrium, the Hamiltonian may depend on time. As the physical evolution of the system only starts at  $t = 0$ , the time dependence of  $H$  can be constrained to positive times. For  $t \leq 0$  the Hamiltonian can be chosen to be constant. This can be thought of as preparing the system in thermal equilibrium during  $t \leq 0$  and then letting it evolve freely starting at  $t = 0$ . Thus,  $\rho = \rho_{eq}$  at negative times, while for positive times, the density matrix follows the Liouville equation (2.7) with a time-dependent Hamiltonian  $H(t)$ . The evolution of the system is then given by

$$\rho(t) = U(t,0)\rho(0)U^\dagger(t,0) = U(t,0)\rho(0)U(0,t), \quad (2.8)$$

where

$$U(t,t') = \mathcal{T} \exp \left[ -i \int_{t'}^t dt'' H(t'') \right] \quad (2.9)$$

is the time evolution operator familiar from classical quantum mechanics. A similarity exists between the time evolution operator  $U$  and the equilibrium density matrix  $\rho_{eq}$ . This allows to express the initial state of the system in terms of an evolution along the imaginary time axis

$$\rho_{eq} = \frac{U(T - i\beta, T)}{\text{tr}[U(T - i\beta, T)]}, \quad (2.10)$$

where  $T$  is an arbitrary negative time during which the system was in equilibrium. Inserting (2.5) and (2.10) into (2.8) then leads to

$$\rho(t) = \frac{U(t,0)U(T - i\beta, T)U(0,t)}{\text{tr}[U(T - i\beta, T)]}. \quad (2.11)$$

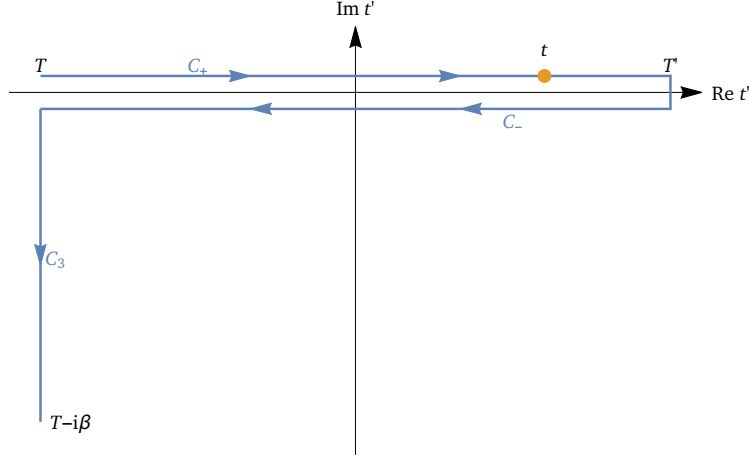


**Figure 2.1:** Contour  $C$  in complex time in the CTP formalism. Integrals over  $t'$  follow  $C$ , starting at  $T < 0$  and ending at  $T - i\beta$ . An operator is picked up at  $t \in [0, T']$  with  $T' > 0$ .

Now, substituting this into (2.4) while exploiting the cyclicity of the trace, as well as the property that evolution operators  $U$  commute with each other at negative times and the identity  $U(t, t'')U(t'', t') = U(t, t')$ , the ensemble average of an observable  $\mathcal{A}$  becomes

$$\begin{aligned} \langle \mathcal{A} \rangle(t) &= \frac{\text{tr} U(T - i\beta, T) U(T, t) \mathcal{A} U(t, T)}{\text{tr} [U(T - i\beta, T)]} \\ &= \frac{\text{tr} U(T - i\beta, T) U(T, T') U(T', t) \mathcal{A} U(t, T)}{\text{tr} [U(T - i\beta, T) U(T, T') U(T', T)]}. \end{aligned} \quad (2.12)$$

In the second step, a new positive time  $T' > t$  was introduced in order to bring the expression into the standard form of the Closed Time Path (CTP) formalism - a special case of the RTE. This expression for the ensemble average can be interpreted as evolving the system in time along a contour  $C$ . The inverse temperature  $\beta$  herein extends this contour into the complex plane, because  $\exp[-\beta H]$  has the same form as the time evolution operators. The path is depicted in Figure 2.1: The start is at the arbitrary negative real time  $T$ , from where one follows the contour to the positive time  $t$  along the real axis, picking up the operator  $\mathcal{A}$ . After that, the path is continued until the arbitrary positive time  $T'$ , turned around and retraced back to  $T$  from where it then reaches towards  $T - i\beta$  in the lower half of the complex plane. The path  $C_+$  in positive real direction is shifted infinitesimally above the real axis, whereas the path  $C_-$  in negative real direction is shifted below. The last segment in negative imaginary direction is labeled  $C_3$ .

The trace in the denominator in (2.12) is the partition function that serves as a normalization factor in the calculation of ensemble averages. Inserting the definition (2.9) for the time evolution operators into the trace, one finds an intermediate expression for the partition function as

$$\mathcal{Z} = \text{tr} [U(T - i\beta, T) U(T, T') U(T', T)]$$

$$= \int d\phi \langle \phi | \mathcal{T}_C \exp \left[ -i \int_C dx^0 \int d^3\vec{x} \mathcal{H}(x) \right] | \phi \rangle, \quad (2.13)$$

where the trace over Fock space was expressed as the integral over the diagonal matrix elements in an appropriate basis  $\{|\phi\rangle\}$ . The integration in time  $x^0$  is performed along the contour  $C$ . Consequently, a time ordering of operators must also be understood as an ordering along  $C$ , which is implied by the subscript on the time ordering operator  $\mathcal{T}_C$ . In the next section, the discussion will turn to deriving an equivalent representation of  $Z$  that is more suited to deriving Feynman rules.

## 2.3 Path Integral

The partition function can be used as a generating functional for any  $n$ -point function of the theory. In order to arrive at a representation where these functions can be extracted from  $Z$ , the Feynman path integral is used. This alternative formalism of quantum physics considers all possible evolutions of a system over time and superimposes them. Technically, this is done by first cutting the contour  $C$  into infinitesimal pieces. At each cut, an integral over all Fock space is inserted as an identity operator. Two bases are chosen for the representation of these identities: The eigenstates of the field operators  $|\phi\rangle$  and their conjugated momenta  $|\varpi\rangle$

$$\mathbb{1} = \int d\phi |\phi\rangle \langle \phi|, \quad (2.14a)$$

$$\mathbb{1} = \int \frac{d\varpi}{2\pi} |\varpi\rangle \langle \varpi|. \quad (2.14b)$$

After the insertion of identities, one obtains

$$\begin{aligned} Z &= \int \frac{d\phi d\varpi}{2\pi} \int \lim_{N \rightarrow \infty} \prod_{n=1}^N \left( \frac{d\phi_n d\varpi_n}{2\pi} \right) \\ &\quad \langle \phi | \varpi_N \rangle \langle \varpi_N | \mathcal{T}_C \exp \left[ -i \int_{t_N}^{T-i\beta} dx^0 \int d^3\vec{x} \mathcal{H}(x) \right] | \phi_N \rangle \dots \\ &\quad \dots \langle \phi_1 | \varpi \rangle \langle \varpi | \mathcal{T}_C \exp \left[ -i \int_T^{t_1} dx^0 \int d^3\vec{x} \mathcal{H}(x) \right] | \phi \rangle. \end{aligned} \quad (2.15)$$

The  $\{t_i\}$ ,  $i = 1, \dots, N$  are the points where  $C$  is cut. In order to proceed, first note that

$$\langle \phi_i | \varpi_{i-1} \rangle = \exp \left[ i \int_{t_{i-1}}^{t_i} dx^0 \int d^3\vec{x} \dot{\phi}(x) \varpi(x) \right], \quad (2.16)$$

where classical fields appear in the integral. In the same way, field operators in the Hamiltonian

inside (2.15) can be replaced by classical fields by letting them act on the states to the left and right of the exponential. For this to work, normal ordering of the operators in  $\mathcal{H}$  is essential. Then, one obtains the following expression for the partition function

$$Z = \mathcal{N} \int \mathcal{D}\phi \mathcal{D}\varpi \exp \left\{ i \int_C d^4x [\dot{\phi}(x) \varpi(x) - \mathcal{H}[\phi(x), \varpi(x)]] \right\}. \quad (2.17)$$

The integrals over Fock space at each point  $t_i$  along the contour have been expressed as integration measures over all classical field configurations  $\mathcal{D}\phi$  and  $\mathcal{D}\varpi$  that are subject to one boundary condition that arises from a subtlety in the derivation of the path integral formula: In (2.13), the bra-vector to the left of the time evolution operator is the same as the ket-vector to the right as they arise from the same trace over Fock space. However, in order for the picture of evolving the system along  $C$  to be consistent, one needs a state at  $T - i\beta$  to the left and a state at  $T$  to the right of the operator. For this reason, one must impose the condition

$$\phi(T - i\beta, \vec{x}) = \pm \phi(T, \vec{x}). \quad (2.18)$$

This (anti-) periodicity relation for the fields in thermal equilibrium is known as the **Kubo-Martin-Schwinger (KMS)** boundary condition [29, 40, 43]. While this constraints the allowed field configurations  $\phi(x)$ , no such rule is imposed on the conjugated momenta  $\varpi(x)$ . The prefactor  $\mathcal{N}$  is a normalization constant from the integration measure. In a final step, the integral over the conjugated momenta can be carried out in case that the Hamiltonian is quadratic in those momenta. Then, the integral is Gaussian and one finds

$$Z = \mathcal{N}' \int \mathcal{D}\phi \exp \left\{ i \int_C d^4x \mathcal{L}[\phi(x), \dot{\phi}(x)] \right\}. \quad (2.19)$$

Again,  $\mathcal{N}'$  is a normalization factor and  $\mathcal{L}$  is the Lagrangian of the theory. The path integral formulation of the partition function can now be used in order to construct a generating functional for Green functions. For this purpose, an external current  $j(x)$  is introduced, defined along  $C$  like the classical fields  $\phi(x)$ . The functional  $Z[j]$  then denotes the partition function of the system in presence of this external source

$$Z[j] = \int \mathcal{D}\phi \exp \left\{ i \int_C d^4x [\mathcal{L}[\phi(x), \dot{\phi}(x)] + j(x) \phi(x)] \right\}. \quad (2.20)$$

Here, the prefactor  $\mathcal{N}'$  was dropped, as Green functions are always normalized with the partition function and  $\mathcal{N}'$  cancels in that process. In the limit  $j \rightarrow 0$ , one trivially recovers the partition function of the system. The importance of the generating functional originates from the possibility

to take functional derivatives with respect to  $j(x)$ . Evaluating these derivatives at  $j(x) \equiv 0$  then gives any  $n$ -point function of the theory

$$\langle \mathcal{T}_C \phi(x_1) \dots \phi(x_n) \rangle = \frac{1}{z[j]} \frac{\delta}{i\delta j(x_1)} \dots \frac{\delta}{i\delta j(x_n)} z[j] \Big|_{j=0}. \quad (2.21)$$

For deriving Feynman rules in an interacting theory, one can split the Lagrangian into a free and an interaction part  $\mathcal{L} = \mathcal{L}_0 + \mathcal{L}_I$  and use the same trick of replacing fields with functional derivatives to move the interaction part in front of the integral over field configurations

$$z[j] = \exp \left\{ i \int_C d^4x \mathcal{L}_I \left[ \frac{\delta}{i\delta j(x)} \right] \right\} z_0[j]. \quad (2.22)$$

Here,  $z_0$  denotes the generating functional from (2.20) with the free Lagrangian  $\mathcal{L}_0$ . All couplings of the theory are comprised in the first term. An expansion in perturbation theory then corresponds to the expansion of the former exponential in powers of functional derivatives  $\delta/i\delta j$  that act on the free generating functional.

In the above discussion, it was implicitly assumed in the Gaussian integral that  $\phi(x)$  is a bosonic field. For the fermionic case, the anti-commuting nature of the fields must be taken into account. However, when the Gaussian integral is carried out, the fields are already considered as being classical, so they are not operator valued. Hence, anti-commuting fields call for anti-commuting numbers - the Grassmann numbers

$$\{\theta_i\} : \theta_i \theta_j = -\theta_j \theta_i. \quad (2.23)$$

This identity immediately leads to the conclusion that all higher powers of a Grassmann number vanish and therefore all power series terminate after the linear term. Any function of a Grassmann number can be written as

$$f(\theta) = a + b\theta, \quad (2.24)$$

where  $a, b \in \mathbb{C}$ . Going one step further, one may ask about sensible definitions for differentiation and integration:

$$\frac{\partial}{\partial \theta} (a + b\theta) = b, \quad (2.25a)$$

$$\int d\theta (a + b\theta) = b. \quad (2.25b)$$

The former is exactly what one would expect. For the case of integration however, the situation

is a bit more involved. A simple argument for the integration formula above can be found when considering a Gaussian integral at which this discussion is aimed anyways. Such an integral should be independent of a shift in the integration variable  $\theta \rightarrow \theta + \psi$ , where  $\psi$  is an independent Grassmann-odd number. This leaves the above as the only possible definition. Therefore, differentiation and integration are the same for Grassmann-odd variables. A general Gaussian integral then takes the form

$$\begin{aligned} \int d\theta d\bar{\theta} \exp(\bar{\theta} \Lambda \theta + \bar{\psi} \theta + \bar{\theta} \psi) &= \int d\theta d\bar{\theta} \exp(\bar{\theta} \Lambda \theta - \bar{\psi} \Lambda^{-1} \psi) \\ &= \Lambda \exp(-\bar{\psi} \Lambda^{-1} \psi). \end{aligned} \quad (2.26)$$

$\Lambda$  is a Grassmann-even operator. In the first step, a substitution of the integration variable  $\theta \rightarrow \theta - \Lambda^{-1} \psi$  and  $\bar{\theta} \rightarrow \bar{\theta} - \bar{\psi} \Lambda^{-1}$  was applied to the integrand in order to complete the square. As the second term in the exponential does no longer depend on the integration variables it can be pulled in front of the integral. Integrating over the momenta in the path integral (2.17) in the fermionic case then gives

$$Z[\eta, \bar{\eta}] = \int \mathcal{D}\psi \mathcal{D}\bar{\psi} \exp \left\{ i \int_C d^4x [\mathcal{L}[\psi(x), \bar{\psi}(x)] + \bar{\eta}(x) \psi(x) + \bar{\psi}(x) \eta(x)] \right\}, \quad (2.27)$$

for the generating functional with two currents  $\eta, \bar{\eta}$ . In the following sections, it will be discussed how to derive the Feynman rules from the generating functional.

## 2.4 Klein-Gordon Propagator

A free scalar theory shall serve as an introductory example for the derivation of Feynman rules from the generating functional and at the same time provide the basis for the discussion of more complicated models. The Lagrangian for a real scalar field  $\phi$  with mass  $m$  is given by

$$\mathcal{L} = \frac{1}{2} \partial_\mu \phi \partial^\mu \phi - \frac{m^2}{2} \phi^2. \quad (2.28)$$

It is advantageous to apply a substitution for the field variable when integrating over field configurations

$$\phi(x) \rightarrow \phi(x) - \int_C d^4y D(x-y) j(y), \quad (2.29)$$

where  $D$  is the propagator of the theory. By definition, it obeys the equation of motion of the

system - the Klein-Gordon equation - with a pointlike inhomogeneity added as a source term on the right hand side

$$-(\square + m^2)D(x-y) = \delta_C(x-y). \quad (2.30)$$

The  $\delta_C$ -function is defined along the contour  $C$  for the zero-component of the four-vectors (a definition based on the step function along  $C$  can be found in (2.40) further into the section). Applying this substitution to the generating functional in (2.20) gives

$$\begin{aligned} z[j] = & \int \mathcal{D}\phi \exp \left[ i \int_C d^4x \frac{1}{2} \phi(x) (-\square - m^2) \phi(x) \right] \\ & \exp \left[ -\frac{i}{2} \int_C d^4x d^4y j(x) D(x-y) j(y) \right]. \end{aligned} \quad (2.31)$$

The first exponential holds the Lagrangian and will cancel with the denominator in (2.21). The second exponential however does not depend on the field variable any more and can be pulled out of the integral over field configurations. Then, the two-point function of the theory can be found according to

$$\begin{aligned} G(x-y) &= \frac{\delta}{i\delta j(x)} \frac{\delta}{i\delta j(y)} \exp \left[ -\frac{i}{2} \int_C d^4x' d^4y' j(x') D(x'-y') j(y') \right] \Bigg|_{j=0} \\ &= iD(x-y). \end{aligned} \quad (2.32)$$

Thus, propagator and 2-point function are the same apart from a factor of imaginary  $i$ . One could now solve the inhomogeneous Klein-Gordon equation for  $D$  by using a Fourier ansatz that respects the KMS boundary condition. Alternatively, the 2-point function can be evaluated directly in this case of a free theory:

$$\begin{aligned} G(x-y) &= \langle \mathcal{T}_C \phi(x) \phi(y) \rangle \\ &= \theta_C(x^0 - y^0) \langle \phi(x) \phi(y) \rangle + \theta_C(y^0 - x^0) \langle \phi(y) \phi(x) \rangle. \end{aligned} \quad (2.33)$$

A non-interacting field can be expanded in creation and annihilation operators

$$\phi(x) = \int \frac{d^3\vec{p}}{(2\pi)^3 2\omega_p} [a(\vec{p}) e^{-ipx} + a^\dagger(\vec{p}) e^{ipx}], \quad \omega_p = \sqrt{m^2 + \vec{p}^2}. \quad (2.34)$$

Upon substitution into (2.33), one obtains thermal expectation values  $\langle a \rangle$ ,  $\langle a a^\dagger \rangle$ ,  $\langle a^\dagger a \rangle$  and

$\langle a^\dagger a^\dagger \rangle$ . While the first and last expression vanish, the other two expressions return thermal distribution functions [52]

$$\langle a^\dagger(\vec{p}) a(\vec{k}) \rangle = (2\pi)^3 \delta(\vec{p} - \vec{k}) 2\omega_p f_B(\omega_p), \quad (2.35a)$$

$$\langle a(\vec{p}) a^\dagger(\vec{k}) \rangle = (2\pi)^3 \delta(\vec{p} - \vec{k}) 2\omega_p [1 + f_B(\omega_p)], \quad (2.35b)$$

where  $f_B$  is the Bose-Einstein distribution for bosons in thermal equilibrium

$$f_B(\omega) = \frac{1}{e^{\beta\omega} - 1}. \quad (2.36)$$

With this, the 2-point Green function can be computed and one obtains

$$G(x-y) = \int \frac{d^4p}{(2\pi)^4} \rho_0(p) e^{-ip(x-y)} [\theta_C(x^0 - y^0) + f_B(p^0)], \quad (2.37)$$

with the spectral function

$$\rho_0(p) = 2\pi \delta(p^2 - m^2) [\theta(p^0) - \theta(-p^0)]. \quad (2.38)$$

The exact form of the Green function depends on the contour  $C$  and therefore on the choice of the formalism - ITF or RTF. Here, as was already laid out earlier, the CTP contour in complex time is chosen for the integration. Then, assuming that real time arguments either on  $C_+$  or  $C_-$  (c.f. Figure 2.1), the step function  $\theta_C$  is defined as

$$\theta_C(x^0 - y^0) = \begin{cases} \theta(x^0 - y^0) & \text{for } x^0, y^0 \in C_+ \\ \theta(y^0 - x^0) & \text{for } x^0, y^0 \in C_- \\ 0 & \text{for } x^0 \in C_+, y^0 \in C_- \\ 1 & \text{for } x^0 \in C_-, y^0 \in C_+. \end{cases} \quad (2.39)$$

The definition can be extended analogously to  $C_3$ , however, later in the discussion it will become clear that fields on this last part of the contour will always decouple from those on  $C_+$  or  $C_-$ . The definition of the step function induces an expression for the  $\delta_C$ -function that already appeared earlier in the equation of motion for the propagator:

$$\delta_C(x^0 - y^0) = \frac{d\theta_C(x^0 - y^0)}{d(x^0 - y^0)} = \begin{cases} \delta(x^0 - y^0) & \text{for } x^0, y^0 \in C_+ \\ -\delta(x^0 - y^0) & \text{for } x^0, y^0 \in C_- \\ 0 & \text{otherwise} \end{cases} \quad (2.40)$$

Even if  $x^0 = y^0$  the  $\delta_C$ -function evaluates to zero for arguments on different branches of the path. This highlights the interpretation of fields on  $C_+$  and  $C_-$  being different degrees of freedom.

Furthermore, the negative sign in the  $\delta$ -function on  $C_-$  is a consequence of the anti-chronological ordering of operators on this piece of the contour.

Above, it was already stated that fields on  $C_3$  do not contribute to any physical processes. In order to address this topic, the generating functional can be split into parts according to the time integration being along  $C_{\pm} = C_+ \cup C_-$  or  $C_3$  for the two integration variables  $x^0$  and  $y^0$  in (2.31)

$$\begin{aligned}
 Z[j] = & \exp \left[ -\frac{i}{2} \left( \int_{C_{\pm}} \int_{C_{\pm}} + \int_{C_3} \int_{C_3} \right) d^4x d^4y j(x) D(x-y) j(y) \right] \\
 & \exp \left[ -\frac{i}{2} \left( \int_{C_{\pm}} \int_{C_3} + \int_{C_3} \int_{C_{\pm}} \right) d^4x d^4y j(x) D(x-y) j(y) \right]. \quad (2.41)
 \end{aligned}$$

Two exponentials appear: One where both time arguments are on the same part of the contour respectively and one where the arguments are mixed. The latter gives rise to propagators that couple fields from  $C_{\pm}$  to fields on  $C_3$ . As an example, one may e.g. consider the propagator between  $C_+$  and  $C_3$

$$iD_{+3}(x-y) = \int_{-\infty}^{+\infty} \frac{dp^0}{2\pi} e^{-ip^0(x^0-T)} \int \frac{d^3\vec{p}}{(2\pi)^3} \rho_0(p) e^{i\vec{p}\cdot(\vec{x}-\vec{y})} e^{\tau p^0} f_B(p^0), \quad (2.42)$$

where  $y^0 = T - i\tau \in C_3$  with  $0 < \tau < \beta$ . The terms were intentionally organized in such a way that one can immediately interpret the above as a Fourier transformation of the rightmost integral from energy to time space. A property of Fourier transforms of analytic functions is that they go to zero at infinity. The parameter  $T$  that appears above is only constrained by the condition  $T < 0$ , so it can be sent to negative infinity, hence causing the result to vanish if the integral over the spatial components of the momentum happens to be analytic. However, this requirement seems to cause problems in light of the non-analytic properties of the spectral distribution function  $\rho_0$ . Therefore, it is important to perform a regularization of the integrand. In particular, step- and  $\delta$ -functions should be replaced by  $\varepsilon$ -regularized expressions

$$\delta(x) = \lim_{\varepsilon \rightarrow 0} \frac{1}{2\pi i} \left( \frac{1}{x - i\varepsilon} - \frac{1}{x + i\varepsilon} \right), \quad (2.43a)$$

$$\theta(x) = \lim_{\varepsilon \rightarrow 0} \int_{-\infty}^{+\infty} \frac{d\omega}{2\pi i} \frac{e^{i\omega x}}{x - i\varepsilon}. \quad (2.43b)$$

The limit is only taken at the very end of the computation. But even this trick is of no use in the case where  $x^0 \rightarrow -\infty$ , because the expression  $x^0 - T$  is then no longer well defined. A way out can be found in constraining the external currents  $j$  to compact functions, such that

## 2 Thermal Quantum Field Theory

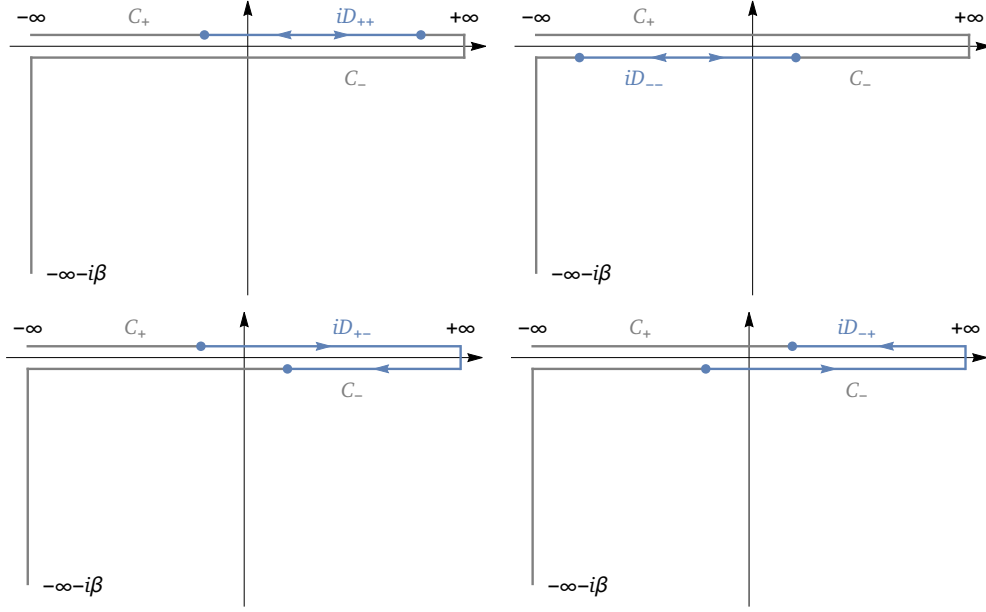


Figure 2.2: The four propagators in the CTP formalism shown in the complex time plane.

$$\lim_{x^0 \rightarrow \pm\infty} j(x) = 0. \quad (2.44)$$

These considerations can analogously be extended to all propagators  $D_{\pm 3}, D_{3\pm}$ , so that altogether one finds that the generating functional mixing the two parts of the contour vanishes

$$\lim_{\substack{T \rightarrow -\infty \\ T' \rightarrow +\infty}} \exp \left[ -\frac{i}{2} \left( \int_{C_{\pm}} \int_{C_3} + \int_{C_3} \int_{C_{\pm}} \right) d^4x d^4y j(x) D(x-y) j(y) \right] = 0 \quad (2.45)$$

and therefore, the generating functional factorizes. Note that this does not imply anything about the evolution of fields on  $C_3$ . What this finding does imply however, is that degrees of freedom on  $C_3$  completely decouple from those on  $C_{\pm}$ .

In light of these two sets of fields, it is customary to define a field and current doublet. The propagators that couple the different fields together are correspondingly organized in a  $2 \times 2$  matrix

$$\phi = \begin{pmatrix} \phi_+ \\ \phi_- \end{pmatrix}, \quad j = \begin{pmatrix} j_+ \\ j_- \end{pmatrix}, \quad D = \begin{pmatrix} D_{++} & D_{+-} \\ D_{-+} & D_{--} \end{pmatrix}. \quad (2.46)$$

In this notation, the integration forth and back along  $C_{\pm}$  can be replaced by an integration from  $-\infty$  to  $+\infty$  while defining a metric  $\text{diag}(1, -1)$  in order to incorporate the anti-chronological operator ordering on  $C_-$

$$\begin{aligned}
z[j_+, j_-] &= \exp \left[ -\frac{i}{2} \int d^4x d^4y \right. \\
&\quad \left. \begin{pmatrix} j_+(x) & j_-(x) \end{pmatrix} \begin{pmatrix} 1 & \\ & -1 \end{pmatrix} \begin{pmatrix} D_{++}(x-y) & D_{+-}(x-y) \\ D_{-+}(x-y) & D_{--}(x-y) \end{pmatrix} \begin{pmatrix} 1 & \\ & -1 \end{pmatrix} \begin{pmatrix} j_+(y) \\ j_-(y) \end{pmatrix} \right].
\end{aligned} \tag{2.47}$$

The four propagators that combine any two fields  $\phi_{\pm}$  can be calculated by substituting the respective step function (2.39) into (2.37). In momentum space, one finds

$$iD_{++}(p) = \left[ \frac{i}{p^2 - m^2 + i\epsilon} + 2\pi \delta(p^2 - m^2) f_B(|p^0|) \right], \tag{2.48a}$$

$$iD_{--}(p) = \left[ \frac{-i}{p^2 - m^2 - i\epsilon} + 2\pi \delta(p^2 - m^2) f_B(|p^0|) \right], \tag{2.48b}$$

$$iD_{+-}(p) = 2\pi \delta(p^2 - m^2) [\theta(-p^0) + f_B(|p^0|)], \tag{2.48c}$$

$$iD_{-+}(p) = 2\pi \delta(p^2 - m^2) [\theta(p^0) + f_B(|p^0|)]. \tag{2.48d}$$

These propagators decompose into non-thermal parts and thermal parts. The first term in  $D_{++}$  and  $D_{--}$  has the familiar form from zero temperature QFT describing the exchange of a virtual particle. The thermal part is proportional to the distribution of states in the thermal bath. It is also important to note that thermal parts are always put on-shell by a  $\delta$  - this describes the absorption or emission of a real particle from or into the heat bath.

## 2.5 Fermion Propagator

In principle, the fermion propagator can be obtained by retracing all the above steps for a fermionic theory with only minor adjustments. There is however also a quite elegant method that allows for the derivation of other propagators directly from the Klein-Gordon propagator. For the sake of introducing this method a general equation of motion is considered:

$$\Lambda_{\alpha\beta} \psi_{\beta} = 0. \tag{2.49}$$

Here,  $\Lambda$  is a differential operator and the Greek indices represent any internal degrees of freedom (e.g. Dirac indices). Now, if there exists a Klein-Gordon divisor  $d_{\alpha\beta}$  that completes the above differential operator in the sense of

$$\Lambda_{\alpha\beta} d_{\beta\gamma} = d_{\alpha\beta} \Lambda_{\beta\gamma} = -\delta_{\alpha\gamma} (\square + m^2), \tag{2.50}$$

then this divisor can be inserted into the differential equation (2.49) and one finds that  $\psi$  also solves the Klein-Gordon equation. Also, this implies that the propagator is just  $d_{\alpha\beta} D$ . A free fermionic theory is the ideal example for this method. The Lagrangian describing a single free fermion with mass  $m$  is given by

$$\mathcal{L} = \bar{\psi} (i\rlap{/}{\partial} - m) \psi. \quad (2.51)$$

For the differential operator  $i\rlap{/}{\partial} - m$  to be completed to a Klein-Gordon operator, the missing factor is

$$d = i\rlap{/}{\partial} + m. \quad (2.52)$$

Before writing down the fermion propagator, one needs to consider the anti-commuting nature of fermionic fields, as a consequence of which, the thermal averages of creation and annihilation operators lead to a different distribution function

$$f_F(\omega) = \frac{1}{e^{\beta\omega} + 1}. \quad (2.53)$$

While the bosonic distribution adhered to the periodic KMS boundary condition, the fermionic one leads to Green functions that are anti-periodic in imaginary time. In position space, the fermion propagator is found to be

$$iS(x-y) = (i\rlap{/}{\partial} + m) \int \frac{d^4p}{(2\pi)^4} \rho_0(p) e^{-ip(x-y)} [\theta_C(x^0 - y^0) - f_F(p^0)]. \quad (2.54)$$

As before, depending on the type of propagator, the step function  $\theta_C$  (2.39) corresponding to the four possible combinations of  $C_+$  and  $C_-$  is inserted into the integral. Then, in analogy to the scalar propagator one finds in momentum space

$$iS_{++}(p) = (\rlap{/}{p} + m) \left[ \frac{i}{p^2 - m^2 + i\epsilon} - 2\pi \delta(p^2 - m^2) f_F(|p^0|) \right], \quad (2.55a)$$

$$iS_{--}(p) = (\rlap{/}{p} + m) \left[ \frac{-i}{p^2 - m^2 - i\epsilon} - 2\pi \delta(p^2 - m^2) f_F(|p^0|) \right], \quad (2.55b)$$

$$iS_{+-}(p) = (\rlap{/}{p} + m) 2\pi \delta(p^2 - m^2) [\theta(-p^0) - f_F(|p^0|)], \quad (2.55c)$$

$$iS_{-+}(p) = (\rlap{/}{p} + m) 2\pi \delta(p^2 - m^2) [\theta(p^0) - f_F(|p^0|)]. \quad (2.55d)$$

These differ from (2.48a)–(2.48d) only in the additional Klein-Gordon divisor and the fermionic distribution function instead of the bosonic one.

## 2.6 Interactions

After having discussed bosonic and fermionic propagators, a short introduction on the treatment of vertices in the CTP formalism is in place. For that purpose, one may reconsider the generating functional in an interacting theory that was already given in (2.22) and apply the CTP doublet notation (2.46) to it:

$$Z[j_+, j_-] = \exp \left\{ i \int d^4x \left[ \mathcal{L}_I \left[ \frac{\delta}{i\delta j_+(x)} \right] - \mathcal{L}_I \left[ \frac{\delta}{i\delta j_-(x)} \right] \right] \right\} Z_0[j_+, j_-]. \quad (2.56)$$

Feynman rules for vertices can be read off directly from this expression. In general, it appears that one will always obtain two vertices from each interaction term in the Lagrangian - one for fields  $\phi_+$  and one for fields  $\phi_-$ . Vertices do not mix fields from different branches like the propagators. This is to be expected, because a vertex does always contain fields at one single point in space-time.

## 2.7 Gauge Theories

With the above formalism, Feynman rules for Yukawa-type interacting theories of bosons and fermions can be derived. An example for such a theory can be found e.g. in the Yukawa sector of the SM. On the other hand, the **G**lashow-**W**einberg-**S**alam (GWS) model of the electroweak interaction and the theory of the strong interaction - **Q**uantum **C**hromo **D**ynamics (QCD) - are so-called Yang-Mills theories [63] that are constructed around fundamental symmetry properties and comprise vector fields in addition to the scalars and fermions that have been considered in this work so far. For the sake of studying this kind of theory, a Lagrangian that is invariant under transformations of a  $SU(n)$  group shall be employed:

$$\mathcal{L} = -\frac{1}{4} F_{\mu\nu}^a F^{\mu\nu a} + \bar{\psi}^i i(\not{D}\psi)^i. \quad (2.57)$$

In the above Lagrangian, there are  $n^2 - 1$  vector fields  $A_\mu^a$ . The field strength of these fields is defined as

$$F_{\mu\nu}^a = \partial_\mu A_\nu^a - \partial_\nu A_\mu^a + f^{abc} A_\mu^b A_\nu^c. \quad (2.58)$$

Therein,  $f^{abc}$  are the completely antisymmetric structure constants of the symmetry group. For any representation of the group, the generators  $t^a$  of symmetry transformations satisfy the Lie-algebra

$$[t^a, t^b] = i f^{abc} t^c. \quad (2.59)$$

The matter fields  $\psi^i$ ,  $i = 1, \dots, N$  transform under a  $N$ -dimensional representation of the symmetry group according to

$$\delta_\epsilon \psi^i = i \epsilon^a (t^a)^{ij} \psi^j, \quad \delta_\epsilon \bar{\psi}^i = -i \bar{\psi}^j \epsilon^a (t^a)^{ji}, \quad (2.60)$$

where  $\epsilon^a$  is the infinitesimal parameter of the transformation. The important principle that leads to a theory of gauge interactions is the invariance under *local* transformations  $\epsilon^a = \epsilon^a(x)$ . Of course, this demand is much stronger than the invariance under global transformations and for

it to be realized, the matter fields must be coupled to the gauge fields such that the latter can compensate any change in the Lagrangian which may arise in a local transformation. This is done through the covariant derivative

$$(\mathbb{D}_\mu \psi)^i = \partial_\mu \psi^i - i(t^a)^{ij} A_\mu^a \psi^j. \quad (2.61)$$

Now, the transformation behavior of the gauge fields must be chosen such that the invariance under local transformations is established. One finds that the requirement is fulfilled for the  $A_\mu^a$  transforming according to the adjoint representation of the symmetry group, wherein the components of the generators are given by the structure constants themselves  $(T^a)^{bc} = -if^{abc}$ :

$$\delta_\epsilon A_\mu^a = (\mathbb{D}_\mu \epsilon)^a = \partial_\mu \epsilon^a + f^{abc} A_\mu^b \epsilon^c. \quad (2.62)$$

It is now easy to verify that the Lagrangian (2.57) is indeed invariant under local transformations.

In an attempt to write down a suitable path integral for the generating functional of this theory, one finds oneself confronted with an immediate problem: the coefficient matrix of the quadratic part of the Lagrangian is singular and as such, it is not possible to introduce a propagator as was done e.g. in (2.31). This may seem like a finishing blow for the concept of perturbation theory, but luckily there is a way to circumvent this issue. The key to obtaining a theory that is accessible by means of perturbation theory is the introduction of so called gauge fixing terms to the Lagrangian. These terms may be of any form, as long as they relieve the above issue of a singular coefficient matrix. This will come at the cost of breaking gauge invariance. Other global symmetries of the theory should be preserved by these terms, keeping as much as possible of the original theory intact. This approach may seem peculiar at first, but there is also a physical motivation to it: In a path integral formulation of the partition function, the integration measure over field configurations would contain all four components of each vector field  $\mathcal{D}A^a = \mathcal{D}A_0^a \mathcal{D}A_1^a \mathcal{D}A_2^a \mathcal{D}A_3^a$ . This means that each field is considered as four independent degrees of freedom in the path integral. In contrast to that, it is known from examples like the photon that a massless spin 1 particle has only two internal degrees of freedom: the two transverse components of the polarization vector. The two unphysical polarizations lead to divergences in the path integral [50] and the reason for this behavior is the gauge invariance of the theory. Gauge transformations create classes of equivalent field configurations. In a naive path integral, those equivalent field configurations are counted redundantly. In order to overcome this issue, it is therefore reasonable to break gauge invariance for the sake of a convergent path integral. A popular choice for such a modification of the Lagrangian in (2.57) is the covariant gauge

$$\mathcal{L}_{\text{GF}} = \partial^\mu F^a A_\mu^a + \frac{\xi}{2} F^a F^a, \quad (2.63)$$

where the field  $F^a$  is an auxiliary field variable, defined by the equation of motion

$$\xi F^a = \partial^\mu A_\mu^a. \quad (2.64)$$

Using the above identity, one could also formulate the gauge fixing Lagrangian as

$$\mathcal{L}_{\text{GF}} = -\frac{1}{2\xi} (\partial_\mu A^{a\mu})^2. \quad (2.65)$$

The parameter  $\xi$  may have any constant value. The most common choices are the Landau gauge  $\xi = 0$  and the Feynman gauge  $\xi = 1$ . Of course, once a theory is modified with a gauge fixing term, the parts that have been superficially added must be compensated for. Through the gauge fixing terms, the equivalence classes created by gauge invariance are eliminated, however the unphysical degrees of freedom are still counted in the path integral. Therefore, the next step is the introduction of new degrees of freedom that are designed to ultimately cancel the unphysical polarization modes: these “negative” degrees of freedom are the Faddeev-Popov ghosts [24]

$$\mathcal{L}_{\text{FP}} = -\int d^4y \bar{c}^a(x) \frac{\delta G^a(x)}{\delta A_\mu^b(y)} (D_\mu c(y))^b. \quad (2.66)$$

$c^a$  and  $\bar{c}^a$  are introduced as having spin zero while fulfilling anti-commutation relations. The gauge fixing condition is obtained from (2.64) as  $G^a = \partial^\mu A_\mu^a - \xi F^a = 0$ . Evaluating the functional derivative and performing a partial integration, one finds

$$\mathcal{L}_{\text{FP}} = \partial^\mu \bar{c}^a (D_\mu c)^a. \quad (2.67)$$

The total Lagrangian with gauge fixing and Faddeev-Popov ghosts now has the form

$$\mathcal{L} = -\frac{1}{4} F_{\mu\nu}^a F^{\mu\nu a} + \bar{\psi}^i i(\not{D}\psi)^i + \partial^\mu F^a A_\mu^a + \frac{\xi}{2} F^a F^a + \partial^\mu \bar{c}^a (D_\mu c)^a. \quad (2.68)$$

The claim that the gauge fixing and ghost terms compensate each other may not be obvious at the level of the Lagrangian. Therefore, it is instructive to study the residual symmetry of the theory, after the local invariance has been broken. Indeed, it is possible to find global symmetries in the modified Lagrangian which are reminiscent of the original invariance under local transformations. Specifically, one can show that the Lagrangian is invariant under the simultaneous transformations

$$\delta_\omega \psi^i = i\omega c^a (t^a)^{ij} \psi^j, \quad (2.69a)$$

$$\delta_\omega \bar{\psi}^i = i\omega \bar{\psi}^j c^a (t^a)^{ji}, \quad (2.69b)$$

$$\delta_\omega A_\mu^a = \omega (D_\mu c)^a, \quad (2.69c)$$

$$\delta_\omega c^a = -\frac{\omega}{2} f^{abc} c^b c^c, \quad (2.69d)$$

$$\delta_\omega \bar{c}^a = -\omega F^a, \quad (2.69e)$$

$$\delta_\omega F^a = 0, \quad (2.69f)$$

where  $\omega$  is a Grassmann-odd parameter of the global symmetry. These so called BRST transformations play an important role in the study of gauge theories. Note how the gauge fields still show the transformation behavior of the original gauge symmetry, but now with the local parameter  $\epsilon^a(x) = \omega c^a(x)$ . The important feature of this residual symmetry is the nilpotency of the transformations: a second variation of any field variable always vanishes as can be easily verified by looking at (2.69a)–(2.69f):

$$\delta_\omega^2 = 0. \quad (2.70)$$

This will be very important for proving that gauge fixing and ghost terms in the Lagrangian hold no physical implications. But first, it should be noted that another global symmetry exists in the ghost sector of the Lagrangian that will also become important later:

$$\delta_\theta c^a = \theta c^a, \quad (2.71a)$$

$$\delta_\theta \bar{c}^a = -\theta \bar{c}^a. \quad (2.71b)$$

The global parameter  $\theta$  of the transformation is Grassmann-even, acting as a scaling factor for the ghosts in the above transformations.

The ghosts as well as two components of each gauge field are unphysical degrees of freedom and it is clear that they cannot appear as external states for physical processes. In order to identify the physical states  $|\Psi\rangle \in \mathcal{V}'_{\text{phys.}}$ , one can exploit the nilpotency of the BRST transformation. For this purpose, it is instructive to consider the Noether currents of the BRST- and ghost scaling symmetry

$$J_{\text{BRST}}^{\mu a} = F^{\mu\nu a} (D_\nu c)^a + F^a (D^\mu c)^a - \frac{1}{2} f^{abc} \partial^\mu \bar{c}^a c^b c^c, \quad (2.72a)$$

$$J_{\text{ghost}}^\mu = \partial^\mu \bar{c}^a c^a - \bar{c}^a (D^\mu c)^a. \quad (2.72b)$$

The charges follow directly.

$$Q_{\text{BRST}} = \int d^3\vec{x} \left[ F^{0\nu a}(x) (D_\nu c(x))^a - \frac{1}{2} f^{abc} \dot{\bar{c}}^a(x) c^b(x) c^c(x) \right], \quad (2.73a)$$

$$Q_{\text{ghost}} = \int d^3\vec{x} \left[ \dot{\bar{c}}^a(x) c^a(x) - \bar{c}^a(x) (D^0 c(x))^a \right]. \quad (2.73b)$$

Using the fundamental (anti-) commutator relations for the fields and their conjugated momenta, one can show that

$$[c^a(x), Q_{\text{ghost}}] = -i c^a(x), \quad (2.74a)$$

$$[\bar{c}^a(x), Q_{\text{ghost}}] = i \bar{c}^a(x). \quad (2.74b)$$

This implies that the operator  $iQ_{\text{ghost}}$  acts as a ghost number operator, counting  $+1$  for every ghost  $c^a$  and  $-1$  for every anti-ghost  $\bar{c}^a$ . The BRST charge itself carries a unit ghost number as one might already read off directly from the definition in (2.73a) or by evaluating the commutator

$$[Q_{\text{BRST}}, Q_{\text{ghost}}] = -iQ_{\text{BRST}}. \quad (2.75)$$

With (2.74a), (2.74b) and (2.75),  $Q_{\text{BRST}}$  and  $Q_{\text{ghost}}$  appear as suitable operators for the selection of physical states. Conditions for a physical state are

$$Q_{\text{BRST}}|\Psi\rangle = 0, \quad (2.76a)$$

$$Q_{\text{ghost}}|\Psi\rangle = 0. \quad (2.76b)$$

Looking at the transformations (2.69c)–(2.69f), it is possible to write the gauge fixing and ghost terms in the Lagrangian as a BRST variation

$$\mathcal{L}_{\text{GF}} + \mathcal{L}_{\text{FP}} = \left\{ Q_{\text{BRST}}, -\partial^\mu \bar{c}^a A_\mu^a - \frac{\xi}{2} \bar{c}^a F^a \right\} \quad (2.77)$$

and due to the criteria for physical states, this implies

$$\langle \Psi' | \mathcal{L}_{\text{GF}} + \mathcal{L}_{\text{FP}} | \Psi \rangle = 0 \quad (2.78)$$

for arbitrary physical states  $|\Psi\rangle, |\Psi'\rangle \in \mathcal{V}'_{\text{phys}}$ . This is the formal proof that the modifications of the Lagrangian hold no physical implications.

The physical states that are selected by the above criteria can be used for a consistent ansatz for the partition function. For this purpose, projection operators  $P_n$  that project onto the subspace with  $n$  ghosts are defined. Obviously, these projectors form a complete orthonormal set

$$\sum_{n=0}^{\infty} P_n = \mathbb{1}, \quad (2.79a)$$

$$P_n P_m = \delta_{nm} P_n. \quad (2.79b)$$

$P_0$  projects out the physical part of a state, that is, it can be used in order to define a trace over only physical states

$$\mathcal{Z} = \text{tr}[P_0 e^{-\beta H}]. \quad (2.80)$$

But still, using this partition function for the definition of a generating functional, one will encounter a problem in the context of BRST invariance when writing down a path integral. At

this point, the BRST symmetry has already proven of great importance to the concept of gauge theories. But in a path integral, the question for the boundary conditions for ghosts arises: Should they obey the periodic or the anti-periodic KMS relation? They are introduced as spin 0 fields, so in analogy to scalars, one could be tempted to argue for symmetric boundary conditions. But on the other hand, they are also anti-commuting degrees of freedom which in the case of spin 1/2 fermions lead to anti-periodic Green functions. However, looking at the infinitesimal BRST transformations in (2.69a)–(2.69e), it becomes clear that the latter leads to inconsistencies: antisymmetric fields obtain symmetric parts in a BRST transformation. Does this mean that BRST invariance is broken at finite temperature? Fortunately, this is not the case, because the above issue is merely a problem with the definition of the partition function. This can be illustrated on a simplified example.

Let  $\mathcal{H}$  be a two-dimensional Hilbert space with the fermionic basis  $|0\rangle$  and  $|1\rangle$ . The previously introduced Grassmann variables can then be used in order to define fermionic coherent states

$$|\psi\rangle = e^{-\psi a^\dagger} |0\rangle = |0\rangle - \psi |1\rangle, \quad (2.81a)$$

$$\langle\psi| = \langle 0| e^{-\bar{\psi} a} = \langle 0| + \bar{\psi} \langle 1|. \quad (2.81b)$$

Here,  $\psi, \bar{\psi}$  is a pair of conjugated Grassmann-odd parameters that anticommutes with fermionic operators of the theory such as  $a$  and  $a^\dagger$ . This property gives rise to the relative sign in (2.81a) and (2.81b). The coherent states provide an alternative complete basis with the completeness relation

$$\begin{aligned} \int d\bar{\psi} d\psi e^{-\bar{\psi}\psi} |\psi\rangle\langle\psi| &= \int d\bar{\psi} d\psi (1 - \bar{\psi}\psi) (|0\rangle\langle 0| - \psi |1\rangle\langle 0| + \bar{\psi} |0\rangle\langle 1| - \bar{\psi}\psi |1\rangle\langle 1|) \\ &= \mathbb{1}. \end{aligned} \quad (2.82)$$

Inserting this into the trace over a bosonic operator  $\mathcal{B}$  - like e.g. the exponential  $e^{-\beta H}$  - one then finds

$$\begin{aligned} \text{tr}[\mathcal{B}] &= \text{tr} \left[ \int d\bar{\psi} d\psi e^{-\bar{\psi}\psi} |\psi\rangle\langle\psi| \mathcal{B} \right] \\ &= \int d\bar{\psi} d\psi e^{-\bar{\psi}\psi} (\langle\psi| \mathcal{B} |0\rangle + \psi \langle\psi| \mathcal{B} |1\rangle) \\ &= \int d\bar{\psi} d\psi e^{-\bar{\psi}\psi} \langle\psi| \mathcal{B} | - \psi\rangle. \end{aligned} \quad (2.83)$$

This is the antisymmetric KMS boundary condition for fermionic fields in the path integral formulation of the generating functional shown explicitly in this simplified example of a two-dimensional Hilbert space. In the case of a gauge theory, it is this very property that leads to problems with ghosts and BRST invariance. The key to alleviating this problem can be found in the already introduced limitation to physical states in the trace over Fock space. In the simplified

example above, the sign in the coherent state is determined by the sign in front of the  $|1\rangle$  state in (2.81a). However, in the partition function, this part is projected out of the trace anyway. A trick can be used to exploit this: A ghost number operator will leave the physical states unaltered, but flips the sign in a coherent state

$$e^{-i\pi N} |\psi\rangle = (1 - 2N)(|0\rangle - \psi|1\rangle) = |0\rangle + \psi|1\rangle = |-\psi\rangle. \quad (2.84)$$

In the first step, the idempotency of the fermion number operator  $N^2 = N$  was used in order to simplify the exponential series. Obviously, the presence of such a number operator in the trace (2.83) leads to periodic boundary conditions for the fermion modes it applies to. This is exactly what is needed for the consistency of ghost fields in a path integral with BRST symmetry. In analogy to the discussion of this simplified example, a ghost number operator  $iQ_{\text{ghost}}$  is inserted into (2.80), leading to

$$\mathcal{Z} = \text{tr} [P_0 e^{\pi Q_{\text{ghost}}} e^{-\beta H}]. \quad (2.85)$$

In order to obtain the propagator for the gauge fields, the free limit for the Lagrangian with gauge fixing and ghosts can be considered. In the covariant gauge, one finds

$$\begin{aligned} \mathcal{L} &= -\frac{1}{4} F_{\mu\nu}^a F^{\mu\nu a} - \frac{1}{2\xi} (\partial^\mu A_\mu^a)^2 + \bar{\psi}^i i \not{\partial} \psi^i + \partial^\mu \bar{c}^a \partial_\mu c^a \\ &= \frac{1}{2} A_\mu^a \left[ g^{\mu\nu} \square - \left(1 - \frac{1}{\xi}\right) \partial^\mu \partial^\nu \right] A_\nu^a + \bar{\psi}^i i \not{\partial} \psi^i - \bar{c}^a \square c^a. \end{aligned} \quad (2.86)$$

Following the same approach that was already used for the fermion propagator, a Klein-Gordon divisor can be found for the differential operator

$$d^{\mu\nu ab}(i\partial) = \delta^{ab} \left[ -g^{\mu\nu} + (1 - \xi) \frac{\partial^\mu \partial^\nu}{\square} \right] \quad (2.87)$$

and the four propagators in the CTP formalism are instantly found to be

$$iD_{++}^{\mu\nu ab}(p) = \delta^{ab} \left[ -g^{\mu\nu} + (1 - \xi) \frac{p^\mu p^\nu}{p^2} \right] \left[ \frac{i}{p^2 + i\epsilon} + 2\pi \delta(p^2) f_B(|p^0|) \right], \quad (2.88a)$$

$$iD_{--}^{\mu\nu ab}(p) = \delta^{ab} \left[ -g^{\mu\nu} + (1 - \xi) \frac{p^\mu p^\nu}{p^2} \right] \left[ \frac{-i}{p^2 - i\epsilon} + 2\pi \delta(p^2) f_B(|p^0|) \right], \quad (2.88b)$$

$$iD_{+-}^{\mu\nu ab}(p) = \delta^{ab} \left[ -g^{\mu\nu} + (1 - \xi) \frac{p^\mu p^\nu}{p^2} \right] 2\pi \delta(p^2) [\theta(-p^0) + f_B(|p^0|)], \quad (2.88c)$$

$$iD_{-+}^{\mu\nu ab}(p) = \delta^{ab} \left[ -g^{\mu\nu} + (1 - \xi) \frac{p^\mu p^\nu}{p^2} \right] 2\pi \delta(p^2) [\theta(p^0) + f_B(|p^0|)]. \quad (2.88d)$$

For calculations, the explicit choice  $\xi = 1$  for the gauge will be adopted. Ghost propagators will not be needed for the upcoming discussions, so they are not given here. However, they can of

## 2 *Thermal Quantum Field Theory*

course be derived from the above Lagrangian in the usual way, using the bosonic distribution function in order to satisfy the periodic boundary condition.

# 3

## The $\nu$ MSM

One of the questions the SM leaves unanswered is: "Why is there more matter than antimatter in the universe?". It was already addressed briefly in Chapter 1, how the baryon over photon ratio inferred from observations like the Planck mission is greatly underestimated by calculations based on the SM. Therefore, extensions of the SM are very interesting to cosmology as a source for additional  $CP$  violation. One model with the ability to provide this is the  $\nu$ MSM - the Neutrino Minimal Standard Model. In the following, the electroweak sector of the SM will be reviewed, followed by an introduction to its extension with right-handed neutrinos. The further is necessary, because leptons, gauge bosons of the electroweak interaction and the Higgs play a role in thermal reactions of the neutrinos and also for the sake of fixing notation. For the latter, the coupling between neutrinos and the SM will be discussed, as well as the parameter space of the model and Majorana properties of the new fields.

### 3.1 Standard Model of electroweak Interactions

Since the discovery of the Higgs in 2012 [19], the Standard Model is considered complete. The electroweak sector contains two out of three interactions, described within a  $SU(2)_L \otimes U(1)_Y$  gauge group. The first subscript  $L$  denotes the breaking of the chiral symmetry by weak interactions: The gauge bosons  $W_\mu^a$  associated with this group only couple to the left-chiral projections of matter fields, but not to the right-handed parts. The charge carried by fields that are subject to this interaction is the weak isospin  $I$ . The second gauge group is abelian with one gauge field  $B_\mu$  and hypercharge  $Y$  - as implied by the subscript in the group.

The electroweak Lagrangian can be partitioned into four pieces: the gauge Lagrangian  $\mathcal{L}_{\text{gauge}}$ , containing the kinetic terms for the gauge fields, the Yang-Mills sector  $\mathcal{L}_{\text{YM}}$  with the kinetic terms for the fermionic matter fields, including gauge couplings in the covariant derivatives, the Higgs sector  $\mathcal{L}_{\text{Higgs}}$ , introducing kinetic terms and self interactions of the Higgs field and finally the Yukawa sector  $\mathcal{L}_{\text{Yukawa}}$  with the couplings between fermions and the Higgs. These four pieces will be discussed one after another in the following.

### 3 The $\nu$ MSM

The gauge sector is given by the two terms

$$\mathcal{L}_{\text{gauge}} = -\frac{1}{4} W_{\mu\nu}^a W^{a\mu\nu} - \frac{1}{4} B_{\mu\nu} B^{\mu\nu}, \quad (3.1)$$

where  $W_{\mu\nu}^a = \partial_\mu W_\nu^a - \partial_\nu W_\mu^a - g_L \varepsilon^{abc} W_\mu^b W_\nu^c$  and  $B_{\mu\nu} = \partial_\mu B_\nu - \partial_\nu B_\mu$  are the field strengths of the gauge fields  $W_\mu^a$  and  $B_\mu$ . The third term in  $W_{\mu\nu}^a$  appears due to the non-abelian algebra of the gauge group  $SU(2)_L$  with  $g_L$  as the corresponding coupling.

Next is the Yang-Mills sector

$$\mathcal{L}_{\text{YM}} = i\bar{q}_{iL} \not{D} q_{iL} + i\bar{d}_{iR} \not{D} d_{iR} + i\bar{u}_{iR} \not{D} u_{iR} + i\bar{\ell}_{iL} \not{D} \ell_{iL} + i\bar{e}_{iR} \not{D} e_{iR}, \quad (3.2)$$

with the covariant derivative

$$D_\mu f_L = \left( \partial_\mu - i g_L \tau^a W_\mu^a - i g_Y \frac{Y}{2} B_\mu \right) f_L, \quad (3.3a)$$

$$D_\mu f_R = \left( \partial_\mu - i g_Y \frac{Y}{2} B_\mu \right) f_R. \quad (3.3b)$$

The matrices  $\tau^a = \sigma^a/2$  are the generators of the  $SU(2)_L$  that are normalized according to

$$\text{tr}[\tau^a \tau^b] = \frac{1}{2} \delta^{ab} \mathbb{1}. \quad (3.4)$$

$g_Y$  is the coupling of the U(1) interaction. Left-handed fields are organized in a doublet structure with weak isospin  $I = 1/2$  and the three component  $I_3 = \pm 1/2$ .  $q_i$  are the quark doublets with up-type  $u_i$  and down-type  $d_i$ ,  $i = 1, 2, 3$  for the three quark families. They carry the hypercharge  $Y = 1/3$ .  $\ell_i$  are the three lepton families with  $I = 1/2$  and  $Y = -1$ :

$$q_{iL} = \begin{pmatrix} u_i \\ d_i \end{pmatrix}_L, \quad \begin{aligned} \{u_i\} &= \{u, c, t\} \\ \{d_i\} &= \{d, s, b\} \end{aligned} \quad (3.5a)$$

$$\ell_{iL} = \begin{pmatrix} \nu_i \\ e_i \end{pmatrix}_L, \quad \begin{aligned} \{e_i\} &= \{e, \mu, \tau\} \\ \{\nu_i\} &= \{\nu_e, \nu_\mu, \nu_\tau\} \end{aligned} \quad (3.5b)$$

The right-handed fields are singlets in the  $SU(2)_L$  with  $I = 0$ . Note that there is no right-handed neutrino in the SM because it would also have no hypercharge  $Y = 0$  and therefore no gauge interactions at all.

The Higgs sector introduces the Higgs field  $\Phi$  as a  $SU(2)_L$  doublet with  $I = 1/2$  and hypercharge  $Y = 1$

$$\mathcal{L}_{\text{Higgs}} = (\mathbb{D}_\mu \Phi)^\dagger \mathbb{D}^\mu \Phi - \mu^2 \Phi^\dagger \Phi - \lambda (\Phi^\dagger \Phi)^2, \quad (3.6)$$

with

$$\Phi = \begin{pmatrix} \phi^+ \\ \phi^0 \end{pmatrix}. \quad (3.7)$$

The covariant derivative is the same as for the left-handed fermions in (3.3a) with the proper hypercharge substituted.  $\mu^2$  could be interpreted as a mass squared term in a scalar theory, however, in the SM, this parameter is chosen negative such that  $\Phi$  develops a non-zero vacuum expectation value (VEV).  $\lambda$  is the coupling of the quartic self-interaction.

In the cold theory, the Higgs VEV is used to generate mass terms for all matter fields in the SM except the neutrinos. This is achieved via couplings between the fields in question and the  $\phi^0$  component that generates the VEV in the Yukawa sector

$$\mathcal{L}_{\text{Yukawa}} = -\bar{q}_{iL} (h_d)_{ij} \Phi d_{jR} - \bar{q}_{iL} (h_u)_{ij} \tilde{\Phi} u_{jR} - \bar{\ell}_{iL} (h_\ell)_{ij} \Phi e_{jR}. \quad (3.8)$$

Above,  $h_d, h_u$  and  $h_\ell$  are the Yukawa coupling matrices. Writing the fermion fields as mass eigenstates, the Yukawa couplings are real and diagonal. This procedure requires different unitary transformations of left- and right-handed fields, which leads to flavor changing charged currents in the interactions of quarks. Their mixing is quantified in the CKM mixing matrix which also holds one  $CP$  violating complex phase. This is the only source of  $CP$  violation within the SM.  $\tilde{\Phi}$  is the isospin conjugated Higgs field which, in the case of the  $SU(2)$ , happens to transform in the same way as the original doublet so that gauge invariance of the Lagrangian is guaranteed:

$$\tilde{\Phi} = i\sigma^2 \Phi^\dagger = \begin{pmatrix} \phi^{0*} \\ -\phi^- \end{pmatrix}. \quad (3.9)$$

Coming back to the case of right-handed neutrinos, it was noted above that the right chiral part of such a field would neither carry a weak isospin nor a hypercharge. Thus, these fields are not forbidden in any way but simply would not participate in any gauge interactions of the theory. However, there is still the possibility of a Yukawa coupling to the isospin conjugate Higgs in analogy to the right-handed up-type quarks. This motivates the extension of the SM which will be considered in the next section.

## 3.2 Extension with right-handed Neutrinos

### 3.2.1 Lagrangian and Parametrization

An arbitrary number of right-handed neutrinos  $N_{IR}$ ,  $I = 1, 2, \dots, n$  can be added to the spectrum of the SM in a straight forward way. The additional neutrino sector Lagrangian then incorporates the

### 3 The $\nu$ MSM

kinetic terms for the new fields, as well as the Yukawa coupling  $h_N$ . Furthermore, as right-handed neutrinos do not carry any charge in this minimal model, there is the possibility to add a Majorana mass term  $M_M$  to the Lagrangian as well [62]:

$$\begin{aligned} \mathcal{L}_{\text{Neutrino}} = & i \bar{N}_{IR} \not{\partial} N_{IR} - \bar{\ell}_{iL} \tilde{\Phi} (h_N)_{iI} N_{IR} - \bar{N}_{IR} (h^\dagger)_{iI} \tilde{\Phi}^\dagger \ell_{iL} \\ & - \frac{1}{2} \left[ \bar{N}_{IR}^C (M_M)_{IJ} N_{JR} + \bar{N}_{IR} (M_M^\dagger)_{IJ} N_{JR}^C \right]. \end{aligned} \quad (3.10)$$

The superscript  $C$  herein denotes charge conjugation  $N_{IR}^C = -\gamma^0 C N_{IR}^*$ . By construction, the right chiral field  $N_{IR}$  can be obtained from the Majorana field

$$N_I = N_{IR} + N_{IR}^C, \quad (3.11)$$

which then satisfies the relation  $N_I^C = N_I$ . The coupling  $h_N$  is a  $3 \times n$  complex matrix that can be parametrized by  $6n$  real numbers. The Majorana mass matrix  $M_M$  on the other hand is a  $n \times n$  matrix in neutrino generation space. The  $N_I$  can always be chosen such that  $M_M$  is real and diagonal. In this case, only  $n$  more parameters are needed to characterize the mass spectrum of the  $\nu$ MSM. With this, the basis of the right-handed neutrinos has been fixed. However, one can still absorb three complex phases in the Yukawas  $h_N$  into the SM-lepton fields  $\ell_{iL}$ . In total, the  $\nu$ MSM requires  $7n - 3$  real numbers to be completely parametrized.

In [7], it was estimated that at least three generations of right-handed neutrinos are needed cosmologically, in order for the  $\nu$ MSM to simultaneously explain the baryon asymmetry of the universe (BAU), neutrino oscillations and dark matter. Numerical studies in [16] can support this claim. In light of these studies, it seems plausible to adopt the choice of  $n = 3$  generations of right-handed neutrinos. In this scenario, 18 parameters in addition to the bar code of the SM are needed to characterize the  $\nu$ MSM. A sensible arrangement for 15 of those numbers to parametrize the  $3 \times 3$  complex Yukawa coupling matrix can be obtained from the singular value decomposition theorem [28]

$$h_N = U_L h_{\text{diag}} U_R^\dagger, \quad (3.12)$$

where  $U_{L/R}$  are unitary matrices and  $h_{\text{diag}} = \text{diag}(h_1, h_2, h_3)$  with 3 real entries  $h_i$ . The left and right unitary matrices can be understood as complex rotations in three dimensions, i.e. [8]

$$\begin{aligned} U_L = & \begin{pmatrix} 1 & 0 & 0 \\ 0 & \cos \theta_{L23} & \sin \theta_{L23} \\ 0 & -\sin \theta_{L23} & \cos \theta_{L23} \end{pmatrix} \begin{pmatrix} \cos \theta_{L13} & 0 & \sin \theta_{L13} e^{-i\delta_L} \\ 0 & 1 & 0 \\ -\sin \theta_{L13} e^{i\delta_L} & 0 & \cos \theta_{L13} \end{pmatrix} \\ & \begin{pmatrix} \cos \theta_{L12} & \sin \theta_{L12} & 0 \\ -\sin \theta_{L12} & \cos \theta_{L12} & 0 \\ 0 & 0 & 1 \end{pmatrix} \begin{pmatrix} e^{i\alpha_1} & 0 & 0 \\ 0 & e^{i\alpha_2} & 0 \\ 0 & 0 & 1 \end{pmatrix}, \end{aligned} \quad (3.13a)$$

$$U_R^\dagger = \begin{pmatrix} \cos \theta_{R12} & -\sin \theta_{R12} & 0 \\ \sin \theta_{R12} & \cos \theta_{R12} & 0 \\ 0 & 0 & 1 \end{pmatrix} \begin{pmatrix} \cos \theta_{R13} & 0 & -\sin \theta_{R13} e^{-i\delta_R} \\ 0 & 1 & 0 \\ \sin \theta_{R13} e^{i\delta_R} & 0 & \cos \theta_{R13} \end{pmatrix} \\
 \begin{pmatrix} 1 & 0 & 0 \\ 0 & \cos \theta_{R23} & -\sin \theta_{R23} \\ 0 & \sin \theta_{R23} & \cos \theta_{R23} \end{pmatrix} \begin{pmatrix} e^{i\beta_1} & 0 & 0 \\ 0 & e^{i\beta_2} & 0 \\ 0 & 0 & 1 \end{pmatrix}. \quad (3.13b)$$

$\theta_{L/Rij}$  are 6 mixing angles. Furthermore, with  $\delta_{L/R}$ ,  $\alpha_i$  and  $\beta_i$  there exist 6 additional CP violating phases. The last three missing parameters are the Majorana masses in the diagonal mass matrix

$$M_M = \text{diag}(M_1, M_2, M_3). \quad (3.14)$$

The decays of right-handed neutrinos violate lepton number and therefore, their mass scale is often considered as being large, e.g.  $M_i \sim 10^7$  GeV in [44]. However, recent works also focus on lighter Majorana masses at the electroweak scale. These scenarios require smaller Yukawa couplings and a nearly degenerate mass spectrum in order to resonantly enhance CP-violating decays in the early universe without spoiling SM predictions and still accounting for the current bounds on active neutrino masses [51].

In the cold universe of today, the Yukawa coupling to the Higgs creates a Dirac mass term for the neutrinos as a consequence of the non-vanishing VEV after the electroweak symmetry breaking at  $T_{EW} \sim 100$  GeV [38]:

$$\langle \tilde{\Phi} \rangle = \begin{pmatrix} \nu \\ 0 \end{pmatrix}, \quad (3.15)$$

where  $\nu = 174$  GeV [12]. The Dirac mass term  $M_D = \nu h$  then mixes left- and right-handed neutrinos with each other

$$\mathcal{L}_{\text{Neutrino}}|_{T \ll T_{EW}} = i \bar{N}_{IR} \not{\partial} N_{IR} - \bar{\nu}_{iL} (M_D)_{iI} N_{IR} - \bar{N}_{IR} (M_D^\dagger)_{iI} \nu_{iL} \\
 - \frac{1}{2} \left[ \bar{N}_{IR}^C (M_M)_{IJ} N_{JR} + \bar{N}_{IR} (M_M^\dagger)_{IJ} N_{JR}^C \right]. \quad (3.16)$$

In order to illustrate the mixing between left- and right-handed neutrinos even better, Dirac- and Majorana mass terms are often assembled into a matrix scheme [44]

$$\mathcal{L}_{\nu\text{MSM}}|_{T \ll T_{EW}} = \dots - \frac{1}{2} \left[ \begin{pmatrix} \bar{\nu}_L & \bar{N}_R^C \end{pmatrix} \begin{pmatrix} 0 & M_D \\ M_D^T & M_M \end{pmatrix} \begin{pmatrix} \nu_L^C \\ N_R \end{pmatrix} + \begin{pmatrix} \bar{\nu}_L^C & \bar{N}_R \end{pmatrix} \begin{pmatrix} 0 & M_D^* \\ M_D^\dagger & M_M^\dagger \end{pmatrix} \begin{pmatrix} \nu_L \\ N_R^C \end{pmatrix} \right]. \quad (3.17)$$

The generation indices  $i, I$  have been dropped in the above formula for the sake of an easier

### 3 The $\nu$ MSM

notation. There exist two sets of mass eigenstates  $\nu'_L$  and  $N'_R$  that are obtained by diagonalizing the above mass matrix

$$\begin{pmatrix} \nu'^C_L \\ N'^C_R \end{pmatrix} = \mathcal{U} \begin{pmatrix} \nu^C_L \\ N_R \end{pmatrix}, \quad \begin{pmatrix} \nu'_L \\ N'_R \end{pmatrix} = \mathcal{U}^* \begin{pmatrix} \nu_L \\ N^C_R \end{pmatrix}. \quad (3.18)$$

These new fields are the chiral components of Majorana fields  $\nu' = \nu'^C$  and  $N' = N'^C$ . Therefore, the respective other chiral component is fixed by the Majorana condition  $\nu'_R = \nu'^C_L$  and  $N'_L = N'^C_R$ . The mass eigenstates are referred to as active and sterile neutrinos respectively.

An ansatz for the transformation matrix can be found by considering first the simpler case of only one left- and one right-handed neutrino. In this toy model, the entries in the mass matrix are scalar expressions  $m_D, m_M$  and the matrix itself can be easily diagonalized by means of a two-dimensional rotation matrix. The corresponding rotation angle is given up to second order in the Yukawas by  $\theta = m_D/m_M + O(m_D^3/m_M^3)$ . Accordingly, the mass matrix in the multi-generation case is diagonalized in two steps: First, a rotation to a block-diagonal form is applied with  $\theta$  defined as [16]

$$\theta = M_D M_M^{-1} \quad (3.19)$$

in correspondence to the single generation case. Here, the mixing between active and sterile neutrinos is revealed to be fixed by the ratio of Dirac masses over Majorana Masses. In a second step, unitary transformations  $U_\nu$  and  $U_N$  diagonalize the block entries. The composite transformation is given up to second order in the Yukawas by

$$\mathcal{U} = \begin{pmatrix} U_\nu & 0 \\ 0 & U_N \end{pmatrix} \begin{pmatrix} \mathbb{1} - \frac{1}{2} \theta^* \theta^T & -\theta^* \\ \theta^T & \mathbb{1} - \frac{1}{2} \theta^* \theta^T \end{pmatrix}. \quad (3.20)$$

Substituting (3.20) into (3.18) then results in

$$\nu'_L = U_\nu \left[ \left( \mathbb{1} - \frac{1}{2} \theta \theta^\dagger \right) \nu_L - \theta N^C_R \right], \quad (3.21a)$$

$$N'_R = U_N \left[ \left( \mathbb{1} - \frac{1}{2} \theta^* \theta^T \right) N_R + \theta^T \nu^C_L \right]. \quad (3.21b)$$

As was already laid out above,  $\theta$  is usually small, either due to large Majorana masses or small Yukawas, such that the active neutrinos  $\nu'$  are mostly constituted by the left-handed neutrinos and the sterile neutrinos  $N'$  contain predominantly the right-handed ones. Both, active and sterile states do have masses as can be seen by performing the first rotation with (3.19). Consistently keeping only the terms up to second order in  $h_N$ , one can write the block-diagonal entries of the mass matrix as

$$M_\nu = -\theta M_M \theta^T, \quad (3.22a)$$

$$M_N = M_M + \frac{1}{2} (\theta^\dagger \theta M_M + M_M^T \theta^T \theta^*). \quad (3.22b)$$

At this point, it becomes clear how this so-called Seesaw formalism for the generation of neutrino masses generates light active neutrinos with masses  $M_\nu = O(M_D^2/M_M)$  and heavy sterile neutrinos with  $M_N = O(M_M)$  at leading order. For reference, the Planck collaboration has inferred an upper limit for the sum of active neutrino masses from their measurements of the CMB of  $\sum_j m_j < 0.66 \text{ eV}$  at 95% confidence level [3]. On the other hand, in [15] an emission line in the stacked X-ray spectrum of galaxy clusters was reported at  $> 3\sigma$  that can be interpreted as the signature of sterile neutrino decay at the mass of 7.1 keV. This observation falls within the allowed region in parameter space and is also consistent with resonant leptogenesis scenarios if one assumes the two other generations to have nearly degenerate masses of order 1...10 GeV [16]. In a rough approximation, neglecting the mixing angles, one Yukawa can be estimated to be of order  $10^{-11}$  and the others  $10^{-7}$ .

### 3.2.2 Majorana Properties

In the era before the electroweak symmetry breaking, the Majorana fields  $N_i$  are mass eigenstates themselves. The Majorana condition holds some implications for the calculation of Feynman diagrams that shall be investigated in the following.

For studying the properties of Majorana fields, it may be instructive to start with a free fermionic toy model

$$\mathcal{L} = \bar{\psi} (i\cancel{\partial} - m) \psi \quad (3.23)$$

and use the Majorana representation for the Dirac matrices appearing in the Feynman dagger  $\cancel{\partial} = \tilde{\gamma}^\mu \partial_\mu$  which is special in that all Dirac matrices are purely imaginary  $\tilde{\gamma}^{\mu*} = -\tilde{\gamma}^\mu$ :

$$\begin{aligned} \tilde{\gamma}^0 &= \begin{pmatrix} 0 & \sigma^2 \\ \sigma^2 & 0 \end{pmatrix}, & \tilde{\gamma}^1 &= \begin{pmatrix} i\sigma^1 & 0 \\ 0 & i\sigma^1 \end{pmatrix}, \\ \tilde{\gamma}^2 &= \begin{pmatrix} 0 & \sigma^2 \\ -\sigma^2 & 0 \end{pmatrix}, & \tilde{\gamma}^3 &= \begin{pmatrix} i\sigma^3 & 0 \\ 0 & i\sigma^3 \end{pmatrix}. \end{aligned} \quad (3.24)$$

Thus, the Dirac equation is real and one can find purely real solutions  $\tilde{\psi}^* = \tilde{\psi}$  to it. These solutions represent the Majorana fermions. At this point, the question arises as to how this condition translates into arbitrary representations of the Dirac matrices. Using the theorem that states that all equivalent representations of Dirac matrices are connected by a unitary similarity transformation  $U$ , one obtains

$$\gamma^\mu = U \tilde{\gamma}^\mu U^\dagger. \quad (3.25)$$

### 3 The $\nu$ MSM

Then, the Majorana condition translates into the arbitrary representation as

$$U U^T \psi^* = \psi. \quad (3.26)$$

The customary form of this condition that was already given in the previous section for the Majorana neutrino fields uses a definition of the unitary matrix  $C$

$$-\gamma^0 C = U U^T. \quad (3.27)$$

The Majorana condition  $\psi^C = -\gamma^0 C \psi^* = \psi$  then consequently leads to new non-vanishing pairings of field operators in two-point functions:

$$\langle \mathcal{T}_C \psi(x) \psi^T(y) \rangle = \text{---} \text{---} \text{---} = \langle \mathcal{T}_C \psi(x) \bar{\psi}(y) \rangle C^T, \quad (3.28a)$$

$$\langle \mathcal{T}_C \bar{\psi}^T(x) \bar{\psi}(y) \rangle = \text{---} \text{---} \text{---} = C^\dagger \langle \mathcal{T}_C \psi(x) \bar{\psi}(y) \rangle. \quad (3.28b)$$

Thus, these new Majorana propagators differ from the usual fermion propagators only by the matrix  $C^T$  or  $C^\dagger$ . Knowing that these two-point functions exist will be of great importance when the self-energies of the right-handed neutrinos are calculated.

# 4

## Self-Energies

Green functions are the dynamic quantities that encode all information of a theory. The following discussion will revolve around two-point functions in the  $\nu$ MSM at finite temperature. These objects are invaluable to many cosmological questions - including leptogenesis - as one can e.g. extract decay- and oscillation rates from them.

### 4.1 Dressed Propagators

In the era before the electroweak phase transition  $T > T_{EW}$ , thermal corrections to the Higgs potential lead to a symmetric vacuum state [38]. Without the non-vanishing vacuum expectation value of the Higgs field, leptons, quarks and gauge bosons are massless. While the Higgs itself is still massive and the right-handed neutrinos still have Majorana masses, these can be neglected in resonant leptogenesis scenarios because the energy scale is given by the temperature  $T \gg M_I$ . Through this reasoning, one might be tempted to consider all degrees of freedom in the early universe to be massless. However, it is a well established fact that at high temperature, thermal effects shift the poles of propagators when considering radiative corrections [23, 61] and therefore alter the dispersion relations of fields that interact with the thermal plasma. This effect becomes visible in the *dressed* propagators one obtains from the resummation in the Dyson series. The need for the resummation as proposed by Braaten and Pisarski [14] arises from infrared divergences in thermal self energies. When calculating the same self energies with resummed propagators, the presence of thermal masses cures this issue. Considering hot gauge theories, the situation becomes even more dramatic as matrix elements from bare propagators depend on the gauge chosen [14]. The reason for this peculiar behavior can be found in perturbation theory: At zero temperature, one is used to calculate diagrams up to a fixed order of vertices. However, in a thermal theory, diagrams with any number of vertices contribute already at leading order in the coupling constants. The application of dressed propagators to the calculation of Green functions bears a rich phenomenology. Thermal effects in leptogenesis have been considered by many authors [6, 4, 11, 10, 20, 26, 27], however, dressed propagators are often approximated by inserting thermal masses by hand into the bare propagators. This treatment is indeed exact

for scalar propagators but may be questionable in the case of fermions.

The ultimate goal of this chapter is the computation of the right-handed neutrino self energies. At leading order, these do only couple to the left-handed SM leptons as well as the Higgs, so in the following, the resummed propagators for these fields will be derived. The resummed propagator is defined via the Dyson series that can be diagrammatically represented as

$$\begin{aligned}
 \text{---} \bullet \text{---} &= \text{---} + \text{---} \circ \text{---} + \text{---} \circ \circ \text{---} + \dots \\
 &= \text{---} + \text{---} \bullet \text{---} .
 \end{aligned} \tag{4.1}$$

The line with the filled blob on the left hand side denotes the dressed propagator, the lines on the right hand side are bare propagators and empty blobs are bare self energies. In the second step, the series was factorized, leading to a recursive definition of the dressed propagator. Writing the above relation explicitly in terms of bare propagators  $iD$  and self-energies  $-i\Pi$ , one can solve for the dressed propagator  $iD^*$ :

$$\begin{aligned}
 iD^* &= iD + iD(-i\Pi)iD + \dots = iD + iD\Pi D^* \\
 \Leftrightarrow iD^* &= \frac{i}{D^{-1} - \Pi}.
 \end{aligned} \tag{4.2}$$

This resummation technique for thermal propagators was originally developed in the ITF [14], where the propagators do not have the  $2 \times 2$  matrix structure that is characteristic for the RTF. The inverse of said matrices is proportional to the inverse of the determinant  $\det D = D^{++} D^{--} - D^{+-} D^{-+}$ . These products of propagators can lead to expressions that contain squares of  $\delta$ -distributions and may therefore be considered as ill defined. One could still do calculations to see that those singular expressions always drop out in the final result, however, it is still desirable to have an approach where these singularities do not appear in the first place. A solution to this is found in the Keldysh representation [33] where a unitary transformation of the propagator matrix is used:

$$U = \frac{1}{\sqrt{2}} \begin{pmatrix} 1 & -1 \\ 1 & 1 \end{pmatrix}. \tag{4.3}$$

Applying the transformation, one obtains the advanced, retarded and statistical propagators  $D^A$ ,  $D^R$  and  $D^F$ . The (1, 1)-element vanishes due to the relation [17]

$$D^{++} - D^{+-} - D^{-+} + D^{--} = 0, \tag{4.4}$$

which can be proven by inserting the corresponding definitions in terms of time ordered field operators. The remaining entries are

$$iD^A(p) = iD^{++}(p) - iD^{-+}(p) = \frac{i}{p^2 - i \operatorname{sgn}(p^0) \varepsilon}, \quad (4.5a)$$

$$iD^R(p) = iD^{++}(p) - iD^{+-}(p) = \frac{i}{p^2 + i \operatorname{sgn}(p^0) \varepsilon}, \quad (4.5b)$$

$$iD^F(p) = iD^{++}(p) + iD^{--}(p) = 2\pi \delta(p^2) [1 + 2f_B(|p^0|)]. \quad (4.5c)$$

The same transformation can be applied to the matrix of self-energies  $-i\Pi$ . In noting that (4.4) holds to all orders in perturbation theory, one can write down a similar relation for the self energies

$$\Pi^{++} + \Pi^{+-} + \Pi^{-+} + \Pi^{--} = 0. \quad (4.6)$$

The careful reader may spot a change in sign for the  $\Pi^{+-}$  and  $\Pi^{-+}$  which arises due to a subtlety in the RTF: While  $\Pi^{++}$  and  $\Pi^{--}$  both comprise two vertices on the same part of the contour  $C$  in complex time (see Chapter 2),  $\Pi^{+-}$  and  $\Pi^{-+}$  contain one vertex on  $C_+$  and one vertex on  $C_-$  each. The additional negative sign from vertices on  $C_-$  switches the signs in the respective terms in the above relation. The new self energies that correspond to (4.5a)–(4.5c) are

$$\Pi^A = \Pi^{++} + \Pi^{-+}, \quad (4.7a)$$

$$\Pi^R = \Pi^{++} + \Pi^{+-}, \quad (4.7b)$$

$$\Pi^F = \Pi^{++} + \Pi^{--}. \quad (4.7c)$$

Note that even after reducing the number of propagators from four in the original RTF formalism to three in the Keldysh formalism, these are still not independent of each other and one can obtain the statistical propagator and self energy directly from the advanced and retarded ones:

$$D^F(p) = [1 + 2f_B(|p^0|)] \operatorname{sgn}(p^0) [D^R(p) - D^A(p)], \quad (4.8a)$$

$$\Pi^F(p) = [1 + 2f_B(|p^0|)] \operatorname{sgn}(p^0) [\Pi^R(p) - \Pi^A(p)]. \quad (4.8b)$$

This relation can be checked for the bare propagators by using the principal value decomposition for the  $\delta$ -distribution from the advanced and retarded propagators in (4.5a), (4.5b)

$$\frac{1}{x - x_0 \pm i\varepsilon} = \mathcal{P} \left( \frac{1}{x - x_0} \right) \mp i\pi \delta(x - x_0). \quad (4.9)$$

The principle value of an integral is obtained when an  $\varepsilon$ -region around a pole residing on the integrated path is cut out. By adding back a circular part that goes around the pole either above or below in the complex plane, one obtains the right-hand side of (4.9) that is sketched on the

#### 4 Self-Energies

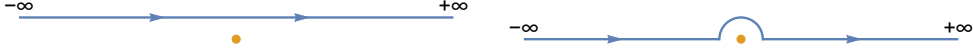


**Figure 4.1:** Graphical representation of the two sides of the principal value decomposition (4.9). Blue is an integration contour that here is chosen to go from  $-\infty$  to  $+\infty$  and yellow is the position of the pole in the integrand.

right side of Figure 4.1. Taking the limit  $\varepsilon \rightarrow 0$  only after the integration, this is the same not cutting out the pole but shifting it by  $\varepsilon$  below or above the contour, as in the left-hand side of (4.9) and Figure 4.1.

The advantage of using the Keldysh formalism over the original RTF propagator matrix becomes obvious in the dressed propagator in (4.2). Due to the vanishing entry in the Keldysh propagator and self energy matrix, the retarded and advanced dressed propagator decouple:

$$\begin{pmatrix} 0 & D^{A*} \\ D^{R*} & D^{F*} \end{pmatrix} = \begin{pmatrix} 0 & D^A + D^A \Pi^A D^{A*} \\ D^R + D^R \Pi^R D^{R*} & D^F + D^R \Pi^F D^{A*} + D^F \Pi^A D^{A*} + D^R \Pi^R D^{F*} \end{pmatrix}. \quad (4.10)$$

While the statistical dressed propagator is more complicated, it can also be computed with (4.8a).

## 4.2 Higgs Self Energy

In the  $\nu$ MSM, there are contributions from vector bosons, scalars and fermions to the Higgs self energy. The respective couplings are found in the Higgs and Yukawa sector of the SM (3.6) and (3.8)

### 4.2.1 Contributions from Vector Bosons

All couplings between the Higgs and vector bosons are comprised in the kinetic term for the Higgs. As is the case in scalar QED, cubic and quartic vertices between vectors and scalars are present in the Lagrangian:

$$\begin{aligned} \mathcal{L}_{\text{Higgs}} &= (\partial_\mu \Phi_i)^\dagger \partial^\mu \Phi_i \\ &\quad -i \left[ g_L (\tau^a)_{ij} W_\mu^a + \frac{g_Y}{2} B_\mu \right] [(\partial^\mu \Phi_i)^\dagger \Phi_j - \Phi_i^\dagger (\partial^\mu \Phi_j)] \\ &\quad + \left[ \frac{g_L^2}{4} \delta_{ij} W_\mu^a W^{a\mu} + \frac{g_Y^2}{4} \delta_{ij} B_\mu B^\mu + g_L g_Y (\tau^a)_{ij} W_\mu^a B^\mu \right] \Phi_i^\dagger \Phi_j \\ &\quad -\mu^2 \Phi_i^\dagger \Phi_i - \lambda (\Phi_i^\dagger \Phi_i)^2. \end{aligned} \quad (4.11)$$

The Feynman rules for the scalar-vector couplings can be read off directly

$$\Phi_j \xrightarrow{p_1} \text{---} \bullet \begin{cases} \text{---} \xrightarrow{p_2} \Phi_i \\ \text{---} \text{---} W^{a\mu} \end{cases} = i g_L (\tau^a)_{ij} (p_1^\mu + p_2^\mu), \quad (4.12a)$$

$$\Phi_j \xrightarrow{p_1} \text{---} \bullet \begin{cases} \text{---} \xrightarrow{p_2} \Phi_i \\ \text{---} \text{---} B^\mu \end{cases} = i \frac{g_Y}{2} \delta_{ij} (p_1^\mu + p_2^\mu), \quad (4.12b)$$

$$\Phi_j \xrightarrow{p_1} \text{---} \bullet \begin{cases} \text{---} \xrightarrow{p_2} \Phi_i \\ \text{---} \text{---} W^{b\nu} \end{cases} = i \frac{g_L^2}{2} \delta^{ab} \delta_{ij} g^{\mu\nu}, \quad (4.12c)$$

$$\Phi_i \xrightarrow{p_1} \text{---} \bullet \begin{cases} \text{---} \xrightarrow{p_2} \Phi_j \\ \text{---} \text{---} W^{a\mu} \\ \text{---} \text{---} B^\nu \end{cases} = i \frac{g_Y^2}{2} \delta_{ij} g^{\mu\nu}, \quad (4.12d)$$

$$\Phi_i \xrightarrow{p_1} \text{---} \bullet \begin{cases} \text{---} \xrightarrow{p_2} \Phi_j \\ \text{---} \text{---} B^\mu \\ \text{---} \text{---} B^\nu \\ \text{---} \text{---} W^{a\mu} \end{cases} = i g_L g_Y (\tau^a)_{ij} g^{\mu\nu}. \quad (4.12e)$$

At leading order, two types of diagrams contribute to the Higgs self energy, comprising either two cubic or one quartic vertex. It may be instructive to first consider the quartic coupling contributions which have an inherently simple structure

$$\Pi_{\text{ssvv}}(p) = \text{---} \xrightarrow{p} \text{---} \bullet \begin{matrix} \text{---} k \\ \text{---} \end{matrix} \text{---} \xrightarrow{p} \text{---} = -i \delta^{aa} g^2 g^{\mu\nu} \int \frac{d^D k}{(2\pi)^D} D_{\mu\nu}(k). \quad (4.13)$$

In the loop, the generations of vector bosons are summed over in  $\delta^{aa} = \mathcal{N}$ , where  $\mathcal{N}$  is the

#### 4 Self-Energies

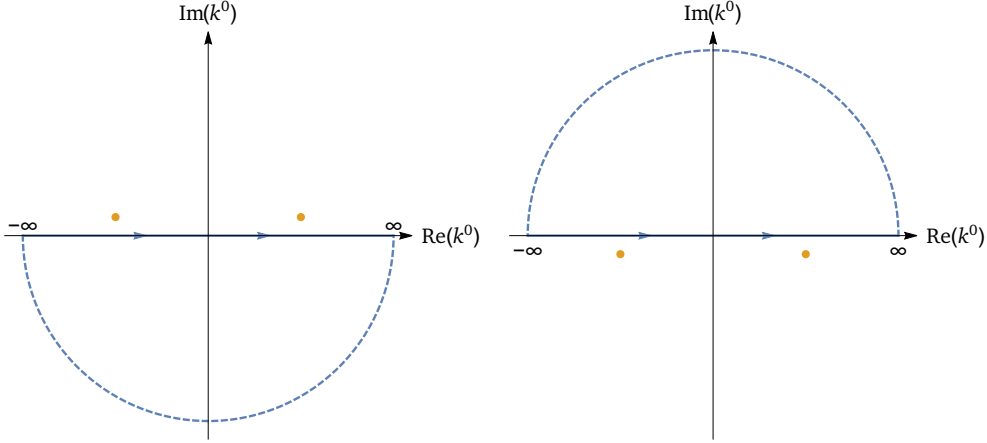


**Figure 4.2:** Poles of the advanced (left) and retarded (right) propagators are depicted in yellow in the complex  $k^0$ -plane. An integral where the contour (blue) can be closed at  $\pm i\infty$  will vanish due to the residue theorem.

number of generators of the underlying gauge group.  $g^2$  denotes the coupling constant from the quartic vertex that shall only be substituted with the respective terms from the  $SU(2)_L$  and  $U(1)_Y$  in the final result. Note that in the above expression, only the topology of the self energy diagram was considered, but not the contractions between space-time points on different contour parts  $C_{\pm}$ . For obtaining the advanced/retarded self energy, (4.7a) and (4.7b) can be used:

$$\Pi_{\text{ssvv}}^{A/R}(p) = \Pi_{\text{ssvv}}^{++}(p) + \Pi_{\text{ssvv}}^{\mp\pm}(p) = -i\mathcal{N}g^2 g^{\mu\nu} \int \frac{d^D k}{(2\pi)^D} D_{\mu\nu}^{++}(k). \quad (4.14)$$

The part with  $\Pi_{\text{ssvv}}^{\mp\pm}$  vanishes as there is only one vertex present in the diagram at leading order and therefore, mixing between  $C_+$  and  $C_-$  are impossible. Inverting the relations in (4.5a) – (4.5c) now allows to translate the above expression back into the Keldysh representation

$$\begin{aligned} \Pi_{\text{ssvv}}^{A/R}(p) &= -\frac{i}{2} \mathcal{N}g^2 g^{\mu\nu} \int \frac{d^D k}{(2\pi)^D} [D_{\mu\nu}^A(k) + D_{\mu\nu}^R(k) + D_{\mu\nu}^F(k)] \\ &= \frac{i}{2} \mathcal{N}g^2 g^{\mu\nu} \int \frac{d^D k}{(2\pi)^D} \\ &\quad \left\{ \frac{g_{\mu\nu}}{k^2 - i\text{sgn}(k^0)\varepsilon} + \frac{g_{\mu\nu}}{k^2 + i\text{sgn}(k^0)\varepsilon} - g_{\mu\nu} 2\pi i \delta(k^2) [1 + 2f_B(|k^0|)] \right\}, \end{aligned} \quad (4.15)$$

where the vector propagators corresponding to (4.5a) – (4.5c) have been inserted in the last step. The first two terms in the above expression are purely advanced/retarded. Structures like these will always vanish upon integration over the zero component of the loop momentum as long as one can close the contour at  $\pm i\infty$ . This is due to the signum function in the denominator that places all poles on the same side of the integration contour as sketched in Figure 4.2. The only remaining contribution comes from the statistical propagator that involves a  $\delta$ -distribution, taking the loop momentum on-shell. Since there are no scalar products of external momentum  $p$  and loop momentum  $k$  present, the remaining  $d = D - 1$  dimensional integral can be formulated



#### 4 Self-Energies

$$\begin{aligned}
\Pi_{\text{ssv}}^{A/R}(p) &= \Pi_{\text{ssv}}^{++}(p) + \Pi_{\text{ssv}}^{\mp\pm}(p) \\
&= i C g^2 \int \frac{d^D k}{(2\pi)^D} \left[ D_{\mu\nu}^{++}(k)(p^\mu + 2k^\mu) D^{++}(p+k)(p^\nu + 2k^\nu) - \right. \\
&\quad \left. D_{\mu\nu}^{\pm\mp}(k)(p^\mu + 2k^\mu) D^{\mp\pm}(p+k)(p^\nu + 2k^\nu) \right]. \tag{4.19}
\end{aligned}$$

An important detail is the relative sign between the two terms above. While the first loop contains only (+) vertices, the second loop connects a (+) and a (−) vertex, the product of which contains an additional factor (−1). Upon translating back into the Keldysh representation, one finds four contributions out of the 9 possible combinations of advanced, retarded and statistical propagators that do not cancel:

$$\begin{aligned}
\Pi_{\text{ssv}}^{A/R}(p) &= -\frac{i}{2} C g^2 \int \frac{d^D k}{(2\pi)^D} (p+2k)^2 \left\{ \right. \\
&\quad 2\pi \delta(k^2) [1 + 2f_B(|k^0|)] \frac{1}{(p+k)^2 \mp i \text{sgn}(p^0 + k^0) \varepsilon} + \\
&\quad 2\pi \delta[(p+k)^2] [1 + 2f_B(|p^0 + k^0|)] \frac{1}{k^2 \pm i \text{sgn}(k^0) \varepsilon} + \\
&\quad \frac{i}{[k^2 - i \text{sgn}(k^0) \varepsilon] [(p+k)^2 - i \text{sgn}(p^0 + k^0) \varepsilon]} + \\
&\quad \left. \frac{i}{[k^2 + i \text{sgn}(k^0) \varepsilon] [(p+k)^2 + i \text{sgn}(p^0 + k^0) \varepsilon]} \right\}. \tag{4.20}
\end{aligned}$$

As was advertised at the beginning of this chapter, no squares of  $\delta$ -distributions appear during the calculation. The two last terms are again purely advanced and purely retarded. As they go like  $1/(k^0)^2$  for large loop momenta, the  $k^0$ -contour can be closed in such a way that no residue is picked up, thus showing that these parts vanish. The remaining terms can be factorized by applying a substitution  $k \rightarrow -p - k$  in the latter one. The integral over  $k^0$  is elementary due to the presence of the  $\delta$ -distribution that puts the loop momentum on-shell. Note that - in contrast to the previously discussed case - scalar products  $kp$  are present in the integrand, which is therefore a function of the angle  $\theta$  between these two momenta. The integration over  $\theta$  can be performed by inserting a logarithmic factor in the integrand and encircling the resulting discontinuity in the complex plane (c.f. Appendix A). One finds

$$\Pi_{\text{ssv}}^{A/R}(p) = -C g^2 \frac{1}{(4\pi)^{d/2}} \frac{1}{\Gamma(\frac{d}{2})} \int_0^\infty d|\vec{k}| |\vec{k}|^{d-2} [1 + 2f_B(|\vec{k}|)] \left[ 1 - \frac{p^2}{2|\vec{p}||\vec{k}|} L_{\pm}^{A/R} \right], \tag{4.21}$$

where

$$L_{\pm}^{A/R} = \ln \frac{|\vec{k}| + (p_+ \mp i\varepsilon)}{|\vec{k}| + (p_- \mp i\varepsilon)} \pm \ln \frac{|\vec{k}| - (p_+ \mp i\varepsilon)}{|\vec{k}| - (p_- \mp i\varepsilon)}, \quad p_{\pm} = \frac{p^0 \pm |\vec{p}|}{2} \tag{4.22}$$

is a shorthand writing for the logarithmic function that appears in the integrand as a consequence of the  $\theta$ -dependence. This type of integrand will also appear in other self energy diagrams in

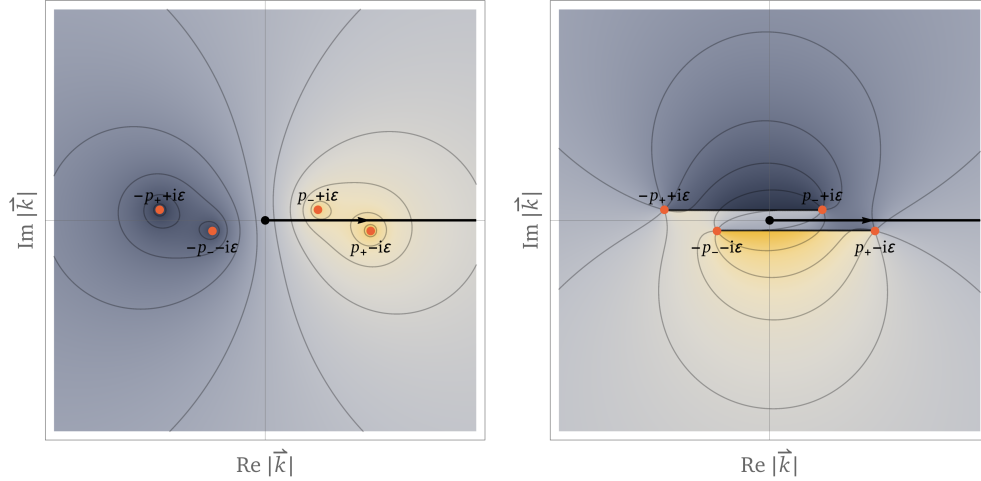


**Figure 4.3:** Real (left) and imaginary (right) part of the logarithmic term  $L^A$  in the integrand in (4.21) for finite  $\varepsilon$ . The poles (red) resulting from the zeros in numerator and denominator of the logarithms can be clearly seen in the real part. The imaginary part on the other hand features discontinuities that join the poles above and below the real axis respectively. Also shown is the integration contour in  $|\vec{k}|$  (black) which does not encounter any of the poles or discontinuities.

various versions: The sign of the  $\varepsilon$  shift depends on the self energy it appears in being advanced or retarded. This has been accounted for with a superscript  $A/R$  in (4.22). Also, in fermionic self energy diagrams, not only the difference  $L_-$ , but also the sum  $L_+$  of the two logarithms will be present. In order to avoid ambiguities in the signs, a color coding was applied in (4.22). Obviously,  $L_-^{A/R}$  features discontinuities in the complex  $|\vec{k}|$ -plane. At this point, the  $\varepsilon$ -regularization is crucial for obtaining a well defined expression: For a finite  $\varepsilon$ , the logarithmic poles are shifted above and below the real axis which in turn are joined pairwise by discontinuity cuts that run parallel to the real axis and the integration contour as shown in Figure 4.3 for the advanced version. Thus,  $L_-^{A/R}$  is analytic along the real axis but still needs to be expanded in order to obtain a non-numeric result for the integral. Note that  $L_-^{A/R}$  depends on the loop momentum  $|\vec{k}|$ , as well as on two external scales  $p_{\pm}$ . The integral itself is dominated by the value of the integrand around  $|\vec{k}| \sim T$  and therefore, a sensible approach is to differentiate between various regions, defined by  $p_{\pm} \lesseqgtr T$  and expand  $L_-^{A/R}$  accordingly.

$$\lim_{\substack{p_+ \rightarrow 0 \\ p_- \rightarrow 0}} L_-^{A/R} = \lim_{\substack{p_+ \rightarrow 0 \\ p_- \rightarrow 0}} \left[ \frac{2|\vec{k}|(p_+ - p_-)}{|\vec{k}|^2 + \varepsilon^2} + o\left(\frac{p_+^2}{|\vec{k}|^2}, \frac{p_-^2}{|\vec{k}|^2}\right) \right] \quad (4.23a)$$

$$\lim_{\substack{p_+ \rightarrow \infty \\ p_- \rightarrow \infty}} L_-^{A/R} = \lim_{\substack{p_+ \rightarrow \infty \\ p_- \rightarrow \infty}} \left[ 2|\vec{k}| \left( \frac{1}{p_+} - \frac{1}{p_-} \right) + o\left(\frac{|\vec{k}|^2}{p_+^2}, \frac{|\vec{k}|^2}{p_-^2}\right) \right] \quad (4.23b)$$

$$\lim_{\substack{p_+ \rightarrow 0 \\ p_- \rightarrow \infty}} L_-^{A/R} = \lim_{\substack{p_+ \rightarrow 0 \\ p_- \rightarrow \infty}} \left[ \ln\left(\frac{|\vec{k}| \mp i\varepsilon}{|\vec{k}| \pm i\varepsilon}\right) - \frac{2|\vec{k}|}{p_-} + \frac{2|\vec{k}|p_+}{|\vec{k}|^2 + \varepsilon^2} + o\left(\frac{p_+^2}{|\vec{k}|^2}, \frac{|\vec{k}|^2}{p_-^2}\right) \right] \quad (4.23c)$$

$$\lim_{\substack{p_+ \rightarrow \infty \\ p_- \rightarrow 0}} L_-^A = \lim_{\substack{p_+ \rightarrow \infty \\ p_- \rightarrow 0}} \left[ \ln\left(\frac{|\vec{k}| \pm i\varepsilon}{|\vec{k}| \mp i\varepsilon}\right) + \frac{2|\vec{k}|}{p_+} - \frac{2|\vec{k}|p_-}{|\vec{k}|^2 + \varepsilon^2} + o\left(\frac{|\vec{k}|^2}{p_+^2}, \frac{p_-^2}{|\vec{k}|^2}\right) \right] \quad (4.23d)$$

(4.23b) corresponds to the infrared limit for the loop momentum. Inserting the expansion into the integral (4.21) reveals the integrand to be infrared finite for  $d = 3$  spatial dimensions. In the

gauge group	$\mathcal{N}$	$\dim(\mathcal{R})$	$C$
U(1)	1	1	1
SU(2)	3	2	3/4

**Table 4.1:** Gauge group and representation specific factors that appear in the Higgs self energy diagrams involving vector bosons.  $\dim(\mathcal{R})$  is the dimension of the representation of the group. In the SM, the Higgs is in the one dimensional representation of the  $U(1)_Y$  and the two dimensional representation of the  $SU(2)_L$ .

ultraviolet, the non-thermal part of the integrand is again quadratically divergent as expected from the  $T = 0$  theory while the thermal part is regulated by the thermal distribution. Evaluating the latter obviously leads to different results, depending on the domain of the external scales  $p_{\pm}$  one chooses to work in. As Pisarski and Braaten [14, 13] have established in the hard thermal loop (HTL) framework, it is sufficient to use bare propagators as long as at least one external momentum is hard. Consequently, the interesting domain where the thermal self energy should be evaluated is characterized by  $p_{\pm} \ll T$ . In this case, the integrand is dominated by the non-logarithmic term since (4.23a) is subleading and the self energy can be approximated as

$$\Pi_{\text{ssv}}^{A/R}(p) = -\frac{1}{12} C g^2 T^2 + [\text{non-thermal parts}]. \quad (4.24)$$

(4.17) and (4.24) make up the leading order self energy contributions from vector bosons. The gauge group and representation specific factors  $\mathcal{N}$  and  $C$  for the SM are tabulated in Table 4.1 [61]. In summing up the discussed diagrams, one arrives at the total vector boson induced self energy of the Higgs in the SM at leading order. In doing so, the couplings in (4.17) and (4.24) have to be replaced by the corresponding couplings of the respective gauge group as listed in (4.12a)–(4.12e)

$$\Pi_{\text{v}}^{A/R}(p) = \left( \frac{3}{16} g_L^2 + \frac{1}{16} g_Y^2 \right) T^2. \quad (4.25)$$

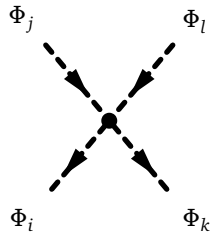
Concluding the discussion on the vector induced self energy diagrams, a short remark on the validity of the HTL approximation for hard external momenta may be appropriate. In [34] it is noted that a resummation of self energy diagrams is always possible and allows to capture the effect of altered dispersion relations in the thermal plasma. Since the thermal masses that appear in the dressed propagators are typically  $\sim 0.1 \dots 1 T$ , the corrections that arise are noticeable even for hard external momenta. While this may justify the usage of dressed propagators beyond the domain of the HTL scheme, one should still reconsider the validity of the approximations that were applied during the computation of (4.25). While the thermal part of the quartic coupling diagram (4.17) is exact and does not depend on the scale of the external momentum, this is not true for the cubic coupling diagram (4.24). Here, it was already noted before that the integrand does depend on the external momentum  $p$  - or more precisely  $p_{\pm}$ . The importance of reconsidering the exact integrand (4.21) and then applying the appropriate approximation can be demonstrated e.g. in the region  $p_{\pm} \gg T$ . Here, one needs to use (4.23b), where the logarithmic term is no longer subleading and leads to

$$\Pi_{\text{ssv}}^{A/R}(p) = -\frac{5}{12} C g^2 T^2 + [\text{non-thermal parts}].$$

This result differs from (4.24) by a factor of 5. It should be noted that this case is highly off-shell, since  $p_- = (p^0 - |\vec{p}|)/2 \gg T$ . Going on-shell while considering thermal masses requires an interpolation between the domains for  $p_- \sim T$ . However, in this case, the integral is dominated by  $|\vec{k}| \sim p_-$ . Attempts to expand around this point lead to  $1/\varepsilon$  singularities. This hints to a breakdown of the overall approximation scheme, caused by the exchange of taking the limit  $\varepsilon \rightarrow 0$  before the integral over  $|\vec{k}|$  is evaluated. The approximations (4.23a)–(4.23d) are not affected by this as the dominant contributions to the integral are far away from the  $\varepsilon$ -shifted poles. Consequently, a treatment for the regions joining the domains  $p_{\pm} \gtrsim T$  requires an alternative method that could not be developed within this work. Hence, the application of resummed propagators should be limited to the HTL case.

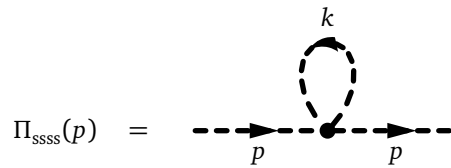
#### 4.2.2 Contributions from Scalars

The Higgs sector of the SM (3.6) also contains the quartic scalar self interaction



$$= -i\lambda (\delta_{ij}\delta_{kl} + \delta_{il}\delta_{jk}). \quad (4.26)$$

This vertex allows for a scalar self energy diagram similar to (4.13) where the vector boson in the loop is replaced by a scalar:



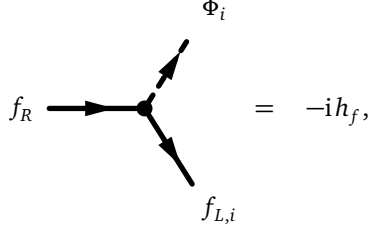
$$\Pi_{\text{ssss}}(p) = \text{diagram} = 6i\lambda \int \frac{d^D k}{(2\pi)^D} D(k). \quad (4.27)$$

Herein, the doublet structure of the Higgs field  $\Phi$  was used in Wick's theorem, giving rise to the numerical prefactor. The rest of the computation of this diagram proceeds in complete analogy to  $\Pi_{\text{ssvv}}$  and one finds

$$\Pi_{\text{ssss}}^{A/R}(p) = \frac{\lambda}{2} T^2 + [\text{non-thermal parts}]. \quad (4.28)$$

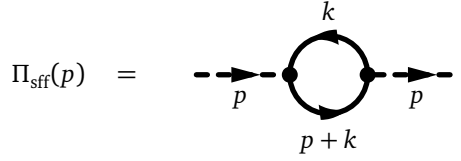
### 4.2.3 Contributions from Fermions

A last self energy diagram can be obtained from the Yukawa sector of the SM Lagrangian (3.8), where the couplings between the Higgs doublet field and quarks and leptons are specified. The vertex for any of the fermions is given by



$$= -i h_f, \quad (4.29)$$

where the index  $i$  is in the  $SU(2)_L$  isospin space.  $h_f$  is the Yukawa coupling that is appropriate for the respective fermion and in general is matrix valued in generation space. One finds the leading order self energy diagram as



$$\Pi_{\text{ssf}}(p) = -\frac{i}{2} \text{tr} [3h_d^\dagger h_d + 3h_u^\dagger h_u + h_\ell^\dagger h_\ell + h_N^\dagger h_N] \int \frac{d^D k}{(2\pi)^D} \text{tr} [S(k)S(p+k)]. \quad (4.30)$$

Factors of 3 in front of the  $h_d^\dagger h_d$  and  $h_u^\dagger h_u$  terms account for the summation of the quark color in the loop. The same approach that was already employed for  $\Pi_{\text{ssv}}$  can be used to find the ansatz in the Keldysh formalism for this case as well. Substituting the fermion propagators and evaluating the trace in the integrand yields a similar function as in the former discussion with scalar products between external and loop momentum. After performing the integration over the enclosed angle, one finds

$$\begin{aligned} \Pi_{\text{ssf}}^{A/R}(p) &= -2 \text{tr} [3h_d^\dagger h_d + 3h_u^\dagger h_u + h_\ell^\dagger h_\ell + h_N^\dagger h_N] \frac{1}{(4\pi)^{d/2}} \frac{1}{\Gamma(\frac{d}{2})} \\ &\int_0^\infty d|\vec{k}| |\vec{k}|^{d-2} [1 - 2f_F(|\vec{k}|)] \left[ 1 + \frac{p^2}{8|\vec{p}||\vec{k}|} L_-^{A/R} \right], \end{aligned} \quad (4.31)$$

with the same logarithmic term appearing in the integrand as before. Evaluating the HTL limit  $p_\pm \ll T$  ultimately leads to the thermal self energy contribution

$$\Pi_{\text{sff}}^{A/R}(p) = \frac{1}{12} \text{tr} [3h_d^\dagger h_d + 3h_u^\dagger h_u + h_\ell^\dagger h_\ell + h_N^\dagger h_N] T^2 + [\text{non-thermal parts}]. \quad (4.32)$$

Among the Yukawas that appear in the above expression, the top coupling  $h_t = (h_u)_{33}$  is by far the most dominant one, such that all other summands can be neglected.

#### 4.2.4 Full thermal Self Energy and dressed Propagator

In adding up all the leading order contributions to the thermal scalar self energy, one arrives at the final result

$$\Pi^{A/R}(p) = \left( \frac{3}{16} g_L^2 + \frac{1}{16} g_Y^2 + \frac{1}{2} \lambda + \frac{1}{4} h_t^2 \right) T^2. \quad (4.33)$$

Within the domain of validity of the HTL approximation, the scalar self energy does not depend on the external momentum  $p$ . Thus, the pole of the dressed propagator  $D^*$  is shifted according to (4.2) and  $\Pi^{A/R}(p)$  can be directly interpreted as a mass term  $m_\phi^2(T) = \Pi^{A/R}$  that occurs due to the interaction between the scalar and the thermal heat bath:

$$iD^{A/R*}(p) = \text{---} \xrightarrow{p} \bullet \xrightarrow{p} \text{---} = \frac{i}{p^2 - m_\phi^2(T) \mp i \text{sgn}(p^0) \varepsilon}, \quad (4.34a)$$

$$iD^{F*}(p) = \text{---} \xrightarrow{p} \bullet \xrightarrow{p} \text{---} = 2\pi \delta [p^2 - m_\phi^2(T)] [1 + 2f_B(|p^0|)]. \quad (4.34b)$$

Equation (4.8a) was used in order to obtain the statistical dressed propagator  $D^{F*}$ . The dispersion relation for the Higgs that can be read off from the shifted poles in  $\Pi^{A/R*}$ , or alternatively from the  $\delta$ -function appearing in the statistical propagator, is exactly that of a particle with mass  $m_{\text{th}}$ .

### 4.3 Lepton Self Energy

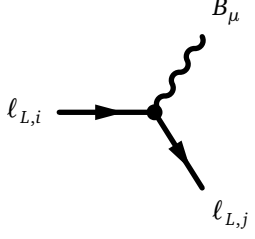
The second field appearing in right-handed neutrino self energy diagrams at leading order besides the Higgs are the left-handed leptons. In the SM, leptons couple to the Higgs as specified in the Yukawa sector (3.8) and to the gauge bosons of the  $SU(2)_L \otimes U(1)_Y$ . Couplings of the latter type can be read off from the Yang-Mills sector (3.2).

#### 4.3.1 Contributions from Vector Bosons

Starting out with vector induced self energy diagrams, two couplings from (3.2) are of interest:

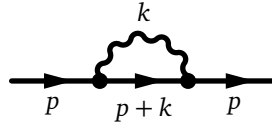
$$\begin{array}{c} \ell_{L,i} \text{---} \xrightarrow{\quad} \bullet \begin{array}{l} \nearrow \text{---} W_\mu^a \\ \searrow \text{---} \ell_{L,j} \end{array} \end{array} = g_L (\tau^a)_{ij} \gamma_\mu, \quad (4.35a)$$

#### 4 Self-Energies



$$= -\frac{g_Y}{2} \delta_{ij} \gamma_\mu. \quad (4.35b)$$

One finds a self energy  $\Sigma_{\text{ffv}}$ , very similar to the scalar case  $\Pi_{\text{ssv}}$ , including the same Casimir factors  $C$  that already appeared earlier as the left-handed lepton fields in the SM are in the same representation of the  $SU(2)_L \otimes U(1)_Y$  as the Higgs doublet



$$\Sigma_{\text{ffv}}(p) = i C g^2 \int \frac{d^D k}{(2\pi)^D} D_{\mu\nu}(k) \gamma^\mu S(p+k) \gamma^\nu. \quad (4.36)$$

Again, the diagram is evaluated for a general gauge theory with coupling  $g$ . The usual ansatz for the advanced and retarded function leads to

$$\begin{aligned} \Sigma_{\text{ffv}}^{A/R}(p) &= \frac{D-2}{2} C g^2 \int \frac{d^D k}{(2\pi)^D} (\not{p} + \not{k}) \\ &\left\{ 2\pi \delta(k^2) [1 + 2f_B(|k^0|)] \frac{1}{(p+k)^2 \mp i \text{sgn}(p^0 + k^0) \varepsilon} \right. \\ &\left. + 2\pi \delta[(p+k)^2] [1 - 2f_F(|p^0 + k^0|)] \frac{1}{k^2 \pm i \text{sgn}(k^0) \varepsilon} \right\}. \end{aligned} \quad (4.37)$$

In the above expression, a factor  $2 - D$  enters due to  $\gamma^\mu \gamma^\nu \gamma_\mu = (2 - D) \gamma^\nu$  in  $D$  dimensions. Also, the two terms involving either only advanced or only retarded propagators have been dropped as these will evaluate to zero when integrating over  $k^0$ , as has already been discussed in the previous section. This fermionic self energy transforms under the Dirac representation of the Lorentz group and thus, the most general ansatz for  $\Sigma^{A/R}$  is

$$\Sigma^{A/R}(p) = -\not{p} a^{A/R} - \not{u} b^{A/R}, \quad (4.38)$$

where  $u$  is the velocity of the plasma. This is a special feature of the finite temperature theory: the presence of a thermal background introduces an additional reference vector such that the rest frame of the plasma can always be distinguished from other choices of coordinates. In the rest frame, the velocity of the relativistic thermal plasma is given by  $u = (1, \vec{0})^T$ . This explicit choice will be adopted for the following computations. In order to obtain the coefficients  $a^{A/R}$  and  $b^{A/R}$ , the following traces can be considered:

$$\begin{aligned} \frac{1}{4} \text{tr} [\not{p} \Sigma_{\text{ffv}}^{A/R}(p)] &= \frac{D-2}{2} C g^2 \frac{1}{(4\pi)^{d/2}} \frac{1}{\Gamma(\frac{d}{2})} \int_0^\infty d|\vec{k}| |\vec{k}|^{d-2} \\ &\quad \left\{ [1 + 2f_B(|\vec{k}|)] \left[ 1 - \frac{p^2}{2|\vec{p}||\vec{k}|} L_-^{A/R} \right] - [1 - 2f_F(|\vec{k}|)] \left[ 1 + \frac{p^2}{2|\vec{p}||\vec{k}|} L_-^{A/R} \right] \right\}, \end{aligned} \quad (4.39a)$$

$$\begin{aligned} \frac{1}{4} \text{tr} [\not{p} \Sigma_{\text{ffv}}^{A/R}(p)] &= \frac{D-2}{4} C g^2 \frac{1}{(4\pi)^{d/2}} \frac{1}{\Gamma(\frac{d}{2})} \int_0^\infty d|\vec{k}| |\vec{k}|^{d-2} \\ &\quad \left\{ [1 + 2f_B(|\vec{k}|)] \left[ \frac{1}{|\vec{p}|} \ln \frac{p^0 + |\vec{p}| \mp i\varepsilon}{p^0 - |\vec{p}| \mp i\varepsilon} - \frac{1}{2|\vec{p}|} L_+^{A/R} - \frac{p^0}{2|\vec{p}||\vec{k}|} L_-^{A/R} \right] \right. \\ &\quad \left. - [1 - 2f_F(|\vec{k}|)] \left[ \frac{1}{|\vec{p}|} \ln \frac{p^0 + |\vec{p}| \mp i\varepsilon}{p^0 - |\vec{p}| \mp i\varepsilon} - \frac{1}{2|\vec{p}|} L_+^{A/R} \right] \right\}. \end{aligned} \quad (4.39b)$$

The first trace exhibits the same behavior as scalar expressions that have been investigated before. However, the second trace incorporates additional features: So far, there was always a term present which was  $\sim |\vec{k}|^{d-2}$  with no further dependence on the external momentum  $p$ . This term then provided the dominant contribution in the limit  $p^0, |\vec{p}| \rightarrow 0$ , which is the reason for the scalar thermal self energy being independent of  $p$  in the HTL approximation. In the case of (4.39b), the leading term is also  $\sim |\vec{k}|^{d-2}$ , but depends logarithmically on  $p$ . Therefore, one might already anticipate a more complicated behavior for the dressed lepton propagator. Another new aspect is a term  $\sim L_+^{A/R}$  which is plotted in Figure 4.4. It can be expanded in the same domains as  $L_-^{A/R}$  in (4.23a)–(4.23d).

$$\lim_{\substack{p_+ \rightarrow 0 \\ p_- \rightarrow 0}} L_+^{A/R} = \lim_{\substack{p_+ \rightarrow 0 \\ p_- \rightarrow 0}} \left[ \pm 2i\varepsilon \frac{p_+ - p_-}{|\vec{k}|^2 + \varepsilon^2} + O\left(\frac{p_+^2}{|\vec{k}|^2}, \frac{p_-^2}{|\vec{k}|^2}\right) \right] \quad (4.40a)$$

$$\lim_{\substack{p_+ \rightarrow \infty \\ p_- \rightarrow \infty}} L_+^{A/R} = \lim_{\substack{p_+ \rightarrow \infty \\ p_- \rightarrow \infty}} \left[ 2 \ln \frac{p_+}{p_-} \mp 2i\varepsilon \left( \frac{1}{p_+} - \frac{1}{p_-} \right) + O\left(\frac{|\vec{k}|^2}{p_+^2}, \frac{|\vec{k}|^2}{p_-^2}\right) \right] \quad (4.40b)$$

$$\begin{aligned} \lim_{\substack{p_+ \rightarrow 0 \\ p_- \rightarrow \infty}} L_+^{A/R} &= \lim_{\substack{p_+ \rightarrow 0 \\ p_- \rightarrow \infty}} \left[ \ln\left(\pm \frac{|\vec{k}| - i\varepsilon}{p_-}\right) + \ln\left(\mp \frac{|\vec{k}| + i\varepsilon}{p_-}\right) \right. \\ &\quad \left. \pm 2i\varepsilon \left( \frac{p_+}{|\vec{k}|^2 + \varepsilon^2} + \frac{1}{p_-} \right) + O\left(\frac{p_+^2}{|\vec{k}|^2}, \frac{|\vec{k}|^2}{p_-^2}\right) \right] \end{aligned} \quad (4.40c)$$

$$\begin{aligned} \lim_{\substack{p_+ \rightarrow \infty \\ p_- \rightarrow 0}} L_+^{A/R} &= \lim_{\substack{p_+ \rightarrow \infty \\ p_- \rightarrow 0}} \left[ \ln\left(\pm \frac{p_+}{|\vec{k}| - i\varepsilon}\right) + \ln\left(\mp \frac{p_+}{|\vec{k}| + i\varepsilon}\right) \right. \\ &\quad \left. \mp 2i\varepsilon \left( \frac{1}{p_+} + \frac{p_-}{|\vec{k}|^2 + \varepsilon^2} \right) + O\left(\frac{|\vec{k}|^2}{p_+^2}, \frac{p_-^2}{|\vec{k}|^2}\right) \right] \end{aligned} \quad (4.40d)$$

Looking at (4.40a),  $L_+^{A/R}$  is subleading in the HTL limit. For  $D = 4$  and  $d = 3$  (spatial) dimensions, the thermal integrand is again regulated by the presence of bosonic and fermionic distribution functions. Keeping only the thermal part, the remaining dominant contributions are

#### 4 Self-Energies

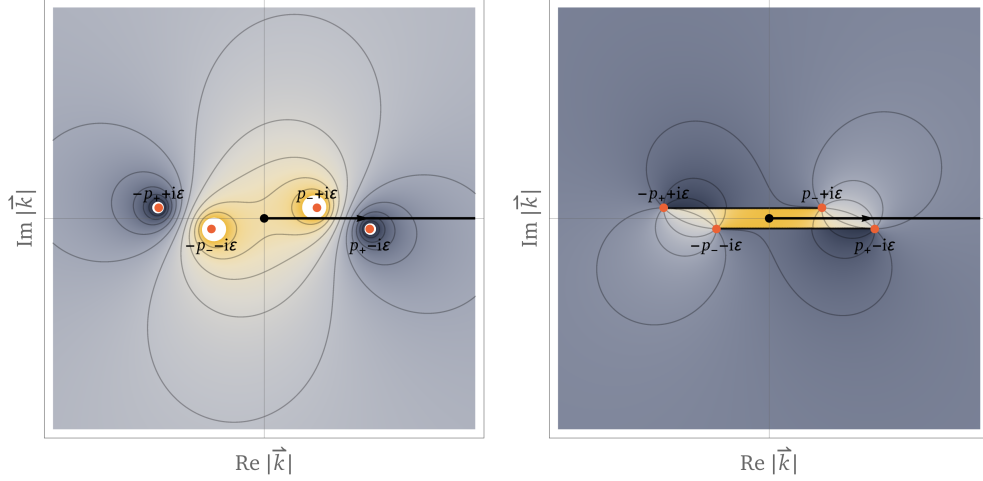


**Figure 4.4:** Real (left) and imaginary (right) part of the logarithmic function  $L_+^A$  for finite  $\epsilon$ . Poles from zeros in numerators and denominators are marked in red and joined pairwise by discontinuity cuts that can be seen as a jump in the imaginary part. The integration contour (black) does not encounter such a discontinuity as long as  $\epsilon$  is kept finite.

$$\frac{1}{4} \text{tr} \left[ \not{p} \Sigma_{\text{ffv}}^{A/R}(p) \right] = \frac{1}{8} C g^2 T^2 + [\text{non-thermal parts}] \quad (4.41a)$$

$$\frac{1}{4} \text{tr} \left[ \not{p} \Sigma_{\text{ffv}}^{A/R}(p) \right] = \frac{1}{16} C g^2 T^2 \frac{1}{|\vec{p}|} \ln \frac{p^0 + |\vec{p}| \mp i \epsilon}{p^0 - |\vec{p}| \mp i \epsilon} + [\text{non-thermal parts}] \quad (4.41b)$$

These results can be compared with the general ansatz for the self energy in (4.38), resulting in two equations from which the coefficients  $a_{\text{ffv}}^{A/R}$  and  $b_{\text{ffv}}^{A/R}$  are obtained:

$$a_{\text{ffv}}^{A/R} = \frac{1}{8} C g^2 \frac{T^2}{|\vec{p}|^2} \left( 1 - \frac{p^0}{2|\vec{p}|} \ln \frac{p^0 + |\vec{p}| \mp i \epsilon}{p^0 - |\vec{p}| \mp i \epsilon} \right), \quad (4.42a)$$

$$b_{\text{ffv}}^{A/R} = -\frac{1}{8} C g^2 \frac{T^2}{|\vec{p}|^2} \left( p^0 - \frac{p^2}{2|\vec{p}|} \ln \frac{p^0 + |\vec{p}| \mp i \epsilon}{p^0 - |\vec{p}| \mp i \epsilon} \right). \quad (4.42b)$$

The same quadratic dependence on the temperature  $T$  that was already found in the discussion on scalars is also present for fermions. Due to the dependence on the external momentum  $p$  however, the shift of the poles and the residues in the dressed propagator are more complicated and one cannot identify the factor  $C g^2 T^2/8$  as a mass term in the same way as for scalars. As is customary, the shorthand  $m_{\text{th}}^2(T)$  will still be used for this prefactor, however, one should bear in mind that this is *not* the mass associated with the fermion in the plasma.

#### 4.3.2 Contributions from Scalars

Before the dressed lepton propagator can be evaluated, the leading order diagrams with a scalar in the loop are also needed. Couplings between leptons and scalars were already investigated for the fermionic contribution to the scalar self energy in (4.29). Here, the needed diagram is of the form



#### 4 Self-Energies

$$\Delta_{\pm}^{A/R} = \left[ p^0 \mp |\vec{p}| \mp \frac{m_{\ell}^2}{|\vec{p}|} \pm \frac{m_{\ell}^2}{2|\vec{p}|^2} (p^0 \mp |\vec{p}|) \ln \frac{p^0 + |\vec{p}| \mp i\varepsilon}{p^0 - |\vec{p}| \mp i\varepsilon} \right]^{-1} \quad (4.49)$$

are the denominators for the two terms that make up the full effective propagator. In these functions, various signs depend on either the propagator being advanced or retarded, or the index  $\pm$  of the denominator. In order to avoid ambiguities, these signs have been color coded with red implying that the sign depends on the distinction advanced/retarded and blue for the index  $\pm$ . Physically, the two terms that make up  $S^{A/R*}$  in (4.48) propagate different fermionic helicity modes: The eigenstates to  $\gamma^0 - \vec{k}\vec{\gamma}/|\vec{k}|$  have helicity  $-1$ , such that their ratio of helicity over chirality is  $+1$ , hence the subscript on the denominator  $\Delta_+$ . This is also the helicity over chirality ratio of massless Dirac fermions at zero temperature. On the other hand,  $\gamma^0 + \vec{k}\vec{\gamma}/|\vec{k}|$  has eigenstates with helicity  $+1$ , so here, the ratio for the propagated mode is  $-1$ , again corresponding to the index of the denominator  $\Delta_-$ . Note that this ratio is a sensible quantity to consider, because the dressed propagator  $S^{A/R*}$  does not brake chirality

$$\{S^{A/R*}, \gamma_5\} = 0 \quad (4.50)$$

unlike a zero temperature massive fermion propagator. Thus, one finds that at non-zero temperature a new fermionic mode can be populated. These new states are presumably excitations of the thermal plasma, commonly referred to as plasminos\* in the literature [36]. The dispersion relations for these two fermionic modes are obtained from the position of the poles  $\omega_{\pm}$  in  $\Delta_{\pm}^{A/R}$ . A closed expression solving the equation ( $\Delta_{\pm}^{A/R}$  was found in [35] by using the Lambert  $W$  function. Neglecting the  $\varepsilon$  shift for a moment and defining a shorthand

$$x_{\pm} = \frac{p^0 \pm |\vec{p}|}{p^0 \mp |\vec{p}|} \quad (4.51)$$

allows to write the pole equation for  $\Delta_{\pm}$  as

$$\frac{m_{\ell}^2}{|\vec{p}|} \frac{1}{x_{\pm} - 1} \left( 2 \frac{|\vec{p}|^2}{m_{\ell}^2} - x_{\pm} + 1 + \ln x_{\pm} \right) = 0. \quad (4.52)$$

If  $x_{\pm} = 1$ , the prefactor diverges. However, this is only possible for  $|\vec{p}| = 0$  and by excluding this case, one can concentrate on the factor in brackets. Applying yet another shorthand

$$y = 2 \frac{|\vec{p}|^2}{m_{\ell}^2} + 1, \quad (4.53)$$

rearranging and raising to powers both sides gives the identity

$$-e^{-y} = -x_{\pm} e^{-x_{\pm}}, \quad (4.54)$$

---

\*in analogy to the bosonic plasmon excitations in solid state physics

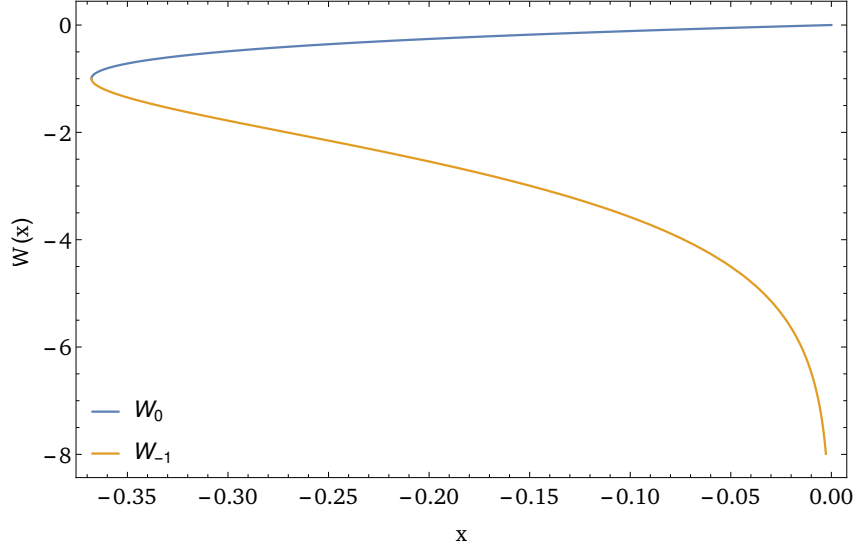


**Figure 4.5:** The two branches  $W_0$  and  $W_{-1}$  of the Lambert  $W$  function that is defined as the inverse of  $f(x) = x e^x$ . The branching point lies at  $(-1/e, -1)$ .

which is satisfied by the Lambert  $W$  function, defined as the inverse of  $f(x) = x e^x$ ,  $W(x) = f^{-1}(x)$ . Note that  $f$  has a minimum at  $x = -1$ ,  $f(-1) = 1/e$ , such that  $W$  has two branches. These are denoted by subscripts 0 and  $-1$

$$W_0(x) \in [-1, \infty) \quad \text{for } x \in \left[-\frac{1}{e}, \infty\right), \quad (4.55a)$$

$$W_{-1}(x) \in (-\infty, -1] \quad \text{for } x \in \left[-\frac{1}{e}, 0\right), \quad (4.55b)$$

as depicted in Figure 4.5. These two branches of  $W$  correspond to two solutions for  $x_p m$  and consequently to the poles of  $\Delta_{\pm}$ . In order to assign them correctly, one might consider the limit  $T \rightarrow 0$ , where the dispersion of a massless particle should be recovered for  $\Delta_+$  as the thermal mass  $m_\ell \rightarrow 0$  in this case. The latter implies  $y \rightarrow \infty$  for non-vanishing momenta  $|\vec{p}| \neq 0$  as can be seen in (4.53) and so the left hand side of (4.54) goes to zero. On the other hand,  $x_+ \rightarrow \infty$  if the massless dispersion relation  $p^0 = |\vec{p}|$  is enforced, identifying  $W_{-1}$  as the branch that holds the solution to  $x_+$ . Resolving the shorthands  $x_{\pm}$ ,  $y$  and solving for the poles  $\omega_{\pm}$ , one arrives at the dispersions for the two modes

$$\omega_+ = |\vec{p}| \frac{W_{-1} \left[ -\exp \left( -\frac{|\vec{p}|^2}{2m_\ell^2} - 1 \right) \right] - 1}{W_{-1} \left[ -\exp \left( -\frac{|\vec{p}|^2}{2m_\ell^2} - 1 \right) \right] + 1}, \quad (4.56a)$$

$$\omega_- = -|\vec{p}| \frac{W_0 \left[ -\exp \left( -\frac{|\vec{p}|^2}{2m_\ell^2} - 1 \right) \right] - 1}{W_0 \left[ -\exp \left( -\frac{|\vec{p}|^2}{2m_\ell^2} - 1 \right) \right] + 1}. \quad (4.56b)$$

Note that earlier,  $|\vec{p}| = 0$  was excluded in the derivation of the dispersion relations and for the sake of completeness, it should be checked if this point is correctly represented in (4.56a) and

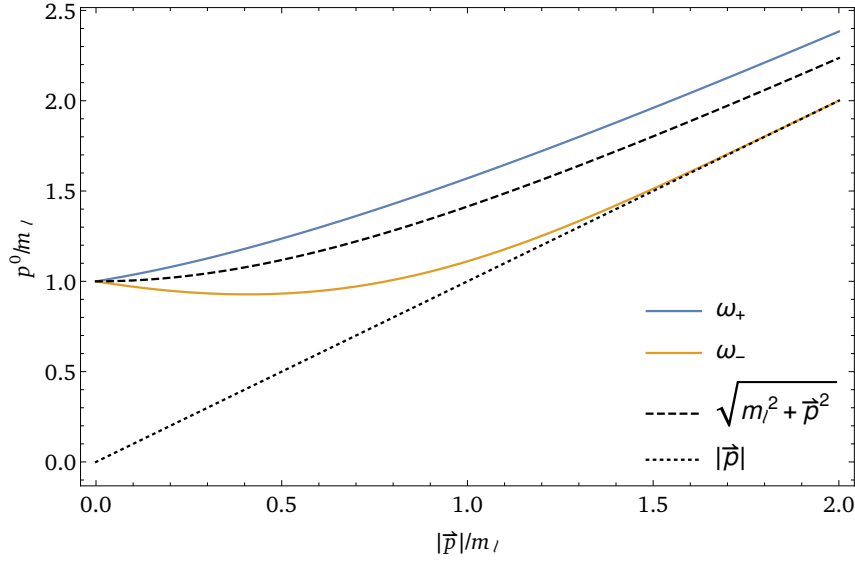


**Figure 4.6:** Dispersion relation for the two fermionic modes found in the dressed lepton propagator (4.48). In blue is the dispersion  $\omega_+$  for the mode with positive ratio of helicity over chirality, in orange is  $\omega_-$  for negative ratio of helicity over chirality. For comparison and as a guide for the eye, the dispersions of a particle with mass  $m_\ell$  (black, dashed) and for a massless particle (black, dotted) are also shown.

(4.56b). The denominators show the asymptotic behavior

$$\lim_{|\vec{p}| \rightarrow 0} \Delta_{\pm}^{-1} = p^0 - \frac{m_\ell^2}{p^0}, \quad (4.57)$$

revealing that  $\omega_{\pm} = m_\ell$  in this case as is already correctly included in the found solution that is depicted in Figure 4.6. One can see how both modes start out just like one would expect for a massive particle with mass  $m_\ell$ . However, the two modes split,  $\omega_+$  exceeding the normal massive dispersion, while  $\omega_-$  falls below and even has a negative slope for small  $|\vec{p}|$  before it asymptotically approaches the dispersion of massless particle.

For  $p^0 \geq 0$  the poles of  $\Delta_{\pm}$  are now known to be  $\omega_{\pm}$ , but how about  $p^0 < 0$ ? Looking back at how the dispersion was derived, substituting  $p^0 \rightarrow -p^0$  corresponds to  $x_{\pm} \rightarrow x_{\mp}$ , revealing that the solutions are switched on the negative side of the  $p^0$ -axis:

$$p^0 = \begin{cases} \pm \omega_{\pm} & \text{for } \Delta_+ \\ \pm \omega_{\mp} & \text{for } \Delta_- \end{cases} \quad \text{for } p^0 \geq 0. \quad (4.58)$$

Finally, the shift of the poles away from the real axis by the  $\varepsilon$  terms in the logarithms shall be investigated. For this reason, one may examine the linear dependence of the denominators on  $\varepsilon$  around  $\varepsilon = 0$ :

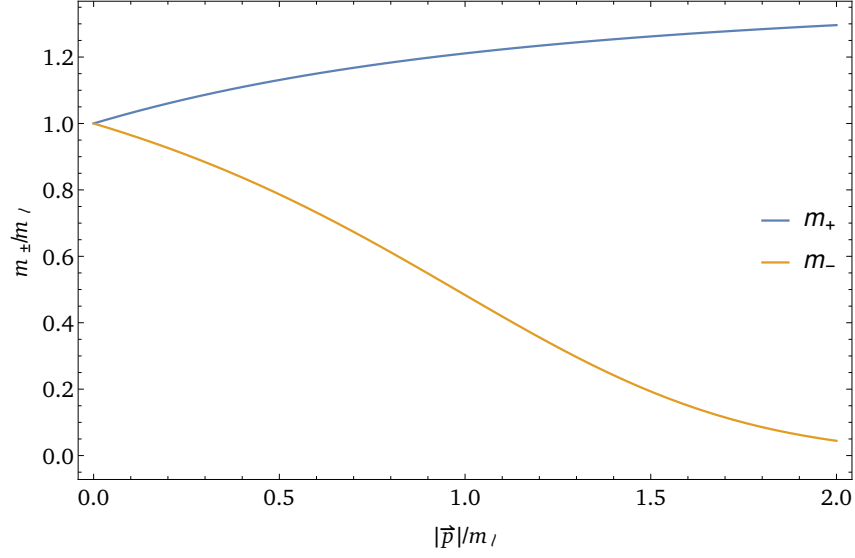


**Figure 4.7:** The effective mass  $m_{\pm}$  as a function of the three-momentum  $|\vec{p}|$ . In blue is the equivalent mass for the fermion mode with positive ratio of helicity over chirality, in orange for negative ratio of helicity over chirality.

$$[\Delta_{\pm}^{A/R}]^{-1} = p^0 \mp |\vec{p}| \mp \frac{m_{\ell}^2}{|\vec{p}|} \pm \frac{m_{\ell}^2}{2|\vec{p}|^2} (p^0 \mp |\vec{p}|) \ln \frac{p^0 + |\vec{p}|}{p^0 - |\vec{p}|} \pm i \frac{m_{\ell}^2}{\pm |\vec{p}| (p^0 \pm |\vec{p}|)} \varepsilon + O(\varepsilon^2). \quad (4.59)$$

Now, the direction of the shift can be obtained from expanding  $\Delta_{\pm}$  at  $\varepsilon = 0$  around the poles  $\omega_{\pm}$ . This is done for the pole on the positive and the negative real axis respectively:

$$[\Delta_{\pm}^{A/R}]^{-1} = \left[ 2 \frac{m_{\ell}^2}{m_{\pm}^2} (p^0 - \omega_{\pm}) + O((p^0)^2) \right] \pm i \frac{m_{\ell}^2}{\pm |\vec{p}| (p^0 \pm |\vec{p}|)} \varepsilon + O(\varepsilon^2), \quad (4.60a)$$

$$[\Delta_{\pm}^{A/R}]^{-1} = \left[ 2 \frac{m_{\ell}^2}{m_{\mp}^2} (p^0 + \omega_{\mp}) + O((p^0)^2) \right] \pm i \frac{m_{\ell}^2}{\pm |\vec{p}| (p^0 \pm |\vec{p}|)} \varepsilon + O(\varepsilon^2). \quad (4.60b)$$

Above, (4.60a) represents the expansion around the positive pole and (4.60b) around the negative one. In the prefactor of the linear term in  $p^0$ , the effective mass  $m_{\pm}$  was introduced which is defined as

$$m_{\pm}^2 = \omega_{\pm}^2 - |\vec{p}|^2, \quad (4.61)$$

so it can be viewed as the momentum dependent equivalent of a mass term that would appear in a normal dispersion relation of a massive particle. Figure 4.7 shows  $m_{\pm}$  as a function of the three-momentum  $|\vec{p}|$ . While  $m_{-}$  asymptotically goes to zero for large momenta, it is still always positive and the same is obviously true for  $m_{+}$ , so  $m_{\pm}^2 > 0$ . Now, equating (4.60a) and (4.60b) with zero and solving for  $p^0$ , one can directly infer the direction of the shift

#### 4 Self-Energies

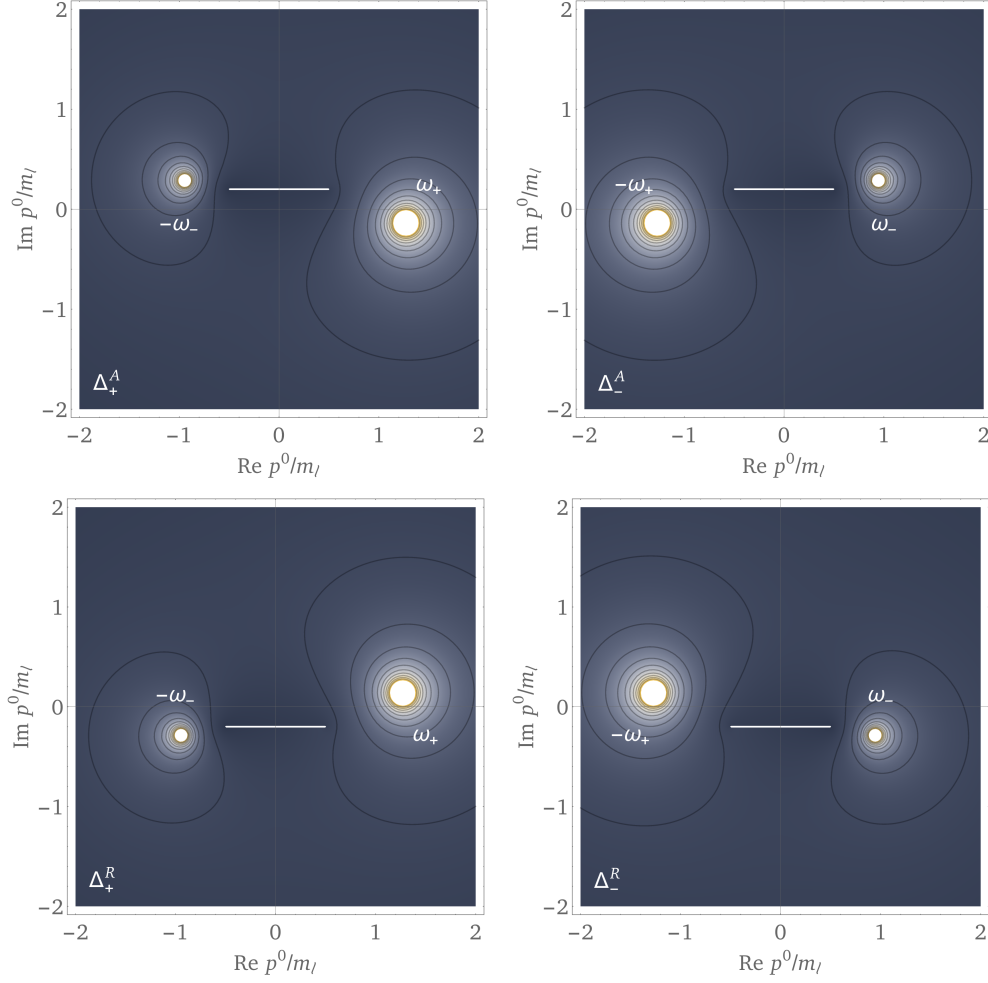


**Figure 4.8:** Poles and discontinuities of the denominator functions  $\Delta_{\pm}^{A/R}$  including a finite  $\varepsilon$ -shift in imaginary direction. Shown is the absolute value, where both discontinuities and poles are visible at the same time.

$$\Delta_{\pm}^{A/R} : p^0 = \omega_{\pm} \mp i \frac{m_{\pm}^2}{\pm 2|\vec{p}|(\omega_{\pm} \pm |\vec{p}|)} \varepsilon \quad \text{for } p^0 > 0, \quad (4.62a)$$

$$\Delta_{\pm}^{A/R} : p^0 = -\omega_{\mp} \mp i \frac{m_{\mp}^2}{\mp 2|\vec{p}|(\omega_{\mp} \pm |\vec{p}|)} \varepsilon \quad \text{for } p^0 < 0. \quad (4.62b)$$

The direction of the shift is explicitly given by the combination of the signs above, as all expressions that appear are positive, including the term  $\omega_{\pm} \pm |\vec{p}|$  in brackets. In Figure 4.8, an arbitrary value was assigned to  $|\vec{p}|$  in order to visualize the shifts from the real axis.

Studying the expansions around the poles (4.60a) and (4.60b) does not only provide insights into the direction of the shift, but also reveals the residues of the poles in  $\Delta_{\pm}^{A/R}$  as

$$\text{res}_{p^0=\omega_{\pm}} \Delta_{\pm}^{A/R} = \frac{m_{\pm}^2}{2m_{\ell}^2}, \quad (4.63a)$$

$$\text{res}_{p^0=-\omega_{\mp}} \Delta_{\pm}^{A/R} = \frac{m_{\mp}^2}{2m_{\ell}^2}. \quad (4.63b)$$

Figure 4.8 does not only show the poles in the complex  $p^0$ -plane, but also branch cuts from  $-|\vec{p}|$  to  $|\vec{p}|$  either above or below the real axis, in case of the advanced or retarded denominator  $\Delta^A$  or  $\Delta^R$  respectively. Those can be traced back to the logarithm that appears in (4.49). For  $p^0 \in [-|\vec{p}|, |\vec{p}|]$ , this logarithm has a discontinuity of  $-2\pi i$  going from infinitesimally above the cut to infinitesimally below it. Based on that, the discontinuity can be calculated as

$$\text{disc } \Delta_{\pm}^{A/R} = 4\pi i \theta(-p^2) \Xi_{\pm} + [\text{poles}], \quad (4.64)$$

where

$$\Xi_{\pm} = \pm \frac{\frac{|\vec{p}|^2}{m_{\ell}^2} \frac{1}{p^0 \mp |\vec{p}|}}{\left( \pm 2 \frac{|\vec{p}|^2}{m_{\ell}^2} - 2 \frac{|\vec{p}|}{p^0 \mp |\vec{p}|} + \ln \frac{p^0 + |\vec{p}|}{p^0 - |\vec{p}|} \right) \left( \pm 2 \frac{|\vec{p}|^2}{m_{\ell}^2} - 2 \frac{|\vec{p}|}{p^0 \mp |\vec{p}|} + 2\pi i + \ln \frac{p^0 + |\vec{p}|}{p^0 - |\vec{p}|} \right)}. \quad (4.65)$$

Poles of the propagator enter as well into the discontinuity, but as the residues were already obtained in (4.63a) and (4.63b), they are not written explicitly here. Note that the discontinuities are calculated by always going from above to below the cut and hence always come with the same overall sign, independent of whether the function is advanced or retarded. In an actual loop integral,  $p^0$  will be integrated along the real axis, so that the contour will be above the discontinuity for an advanced propagator and below for a retarded one. The cut itself represents a continuous spectrum, originating from the interaction between the propagated fermion mode and the particles in the plasma that were considered in the self energy.

Finally, the statistical dressed lepton propagator  $iS^{F*}$  is obtained in analogy to the scalar case by replacing  $1 + 2f_B \rightarrow 1 - 2f_F$  in (4.8a). The difference of retarded and advanced propagator is very similar to the discontinuity calculated before:

$$\begin{aligned} iS^{F*}(p) &= \text{---} \overset{p}{\bullet} \text{---} \\ &= \left\{ - \left( \gamma^0 - \frac{\vec{p}}{|\vec{p}|} \vec{\gamma} \right) \left[ \pi \delta(p^0 - \omega_+) \frac{m_+^2}{2m_{\ell}^2} + \pi \delta(p^0 + \omega_-) \frac{m_-^2}{2m_{\ell}^2} + 2\pi \text{sgn}(p^0) \theta(-p^2) \Xi_+ \right] \right. \\ &\quad \left. + \left( \gamma^0 + \frac{\vec{p}}{|\vec{p}|} \vec{\gamma} \right) \left[ \pi \delta(p^0 - \omega_-) \frac{m_-^2}{2m_{\ell}^2} + \pi \delta(p^0 + \omega_+) \frac{m_+^2}{2m_{\ell}^2} + 2\pi \text{sgn}(p^0) \theta(-p^2) \Xi_- \right] \right\} \\ &\quad [1 - 2f_F(|p^0|)]. \end{aligned} \quad (4.66)$$

The thorough discussion of the dressed propagators, the position of their poles and discontinuities in the complex  $p^0$ -plane and the associated residues facilitates the analytic calculation of integrals over the zero-component of a loop-momentum containing dressed propagators. This will be very important in the next section.

## 4.4 Neutrino Self Energy

Finally, the building blocks that were computed in the previous sections are to be assembled into the self energy of neutrinos in the  $\nu$ MSM. Due to the minimal coupling between the Majorana fields  $N$  and the SM particle content, only one type of diagram enters the calculation at leading order: A loop consisting of one lepton and one Higgs propagator, analogous to the contribution that was already discussed for the SM leptons. There arises however an additional contribution, originating from the additional Majorana propagators. Thus, one obtains for the self energy [5]

$$\begin{aligned}
 \Sigma(p) &= \text{Diagram 1} + \text{Diagram 2} \\
 &= i \left( h^\dagger h P_L + h^T h^* P_R \right) \int \frac{d^D k}{(2\pi)^D} D(k) S(p+k).
 \end{aligned} \tag{4.67}$$

In the second diagram, the momenta point in the same direction along the lines as they do in the first one. As was already the case for the leptons, two four vectors  $p$  and  $u$  can be used to construct an expression that transforms properly under Lorentz transformations as in (4.38):

$$\Sigma^{A/R}(p) = \not{p} \left( P_L a_L^{A/R} + P_R a_R^{A/R} \right) + \not{p} \left( P_L b_L^{A/R} + P_R b_R^{A/R} \right). \tag{4.68}$$

Here, the superscript  $A/R$  refers to advanced and retarded objects as usual, whereas the subscript  $L/R$  denotes right- and left chiral parts. The evaluation of the coefficients now depends on the external momentum: For hard  $p^0$ ,  $|\vec{p}| \gtrsim T$ , the bare propagators can be used. Then, the computation of the self-energy is carried out in analogy to the SM leptons, with the difference that the logarithms appearing in the momentum integrals must be approximated for hard external momentum scales. The leading contributions to  $L_\pm^{A/R}$  in this domain have already been given in (4.23b)–(4.23c) and (4.40b)–(4.40c). It was laid out how these terms depend on three scales: The spatial loop momentum  $|\vec{k}|$ , as well as the two external scales  $p_\pm = (p^0 \pm |\vec{p}|)/2$ . Having a hard external momentum can mean that either both  $p_\pm$  are hard or just one of the two, if  $p^0$  and  $|\vec{p}|$  are much larger as the temperature but take on comparable absolute values.

In this limit  $p_\pm \ll T$ , the logarithms in the loop integral give sizable contributions to the thermal loop integral and the traces of the self-energy are found to be

$$\frac{1}{4} \text{tr} [P_L \not{p} \Sigma^{A/R}(p)] = \frac{7}{24} h_N^\dagger h_N T^2, \tag{4.69a}$$

$$\frac{1}{4} \text{tr} [P_R \not{p} \Sigma^{A/R}(p)] = \frac{7}{24} h_N^T h_N^* T^2, \tag{4.69b}$$

$$\frac{1}{4} \text{tr}[P_L \not{p} \Sigma^{A/R}(p)] = \frac{1}{6} h_N^\dagger h_N \frac{p^0}{p^2} T^2, \quad (4.69c)$$

$$\frac{1}{4} \text{tr}[P_R \not{p} \Sigma^{A/R}(p)] = \frac{1}{6} h_N^T h_N^* \frac{p^0}{p^2} T^2. \quad (4.69d)$$

Upon solving the system of equations for the coefficients  $a_{L/R}^{A/R}$  and  $b_{L/R}^{A/R}$ , one obtains

$$a_L^{A/R} = \frac{1}{24} h_N^\dagger h_N \frac{T^2}{|\vec{p}|^2} \left[ 7 - 4 \frac{(p^0)^2}{p^2} \right], \quad (4.70a)$$

$$a_R^{A/R} = \frac{1}{24} h_N^T h_N^* \frac{T^2}{|\vec{p}|^2} \left[ 7 - 4 \frac{(p^0)^2}{p^2} \right], \quad (4.70b)$$

$$b_L^{A/R} = -\frac{1}{8} h_N^\dagger h_N \frac{T^2}{|\vec{p}|^2} p^0, \quad (4.70c)$$

$$b_R^{A/R} = -\frac{1}{8} h_N^T h_N^* \frac{T^2}{|\vec{p}|^2} p^0. \quad (4.70d)$$

Interestingly, logarithmic dependencies on the external momentum do contribute in the loop integral but cancel each other in this domain of the approximation.

The second case, where one of the two external scales  $p_+$  or  $p_-$  is hard, but the other one is soft, gives a different picture. The corresponding expansions of the logarithmic term  $L_+^{A/R}$  in the loop integral give leading logarithmic dependencies on the loop momentum  $\sim |\vec{k}| \ln(|\vec{k}|/p_\pm)$ . Therefore, the leading contributions to the traces are of the form

$$\int_0^\infty d|\vec{k}| |\vec{k}| \ln \frac{|\vec{k}|}{p_\pm} f_B(|\vec{k}|) = \frac{\pi^2}{6} T^2 \left( 1 - 12 \ln A + \ln \frac{2\pi T}{p_\pm} \right), \quad (4.71a)$$

$$\int_0^\infty d|\vec{k}| |\vec{k}| \ln \frac{|\vec{k}|}{p_\pm} f_F(|\vec{k}|) = \frac{\pi^2}{12} T^2 \left( 1 - 12 \ln A + \ln \frac{4\pi T}{p_\pm} \right), \quad (4.71b)$$

where  $A \approx 1.28243$  is the Glaisher-Kinkelin constant that appears for example in the derivative of the Riemann  $\zeta$ -function. Keeping the leading terms in the temperature, the traces are

$$\frac{1}{4} \text{tr}[P_L \not{p} \Sigma^{A/R}(p)] = \frac{1}{8} h_N^\dagger h_N T^2 \left[ 1 \mp \frac{2}{3} \frac{p^2}{|\vec{p}|(p^0 \pm |\vec{p}|)} \right] \quad (4.72a)$$

$$\frac{1}{4} \text{tr}[P_R \not{p} \Sigma^{A/R}(p)] = \frac{1}{8} h_N^T h_N^* T^2 \left[ 1 \mp \frac{2}{3} \frac{p^2}{|\vec{p}|(p^0 \pm |\vec{p}|)} \right] \quad (4.72b)$$

$$\frac{1}{4} \text{tr}[P_L \not{p} \Sigma^{A/R}(p)] = \pm \frac{1}{16} h_N^\dagger h_N T^2 \frac{1}{|\vec{p}|} \left[ 1 + \frac{\ln 2}{3} - 12 \ln A - \frac{4}{3} \frac{p^0}{p^0 \pm |\vec{p}|} + \ln \frac{\pm 4\pi T}{p^0 \mp |\vec{p}| \mp i\epsilon} \right] \quad (4.72c)$$

$$\frac{1}{4} \text{tr}[P_R \not{p} \Sigma^{A/R}(p)] = \pm \frac{1}{16} h_N^T h_N^* T^2 \frac{1}{|\vec{p}|} \left[ 1 + \frac{\ln 2}{3} - 12 \ln A - \frac{4}{3} \frac{p^0}{p^0 \pm |\vec{p}|} + \ln \frac{\pm 4\pi T}{p^0 \mp |\vec{p}| \mp i\epsilon} \right] \quad (4.72d)$$

#### 4 Self-Energies

Here, the color coding of signs is use to disambiguate between the two cases of advanced and retarded functions (red), as well as between the two domains of approximation ( $p_{\pm} \gg T$ )  $\wedge$  ( $p_{\mp} \ll T$ ) (blue). As usual, the coefficient functions  $a_{L/R}^{A/R}$  and  $b_{L/R}^{A/R}$  are obtained:

$$a_L^{A/R} = \frac{1}{8} h_N^\dagger h_N \frac{T^2}{|\vec{p}|^2} \left[ 1 \mp \frac{1}{2} \left( 1 + \frac{\ln 2}{3} - 12 \ln A + \ln \frac{\pm 4\pi T}{p^0 \mp |\vec{p}| \mp i\epsilon} \right) \frac{p^0}{|\vec{p}|} \pm \frac{2}{3} \frac{|\vec{p}|}{p^0 \pm |\vec{p}|} \right] \quad (4.73a)$$

$$a_R^{A/R} = \frac{1}{8} h_N^T h_N^* \frac{T^2}{|\vec{p}|^2} \left[ 1 \mp \frac{1}{2} \left( 1 + \frac{\ln 2}{3} - 12 \ln A + \ln \frac{\pm 4\pi T}{p^0 \mp |\vec{p}| \mp i\epsilon} \right) \frac{p^0}{|\vec{p}|} \pm \frac{2}{3} \frac{|\vec{p}|}{p^0 \pm |\vec{p}|} \right] \quad (4.73b)$$

$$b_L^{A/R} = -\frac{1}{8} h_N^\dagger h_N \frac{T^2}{|\vec{p}|^2} \left[ p^0 \mp \frac{1}{2} \left( 1 + \frac{\ln 2}{3} - 12 \ln A + \ln \frac{\pm 4\pi T}{p^0 \mp |\vec{p}| \mp i\epsilon} \right) \frac{p^2}{|\vec{p}|} \right] \quad (4.73c)$$

$$b_R^{A/R} = -\frac{1}{8} h_N^T h_N^* \frac{T^2}{|\vec{p}|^2} \left[ p^0 \mp \frac{1}{2} \left( 1 + \frac{\ln 2}{3} - 12 \ln A + \ln \frac{\pm 4\pi T}{p^0 \mp |\vec{p}| \mp i\epsilon} \right) \frac{p^2}{|\vec{p}|} \right] \quad (4.73d)$$

An important result is the changed dependence on temperature in this domain of mixed momentum scales. Where up to now, the self-energy was  $O(T^2)$ , here, an additional dependence  $O(T^2 \ln T)$  appears in the approximation. These logarithms are large as they contain the ratio of temperature over the soft momentum scale  $T/p_{\mp} \gg 1$ .

In the last domain  $p^0, |\vec{p}| \ll T$ , dressed propagators are needed in order to capture all contributions to a fixed order of the Yukawas  $h_N$  in the perturbative expansion. These propagators have been computed above and are now substituted into the self-energy integral

$$\Sigma^{A/R}(p) = \frac{i}{2} (h_N^\dagger h_N P_L + h_N^T h_N^* P_R) \int \frac{d^D k}{(2\pi)^D} \left[ D^{F^*}(k) S^{A/R^*}(p+k) + D^{R/A^*}(k) S^{F^*}(p+k) + D^{A^*}(k) S^{A^*}(p+k) + D^{R^*}(k) S^{R^*}(p+k) \right]. \quad (4.74)$$

When the dressed propagators are inserted above, the integrand becomes a long and complicated expression. For this reason, it is divided into four additive parts that are discussed separately below.

The first part is simply given by the first summand  $D^{F^*}(k) S^{A/R^*}(p+k)$  of the integrand. The statistical Higgs-propagator features a  $\delta$ -distribution that renders the  $k^0$ -integration trivial:

$$\begin{aligned}
& \int \frac{d^D k}{(2\pi)^D} D^{F^*}(k) S^{A/R^*}(p+k) = \\
= & -\frac{i}{4} \int \frac{d^d \vec{k}}{(2\pi)^d} \frac{1}{\omega_\phi(|\vec{k}|)} [1 + 2f_B[\omega_\phi(|\vec{k}|)]] \\
& \left\{ \left[ \Delta_+^{A/R}(p^0 + \omega_\phi(|\vec{k}|), |\vec{p} + \vec{k}|) + \Delta_+^{A/R}(p^0 - \omega_\phi(|\vec{k}|), |\vec{p} + \vec{k}|) \right] \left( \gamma^0 - \frac{\vec{p} + \vec{k}}{|\vec{p} + \vec{k}|} \vec{\gamma} \right) + \right. \\
& \left. \left[ \Delta_-^{A/R}(p^0 + \omega_\phi(|\vec{k}|), |\vec{p} + \vec{k}|) + \Delta_-^{A/R}(p^0 - \omega_\phi(|\vec{k}|), |\vec{p} + \vec{k}|) \right] \left( \gamma^0 + \frac{\vec{p} + \vec{k}}{|\vec{p} + \vec{k}|} \vec{\gamma} \right) \right\}. \tag{4.75}
\end{aligned}$$

The shorthand  $\omega_\phi$  denotes the quasi on-shell energy of the Higgs with thermal mass  $m_\phi(T)$  at which which the zero-component of the loop momentum is fixed by the  $\delta$ -distribution

$$\omega_\phi(|\vec{k}|) = \sqrt{m_\phi^2(T) + |\vec{k}|^2}. \tag{4.76}$$

At this point, problems start to emerge that will also recur in most of the other parts of the self-energy integral. The poles and discontinuity of the denominators  $\Delta_\pm^{A/R}$  were discussed at great lengths in the previous section. The associated residues and discontinuity determine the value of the above integral. Finding the poles for the spatial momentum  $|\vec{k}|$  means solving the equations

$$p^0 + \omega_\phi(|\vec{k}|) = \pm \omega_\pm(|\vec{p} + \vec{k}|), \tag{4.77a}$$

$$p^0 - \omega_\phi(|\vec{k}|) = \pm \omega_\pm(|\vec{p} + \vec{k}|), \tag{4.77b}$$

$$p^0 + \omega_\phi(|\vec{k}|) = \pm \omega_\mp(|\vec{p} + \vec{k}|), \tag{4.77c}$$

$$p^0 - \omega_\phi(|\vec{k}|) = \pm \omega_\mp(|\vec{p} + \vec{k}|) \tag{4.77d}$$

for the four denominators in (4.75) respectively. For these, there is no analytic solution, so they need to be found numerically. Depending on the point  $(p^0, |\vec{p}|)$  in momentum space and the two masses  $m_\ell$  and  $m_\phi$ , large cancellations can occur. Thus, while the overall concept of how to approach this integral is clear, the detailed implementation of an algorithm that works out the numerical integration for the spatial components is non-trivial. Pretending the position of the poles were known, one could compute the principal value of the integral numerically and add the missing residues from the shifted poles by hand. It turns out that the exact same issue occurs in two other parts of the self-energy.

For the second part, the contributions from poles to the lepton statistical propagator in  $D^{R/A^*}(k) S^{F^*}(p+k)$  are considered. These also feature  $\delta$ -distributions and the  $k^0$ -integration can again be performed:

#### 4 Self-Energies

$$\begin{aligned}
& \int \frac{d^D k}{(2\pi)^D} D^{R/A^*}(k) S^{F^*}(p+k) \Big|_{\text{poles}} = \\
& \frac{i}{4} \int \frac{d^d \vec{k}}{(2\pi)^d} \\
& \left\{ \left( \gamma^0 - \frac{\vec{p} + \vec{k}}{|\vec{p} + \vec{k}|} \vec{\gamma} \right) \right. \\
& \left[ \frac{m_+^2(|\vec{p} + \vec{k}|)}{m_\ell^2(T)} \frac{1 - 2f_F[\omega_+(|\vec{p} + \vec{k}|)]}{[p^0 - \omega_+(|\vec{p} + \vec{k}|)]^2 - \omega_\phi^2(|\vec{k}|) \mp i \operatorname{sgn}[p^0 - \omega_+(|\vec{p} + \vec{k}|)] \varepsilon} + \right. \\
& \left. \frac{m_-^2(|\vec{p} + \vec{k}|)}{m_\ell^2(T)} \frac{1 - 2f_F[\omega_-(|\vec{p} + \vec{k}|)]}{[p^0 + \omega_-(|\vec{p} + \vec{k}|)]^2 - \omega_\phi^2(|\vec{k}|) \mp i \operatorname{sgn}[p^0 + \omega_-(|\vec{p} + \vec{k}|)] \varepsilon} \right] - \\
& \left( \gamma^0 + \frac{\vec{p} + \vec{k}}{|\vec{p} + \vec{k}|} \vec{\gamma} \right) \\
& \left[ \frac{m_-^2(|\vec{p} + \vec{k}|)}{m_\ell^2(T)} \frac{1 - 2f_F[\omega_-(|\vec{p} + \vec{k}|)]}{[p^0 - \omega_-(|\vec{p} + \vec{k}|)]^2 - \omega_\phi^2(|\vec{k}|) \mp i \operatorname{sgn}[p^0 - \omega_-(|\vec{p} + \vec{k}|)] \varepsilon} + \right. \\
& \left. \frac{m_+^2(|\vec{p} + \vec{k}|)}{m_\ell^2(T)} \frac{1 - 2f_F[\omega_+(|\vec{p} + \vec{k}|)]}{[p^0 + \omega_+(|\vec{p} + \vec{k}|)]^2 - \omega_\phi^2(|\vec{k}|) \mp i \operatorname{sgn}[p^0 + \omega_+(|\vec{p} + \vec{k}|)] \varepsilon} \right] \Big\}. \quad (4.78)
\end{aligned}$$

This integrand has the same poles and residues as the first part, leaving aside the different thermal distributions  $f_B$  and  $f_F$ . Hence, the same problem occurs that was already pointed out for the first part.

In the third part of the integral, the discontinuity in the statistical lepton propagator is taken into account. Here, a picture different from the two situations before emerges, as the integration over  $k^0$  is not composed of measure zero contributions from  $\delta$ -distributions, but instead spans over a continuous integrand in the finite region of the discontinuity jump:

$$\begin{aligned}
& \int \frac{d^D k}{(2\pi)^D} D^{R/A^*}(k) S^{F^*}(p+k) \Big|_{\text{disc.}} = \\
& = i \int \frac{d^d \vec{k}}{(2\pi)^d} \int_{-p^0 - |\vec{p} + \vec{k}|}^{-p^0 + |\vec{p} + \vec{k}|} \frac{dk^0}{2\pi} \left[ \left( \gamma^0 - \frac{\vec{p} + \vec{k}}{|\vec{p} + \vec{k}|} \vec{\gamma} \right) \Xi_+(p+k) - \left( \gamma^0 + \frac{\vec{p} + \vec{k}}{|\vec{p} + \vec{k}|} \vec{\gamma} \right) \Xi_-(p+k) \right] \\
& \frac{1 - 2f_F(p^0 + k^0)}{(k^0)^2 - \omega_\phi^2(|\vec{k}|) \pm i \operatorname{sgn}(k^0) \varepsilon}. \quad (4.79)
\end{aligned}$$

In an attempt to solve the  $k^0$  integral analytically, one could multiply the above integrand by a logarithmic term

$$\frac{1}{2\pi i} \ln \frac{k^0 + p^0 - |\vec{p} + \vec{k}|}{k^0 + p^0 + |\vec{p} + \vec{k}|},$$

which has a discontinuity of 1 along the original integration contour (c.f. Appendix A). Then,

the integral can be obtained by instead encircle this new discontinuity. One can then add up all residues exterior to the encircled cut. This method has been used in the calculations in the previous sections to perform finite interval integrations with great success. However, in all previous cases, the integration variable did not appear in the argument of the thermal distributions  $f_B$  or  $f_F$ , which  $k^0$  of course does. The problem at this point is the infinite number of  $1/k^0$  singularities these distributions have along the imaginary axis. Hence, one obtains an infinite sum of residues that also contain the complicated functions  $\Xi_{\pm}$ . Thus, the  $k^0$ -integration should also be attempted numerically.

The fourth and last part is not proportional to a thermal distribution function and therefore does not contribute to the thermal part of the self-energy. It is still given here for the sake of completeness and in order to point out an interesting feature of the dressed propagators:

$$\begin{aligned}
& \int \frac{d^D k}{(2\pi)^D} [D^{A^*}(k) S^{A^*}(p+k) + D^{R^*} S^{R^*}(p+k)] = \\
= & \int \frac{d^d \vec{k}}{(2\pi)^d} \frac{1}{\omega_{\phi}(|\vec{k}|)} \frac{m_+^2(|\vec{p} + \vec{k}|)}{m_{\ell}^2(T)} \\
& \left\{ \left( \gamma^0 - \frac{\vec{p} + \vec{k}}{|\vec{p} + \vec{k}|} \vec{\gamma} \right) \left[ -\pi \delta[\omega_+(|\vec{p} + \vec{k}|) - p^0 + \omega_{\phi}(|\vec{k}|)] \right. \right. \\
& \qquad \qquad \qquad \left. \left. + \pi \delta[\omega_+(|\vec{p} + \vec{k}|) - p^0 - \omega_{\phi}(|\vec{k}|)] \right] + \right. \\
& \left. \left( \gamma^0 + \frac{\vec{p} + \vec{k}}{|\vec{p} + \vec{k}|} \vec{\gamma} \right) \left[ -\pi \delta[-\omega_+(|\vec{p} + \vec{k}|) - p^0 + \omega_{\phi}(|\vec{k}|)] \right. \right. \\
& \qquad \qquad \qquad \left. \left. + \pi \delta[-\omega_+(|\vec{p} + \vec{k}|) - p^0 - \omega_{\phi}(|\vec{k}|)] \right] \right\}. \tag{4.80}
\end{aligned}$$

This result is unexpected, since in the case of bare propagators, one is used to products of exclusively advanced or retarded propagators vanishing in a loop integral because all of their poles are situated at the same side of the real axis. This property is lost in the resummed fermion propagator, where - as shown in in Figure 4.8 - at least one pole is always present in each, the lower and upper half of the complex plane. To the knowledge of the author, this feature is undocumented in the literature. The form of the above integral after the  $k^0$ -integration depends on where the contour is closed in the complex plane. Here, an effort was made to avoid picking up contributions from the discontinuity, which results in a somewhat asymmetric expression that only contains  $\omega_+$  but no  $\omega_-$ .

Implementing a numeric algorithm for the above integrals will be a task for future studies. The problems that arise in such a study have been outlined above. While a general method that solves for the positions of the poles in the spatial momentum integrals has to deal with potentially large cancellations over many orders of magnitude, these problems should in principle be resolvable. A thorough examination of the self-energy, based on the results that are presented here, will give insights into the size of contributions e.g. from the plasmino mode in the dressed fermion propagator.



# 5

## Summary and Outlook

In this work, a review on the concepts of thermal Quantum Field Theory was presented. It was shown, how Feynman rules are derived in the context of the Closed Time Path formalism, where field operators live on two distinct contours  $C_+$  and  $C_-$  in complex time along the real axis. This implies a doubling of the degrees of freedom and one obtains two systems: one that is defined along  $C_+$  with operators ordered chronologically in the conventional way and one on  $C_-$ , where operators are ordered anti-chronologically. These two systems are coupled at finite temperature by thermal propagators. At zero temperature, these propagators go to zero, the two systems decouple and one obtains the zero temperature QFT from the fields on  $C_+$ . Naively, this leads to four propagators at finite temperature for every propagator at zero temperature. Later in this work, it has been shown that relations between these propagators exist. An alternative representation of the theory exploits one such relation to reduce the number of propagators to three: an advanced, a retarded and a statistical one. Also, gauge theories at finite temperatures have been considered. A naive definition of the partition function seems to indicate that BRST symmetry breaks down at finite temperature due to inconsistencies in the Kubo-Martin-Schwinger boundary conditions for the Faddeev-Popov ghosts. These issues can be cured by including an additional ghost number operator into the partition function that does not alter contributions from physical states.

In the  $\nu$ MSM,  $n$  right-handed neutrinos are added to the matter content of the SM. These new fields are singlets under all SM gauge groups and therefore, can be obtained as the right chiral components of Majorana fields. They interact with the SM via Yukawa couplings to the Higgs and left-handed leptons. Complex phases in these Yukawas provide sources of  $CP$  violation and it has been argued in the literature, that models with at least three generations of right-handed neutrinos can account for the baryon asymmetry of the universe via the mechanism of leptogenesis, while also giving a candidate for dark matter. The oscillations of active neutrinos are accounted for via the Seesaw I mechanism. These possibilities make the  $\nu$ MSM a promising model for answering many questions simultaneously that point to physics beyond the SM.

The main part of this work was the self-consistent computation of self-energies at finite temperature within the  $\nu$ MSM. In the early 90s, Braaten and Pisarski have pointed out that thermal

## 5 Summary and Outlook

propagators need to be resummed for soft external momenta in order to obtain results that are complete to a given order in perturbation theory. These resummed propagators were computed for the Higgs and SM leptons which appear in leading order self-energy diagrams for the right-handed neutrinos. For scalars, one finds that the self-energy insertions act as a mass-squared term  $m_\phi^2 \sim T^2$  that simply shifts the poles in the corresponding propagators. Care must be taken if one wishes to extend the resummation scheme towards hard external momenta. In this case, the so-called Hard Thermal Loop approximation is no longer valid and a detailed computation shows that the thermal masses also depend on the external momentum. For fermions, the resummed propagators bear a rich phenomenology. In the limit of soft external momenta, one finds that at finite temperature, a new fermionic mode with opposite helicity is populated. The corresponding new states are interpreted as fermionic plasma excitations - the plasminos. Both fermionic modes show dispersion relations that are different from typical massive or massless dispersions. Although these dispersions can be interpreted as originating from momentum dependent masses, the resummed propagators do not break chirality. For the neutrinos, analytic expressions were obtained for the self-energies at hard external momenta. When inserting the dressed propagators in the case of soft external momenta, the resulting integrals become much more complicated and a numerical approach seems in place. This task could not be completed within this work and may be attempted in the future, following the principle strategy that was developed above.

Further interesting challenges are the consistent extension of the resummation technique for thermal propagators to hard external momenta. While the original argument of Braaten and Pisarski indicates that corrections in this regime would be negligible, it would be interesting to verify this explicitly. Especially the crossover region between soft and hard scales should be further investigated. Finally, the self-energies can be used as input for numerical studies on the evolution of baryon asymmetries in the universe.

# Appendix A

## Arbitrary Interval Integrals and the Residue Theorem

In the calculation of self-energies, integrals over loop momenta have to be computed. In this work, the integration over the spatial components is typically performed in spherical coordinates. In the case where the external momentum does not appear inside the integrand, only the integral over the absolute value of the loop momentum is non-trivial. However, scalar products between external- and loop momentum are present in most cases and one has to deal with an additional dependence on the angle between these two momenta. As an example, an integral that appears in the computation of scalar self-energies  $\Pi_{\text{ssv}}^A$  in (4.20) is

$$\begin{aligned}
 & \int \frac{d^D k}{(2\pi)^D} 2\pi \delta(k^2) [1 + 2f_B(|k^0|)] \frac{(2p+k)^2 + (p-k)^2}{(p+k)^2 - i \operatorname{sgn}(p^0 + k^0)\varepsilon} \\
 = & \frac{1}{2} \frac{1}{(4\pi)^{d/2}} \frac{1}{\Gamma(\frac{d}{2})} \int_0^\infty d|\vec{k}| |\vec{k}|^{d-2} [1 + 2f_B(|\vec{k}|)] \int_{-1}^{+1} d\cos\theta \\
 & \left[ \frac{5p^2 + 2p^0|\vec{k}| - 2|\vec{p}||\vec{k}|\cos\theta}{p^2 + 2p^0|\vec{k}| - 2|\vec{p}||\vec{k}|\cos\theta - i \operatorname{sgn}(p^0 + |\vec{k}|)\varepsilon} + \right. \\
 & \left. \frac{5p^2 - 2p^0|\vec{k}| - 2|\vec{p}||\vec{k}|\cos\theta}{p^2 - 2p^0|\vec{k}| - 2|\vec{p}||\vec{k}|\cos\theta - i \operatorname{sgn}(p^0 - |\vec{k}|)\varepsilon} \right] \tag{A.1}
 \end{aligned}$$

The integrand features two poles that are shifted away from the integration contour by the  $\varepsilon$ -term in the denominator.

$$\cos\theta = \frac{1}{2|\vec{p}||\vec{k}|} [p^2 \pm 2p^0|\vec{k}| - i \operatorname{sgn}(p^0 \pm |\vec{k}|)\varepsilon] \tag{A.2}$$

As long as  $\varepsilon$  is kept finite, the integral is well defined. A possibility to evaluate the integral over  $\cos\theta$  is to insert a logarithmic factor into the integrand that is constructed in such a way that

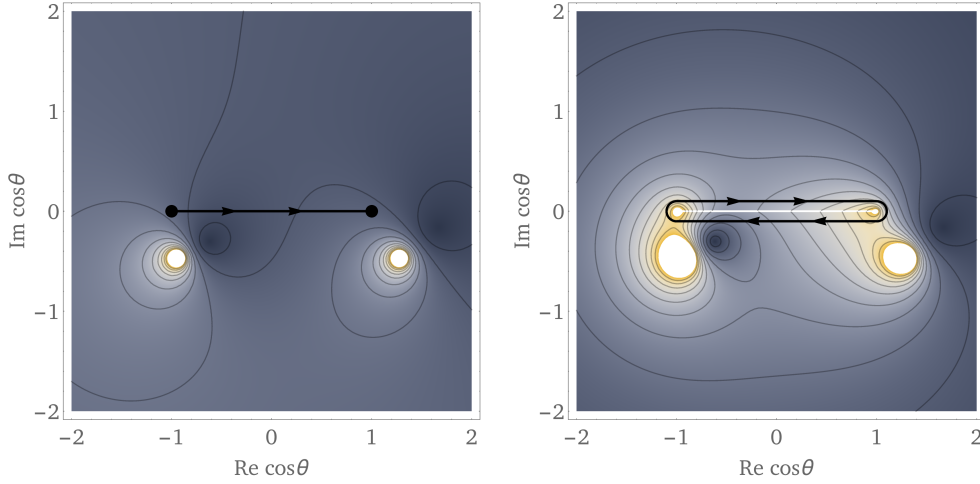


**Figure A.1:** Absolute values of the original integrand (left) and the integrand after the insertion of the logarithmic term in (A.3). Shown in black is the integration contour from  $-1$  to  $+1$  for the original integral and the closed contour after the insertion.

it features a discontinuity of 1 along the original contour, which in turn is then replaced by a closed path that clockwise encircles said discontinuity. The logarithmic term in question is

$$\frac{1}{2\pi i} \ln \frac{\cos \theta - 1}{\cos \theta + 1} \quad (\text{A.3})$$

The prescription for the integration contour is depicted in Figure A.1. After the insertion, the value of the integral can be found in the residues that lie outside the encircled region. These residues then also contain the logarithm, evaluated at the position of the poles, which is the reason for the appearance of logarithms in the self-energies. For the example considered here, one finds

$$2 \frac{1}{(4\pi)^{d/2}} \frac{1}{\Gamma(\frac{d}{2})} \int_0^\infty d|\vec{k}| |\vec{k}|^{d-2} \left[ 1 + f_B(|\vec{k}|) \right] \left\{ 1 - \frac{p^2}{2|\vec{p}||\vec{k}|} \left[ \ln \frac{|\vec{k}| + \frac{1}{2}(p^0 + |\vec{p}| - i\epsilon)}{|\vec{k}| + \frac{1}{2}(p^0 - |\vec{p}| - i\epsilon)} - \ln \frac{|\vec{k}| - \frac{1}{2}(p^0 + |\vec{p}| - i\epsilon)}{|\vec{k}| - \frac{1}{2}(p^0 - |\vec{p}| - i\epsilon)} \right] \right\} \quad (\text{A.4})$$

This is exactly the integral that is given in (4.21).

# Bibliography

- [1] K. Abe et al. (Belle Collaboration). Observation of Large  $cp$  Violation in the neutral  $b$  Meson System. *Phys. Rev. Lett.*, 87(091802), 2001.
- [2] P. A. Ade et al. (Planck Collaboration). Planck 2013 Results. I. Overview of Products and scientific Results. *A & A*, 571:A1, 2014.
- [3] P. A. Ade et al. (Planck Collaboration). Planck 2013 Results. XVI. Cosmological Parameters. *A & A*, 571:A16, 2014.
- [4] A. Anisimov, D. Besak, and D. Boedeker. Thermal production of relativistic Majorana neutrinos: Strong enhancement by multiple soft scattering. *JCAP*, 03:042, 2011.
- [5] A. Anisimov, A. Broncano, and M. Plumacher. The CP-asymmetry in resonant leptogenesis. *Nucl. Phys. B*, 737:176–189, 2006.
- [6] A. Anisimov, W. Buchmüller, and S. Mendizabal. Quantum Leptogenesis I. *Annals Phys.*, 326:1998–2038, 2011.
- [7] T. Asaka, S. Blanchet, and M. Shaposhnikov. The  $\nu$ MSM, Dark Matter and Neutrino Masses. *arXiv:hep-ph/0503065*, 2005.
- [8] T. Asaka and M. Shaposhnikov. The  $\nu$ MSM, Dark Matter and the Baryon Asymmetry of the Universe. *arXiv:hep-ph/0505013*, 2005.
- [9] B. Aubert et al. (BABAR Collaboration). Observation of  $cp$  Violation in the  $b^0$  Meson System. *Phys. Rev. Lett.*, 87(091801), 2001.
- [10] M. Beneke, B. Garbrecht, C. Fidler, and M. Herranen. Flavoured Leptogenesis in the CTP Formalism. *Nucl. Phys. B*, 843:177–212, 2011.
- [11] M. Beneke, B. Garbrecht, M. Herranen, and P. Schwaller. Finite Number Density Corrections to Leptogenesis. *Nucl. Phys. B*, 838:1–27, 2010.
- [12] J. Beringer (Particle Data Group). Status of Higgs Boson Physics. *Phys. Rev. D*, 86(010001), 2012.
- [13] E. Braaten and R. D. Pisarski. Deducing hard thermal Loops from Ward Identities. *Nucl. Phys. B*, 339:310–324, 1990.
- [14] E. Braaten and R. D. Pisarski. Soft Amplitudes in hot Gauge Theories: A general Analysis. *Nucl. Phys. B*, 337:569–634, 1990.

## Bibliography

- [15] E. Bulbul, M. Markevitch, A. Foster, R. K. Smith, M. Loewenstein, and S. Randall. Detection of an unidentified emission line in the stacked X-ray spectrum of galaxy clusters. *arXiv:1402.2301 [astro-ph.CO]*, 2014.
- [16] L. Canetti, M. Drewes, T. Frossard, and M. Shaposhnikov. Dark Matter, Baryogenesis and Neutrino Oscillations from Right Handed Neutrinos. *arXiv:1208.4607 [hep-ph]*, 2012.
- [17] M. E. Carrington, H. Defu, and M. H. Thoma. Equilibrium and Non-Equilibrium Hard Thermal Loop Resummation in the Real Time Formalism. *Eur. Phys. J. C*, 7:347–354, 1999.
- [18] J. H. Christenson, J. Cronin, V. Fitch, and R. Turlay. Evidence for the  $2\pi$  Decay of the  $k^0$ . *Phys. Rev. Lett.*, 13(138), 1964.
- [19] A. Collaboration. Observation of a new particle in the search for the Standard Model Higgs boson with the ATLAS detector at the LHC. *Phys. Rev. B*, 716:1–29, 2012.
- [20] L. Covi, N. Rius, R. E., and V. F. Finite temperature effects on CP violating asymmetries. *Phys. Rev. D*, 57:93–99, 1997.
- [21] A. Das. *Finite Temperature Field Theory*. World Scientific, 1997.
- [22] R. H. Dicke, J. E. Peebles, P. P. G. Roll, and D. T. Wilkinson. Cosmic Black Body Radiation. *APJ*, 142:414–419, 1965.
- [23] P. Elmfors, K. Enqvist, and I. Vilja. Thermalization of the Higgs Field at the Electroweak Phase Transition. *Nucl. Phys. B*, 412:459–478, 1994.
- [24] L. D. Faddeev and V. N. Popov. Feynman Diagrams for the Yang-Mills Field. *Phys. Lett. B*, 25(1):29, 1967.
- [25] G. R. Farrar and M. E. Shaposhnikov. Baryon asymmetry of the Universe in the standard model. *Phys. Rev. D*, 50(2):774–818, 1994.
- [26] B. Garbrecht. Leptogenesis. The Other Cuts. *Nucl. Phys. B*, 847:350–366, 2011.
- [27] G. F. Giudice, A. Notari, M. Raidal, A. Riotto, and A. Strumia. Towards a complete theory of thermal leptogenesis in the SM and MSSM. *Nucl. Phys. B*, 685:89–149, 2004.
- [28] G. Golub and W. Kahan. Calculating the Singular Values and Pseudo-Inverse of a Matrix. *Journal of the Society for Industrial and Applied Mathematics Series B Numerical Analysis*, 2(2):205–224, 1965.
- [29] R. Haag, N. M. Hugenholtz, and M. Winnink. On the equilibrium States in quantum statistical Mechanics. *Commun. math. Phys.*, 5(3):215–236, 1967.
- [30] Y. I. Izotov, T. X. Thuan, and V. A. Lipovetsky. The primordial helium abundance from a new sample of metal-deficient blue compact galaxies. *APJ*, 435:647–667, 1994.
- [31] N. Jarosik et al. Seven-Year Wilkinson Microwave Anisotropy Probe (WMAP) Observations: Sky Maps, systematic Errors and basic Results. *APJ Supplement Series*, 192(14), 2011.

- [32] J. I. Kapusta and C. Gale. *Finite-Temperature Field Theory - Principles and Applications*. Cambridge, 2006.
- [33] L. V. Keldysh. Diagram Technique for Nonequilibrium Processes. *JETP*, 20(4):1018–1026, 1965.
- [34] C. P. Kießig and M. Plümacher. Hard-thermal-Loop Corrections in Leptogenesis I:  $cp$ -Asymmetries. *JCAP*, 07, 2012.
- [35] C. P. Kiessig, M. Plumacher, and M. H. Thoma. Decay of a Yukawa fermion at finite temperature and applications to leptogenesis. *Phys.Rev. D*, 82:036007, 2010.
- [36] V. Klimov. Spectrum of Elementary Fermi Excitations in Quark Gluon Plasma. (In Russian). *Sov.J.Nucl.Phys.*, 33:934–935, 1981.
- [37] M. Kobayashi and T. Maskawa.  $Cp$  Violation in the renormalizable Theory of weak Interaction. *Prog. Theor. Phys.*, 49:652–657, 1973.
- [38] E. W. Kolb and M. S. Turner. The early universe. *Front. Phys.*, Vol. 69,, 1, 1990.
- [39] E. Komatsu et al. Seven-Year Wilkinson Microwave Anisotropy Probe (WMAP) Observations: Cosmological Interpretation. *APJ Supplement Series*, 192(18), 2011.
- [40] R. Kubo. Statistical-Mechanical Theory of irreversible Processes. I. General Theory and simple Applications to magnetic and Conduction Problems. *J. Phys. Soc. Jpn.*, 12:570–586, 1957.
- [41] V. A. Kuzmin, V. A. Rubakov, and M. E. Shaposhnikov. On anomalous electroweak baryon-number non-conservation in the early universe. *Phys. Lett. B*, 155:36–42, 1985.
- [42] M. Le Bellac. *Thermal Field Theory*. Cambridge, 1996.
- [43] P. C. Martin and J. Schwinger. Theory of Many-Particle Systems. I. *Phys. Rev.*, 115:1342, 1959.
- [44] P. Minkowski.  $\mu \rightarrow e \gamma$  at a Rate of one out of  $10^9$  muon Decays? *Phys. Lett. B*, 67(4):421, 1977.
- [45] K. A. Olive and G. Steigman. A new look at neutrino limits from big bang nucleosynthesis. *Phys. Lett. B*, 354:357–362, 1995.
- [46] K. A. Olive et al. (Particle Data Group). Electroweak Model and Constraints on new Physics. *Chin. Phys. C*, 38(090001), 2014.
- [47] K. A. Olive et al. (Particle Data Group). Quantum Chromodynamics. *Chin. Phys. C*, 38(090001), 2014.
- [48] A. Penzias and R. Wilson. A Measurement of excess Antenna Temperature at 4080 Mc/s. *APJ*, 142:419–421, 1965.
- [49] S. Perlmutter et al. Measurements of  $\omega$  and  $\lambda$  from 42 high-redshift Supernovae. *APJ*, 517(2):565, 1999.

*Bibliography*

- [50] M. Peskin and D. V. Schröder. *An Introduction to Quantum Field Theory*. Westview, 1995.
- [51] A. Pilaftsis and T. E. J. Underwood. Resonant leptogenesis. *Nucl. Phys. B*, 692:303–345, 2004.
- [52] M. Quirós. Field theory at finite temperature and phase transitions. *Helv. Phys. Acta*, 67:452–583, 1994.
- [53] M. J. Rees and D. W. Sciama. Large-Scale Density Inhomogeneities in the Universe. *Nature*, 217(5128):511–516, 1968.
- [54] A. Riess et al. Observational Evidence from Supernovae for an accelerating Universe and a cosmological Constant. *A & A*, 116(3):1009, 1998.
- [55] R. K. Sachs and A. M. Wolfe. Perturbations of a Cosmological Model and angular Variations of the Microwave Background. *APJ*, 147:73–90, 1967.
- [56] A. D. Sakharov. *CP Symmetry Violation, C-Asymmetry and Baryonic Asymmetry of the Universe*. *Pisma Zh. Eksp. Theor. Fiz.*, 5, 1967.
- [57] A. D. Sakharov. Violation of *CP* invariance, *C* asymmetry and baryon asymmetry of the universe. *JETP*, 5, 1967.
- [58] G. F. Smoot et al. Structure in the COBE differential Microwave Radiometer first-year Maps. *APJ*, 396:L1–L5, 1992.
- [59] G. 'tHooft. Symmetry breaking through bell-jackiw anomalies. *Phys. Rev. Lett.*, 37:8–11, 1976.
- [60] S. Weinberg. *Cosmology*. Oxford, 2008.
- [61] H. A. Weldon. Effective fermion masses of order  $gt$  in high-temperature gauge theories with exact chiral invariance. *Phys. Rev. D*, 26(10), 1982.
- [62] T. Yanagida. Proceedings of the Workshop on the Unified Theory and the Baryon Number in the Universe, 1979.
- [63] C. N. Yang and R. L. Mills. Conservation of Isotopic Spin and Isotopic Gauge Invariance. *Phys. Rev.*, 96:191, 1954.